High Accuracy Potentials for Quantum Dynamics

Edited by

Andrea Miani
Jonathan Tennyson
Tanja van Mourik

High Accuracy Potentials for Quantum Dynamics

Edited by

Andrea Miani

Jonathan Tennyson

Department of Physics & Astronomy,
University College London,
Gower Street,
London, WC1E 6BT,
United Kingdom

and

Tanja van Mourik

Department of Chemistry,
University College London,
20 Gordon Street,
London, WC1H 0AJ,
United Kingdom

Suggested Dewey classification: 541.2

ISBN 0-9545289-0-5

Published by

Collaborative Computational Project
on Molecular Quantum Dynamics (CCP6),
Daresbury Laboratory,
Daresbury,
Warrington, WA4 4AD,
United Kingdom

Preface vi

Ground-State Potential Energy Surfaces at the Focal Point
Attila G. Császár 1

The Explicitly Correlated Coupled-Cluster Models CC2-R12 and CCSD(R12)
Wim Klopper 8

Exploiting Systematic Basis Set Convergence for Accurate Potential Energy Surfaces
Kirk A. Peterson 14

Relativistic, Quantum Electrodynamic and Electroweak Effects in Molecules
H. M. Quiney 22

The Role of Born-Oppenheimer Breakdown Terms in the Prediction of Accurate Transition Frequencies for Ordinary Molecules
David W. Schwenke 32

The Asymptotic Regions of the Potential Energy Surfaces Relevant for the $O(^3P)$ + $O_2(X^3\Sigma_g^-) \rightleftharpoons O_3$ and
$O(^3P)$ + $OH(X^2\Pi) \rightleftharpoons O_2(X^3\Sigma_g^-)$ + $H(^2S)$ Reactions
Claire Gillery and Pavel Rosmus 37

Two Exothermic Reactions in the "Lithium Chemistry" Network: $LiH + H \rightarrow Li + H_2$ and $LiH^+ + H \rightarrow Li^+ + H_2$. A Comparison of Computed Potential Energy Surfaces.
E. Bodo, R. Martinazzo and F. A. Gianturco 43

Spectroscopic Determination of Ground and Excited State Potential Energy Surfaces.
K. Ahmed, G. G. Balint-Kurti and C. M. Western 48

From Single- to Multi-Sheeted Potential Energy Surfaces: a Dual Strategy for Accurate Global Forms
A. J. C. Varandas 54

Adiabatic and Diabatic Intermolecular Potentials for Open-Shell Complexes and Their Applications.
J. Kłos, W. Zeimen, V. Lotrich, G. C. Groenenboom and A. van der Avoird 59

Intermolecular Interaction Potentials
Krzysztof Szalewicz 66

Accurate Coupled-Cluster Potential Energy Surfaces: Large Calculations on Cyclopropenylidene Anharmonicities
Timothy J. Lee and Christopher E. Dateo 77

Vibrational Effects on Molecular Properties:
the Dalton Approach
Trygve Helgaker and Torgeir A. Ruden, Dan Jonsson, Kenneth Ruud, Peter R. Taylor and Per-Olof Åstrand 81

Subwavenumber Accuracy for the *Ab Initio* Rotation-Vibration Transitions of Water.
Oleg Polyansky 88

Analytical Energy Gradients for Internally Contracted Second-Order Multi-reference Perturbation Theory (CASPT2)
Hans-Joachim Werner and Paolo Celani 94

Model Hamiltonians for Accelerating Orbital Basis Convergence
Peter J. Knowles 99

A. Miani, J. Tennyson and T. van Mourik (eds.)
High Accuracy Potentials for Quantum Dynamics

Preface

This booklet was produced in connection with a workshop on "High Accuracy Potentials for Quantum Dynamics" held at University College London from 31st March to 2nd April 2003. The workshop was sponsored by the
UK Collaborative Computation Project 1 (CCP1) on the electronic structure of molecules,
UK Collaborative Computation Project 6 (CCP6) on Molecular Quantum Dynamics,
ChemReact high performance computing consortium.
The workshop was timely since the growth in computer power and concurrent development of new methods and algorithms has meant that the dream of calculating *ab initio* chemically accurate and spectroscopically accurate potential energy surfaces for chemically significant systems is rapidly becoming a reality.

The objective of the workshop was to bring together leading specialists working on high accuracy potential energy surfaces to share ideas and expertise on how best to construct such surfaces for a range of systems. Each invited speaker was asked to provide a brief article which reviews their work in the field of high accuracy potentials. This booklet should thus provide a good starting point for anyone wishing to learn more about the topic. The booklet undoubtedly conveys the breadth of topic discussed at the workshop, what it probably does not convey is the lively discussions which characterised not only the formal sessions but also breaks between them.

Jonathan Tennyson
London
May 2003

A. Miani, J. Tennyson and T. van Mourik (eds.)
High Accuracy Potentials for Quantum Dynamics

Ground-State Potential Energy Surfaces at the Focal Point

Attila G. Császár

Department of Theoretical Chemistry, Eötvös University, H-1518 Budapest 112, P. O. Box 32, Hungary

I. INTRODUCTION

Much of contemporary experimental physical chemistry, through spectroscopic, scattering, and kinetic studies, is directed toward the elucidation of salient features of potential energy surfaces (PES). Similarly, much of computational quantum chemistry is aimed at understanding given portions or the whole of potential energy surfaces of molecular species or reactive (scattering) systems. Therefore, it is somewhat strange to note that PESs exist only within the so-called Born–Oppenheimer (BO) separation of electronic and nuclear motion [1]. Adiabatic corrections to the BO-PES relax this strict separation, defining an adiabatic (mass-dependent) PES.

In the present report we are concerned neither with the case where several electronic states are to be described equally well (e.g., for processes driven by curve crossings) nor with the evaluation of coupling matrix elements, such as those arising from nonadiabatic BO interactions and detailed spin-orbit couplings. Here we are focusing on well-separated ground-state PESs. Nevertheless, there are still a number of challenges facing quantum chemists interested in computing such surfaces, including [2]: (a) use of wave functions of single- vs multireference (MR) character; (b) use of wave functions obtained from truncated configuration interaction (CI), coupled cluster (CC), or many-body perturbation theory (MBPT); (c) use of variational vs non-variational wave functions; (d) use of size-extensive vs non-size-extensive techniques; (e) instabilities in the (reference) wave functions; (f) basis set incompleteness error (BSIE); (g) basis set superposition error (BSSE); and (h) determination of small energy terms, usually referred to as correction terms.

Within the BO-PES approach, for the computation of well-separated ground electronic states one needs to consider three choices: that of the Hamiltonian, of the one-, and of the n-particle spaces [3].

Several model chemistries have been devised along these lines for refining *ab initio* energetic predictions. One of the earliest systematic efforts is the Gaussian-n series developed by Pople and co-workers, including G1 [4, 5], G2 [6], G3 [7, 8], and a wide number of variants, a very recent one being G3-RAD [9]. The target accuracy of these procedures is ± 4 kJ mol^{-1} but their usual accuracy is less (sometimes considerably less).

A similar approach in common use today is the CBS-n (CBS-4, CBS-q, CBS-Q and variants) scheme of Petersson et al. [10–12]. CBS-Q and G2 show roughly equivalent performance [11]. Certain newer models [12] include (size-consistent) empirical correction factors for the various residual theoretical errors. The parameterized configuration interaction (PCI-X) method of Siegbahn et al. [13, 14] also performs similarly to the Gaussian-n schemes.

An excellent black-box model chemistry is the W1/W2 method of Martin [15]. W1 and W2 follow similar protocols, but only W2 has no empirical parameters. W2 is capable of achieving chemical accuracy in the energetics.

All of the methods discussed but W2 are in some manner empirical. Nevertheless, numerous advances have been made which allow computation of highly accurate results without empirical parameterization. These methods rely on an understanding of the dual asymptotic behavior of the electron correlation energy. The BSIE was originally characterized by Schwartz [16] and Carroll et al. [17] and was investigated subsequently by others [1, 18–21]. Approaches to the full-CI asymptote have also been investigated [23].

II. THE FOCAL-POINT APPROACH

The focal point approach [1, 24, 25], utilized heavily in this work, can be summarized as follows (note that ΔE is a relative energy of two points, whereas δ denotes an incremental change in ΔE with respect to the previous level of theory):

(1) Extrapolate the SCF energy to the complete basis set (CBS) limit according to the three-parameter form [18] $E_{\rm SCF} = E^{\infty}_{\rm SCF} + ae^{-bX}$, where X is the cardinal number of the correlation-consistent (cc) basis sets developed by Dunning [26]. $\Delta E^{\infty}_{\rm SCF}$ is computed using these extrapolated values.

(2) Extrapolate the MP2 correlation energy to the CBS limit according to the two-parameter form $E_{\rm MP2}(X) - E_{\rm SCF}(X) = \epsilon^{\infty}_{\rm MP2} + bX^{-3}$. The extrapolated MP2 correlation energy, $\epsilon^{\infty}_{\rm MP2}$, is added to $E^{\infty}_{\rm SCF}$. The increment to the relative energy is computed as $\delta({\rm MP2}^{\infty}) = \Delta E^{\infty}_{\rm MP2} - \Delta E^{\infty}_{\rm SCF}$.

(3) Assume that basis set effects for correlation energy increments are additive and that the increments converge rapidly as X increases in the (aug-)cc-pVXZ series. The additivity principle is advantageous because valence-only coupled-

cluster calculations employing the $X = 5$ basis set are prohibitive for but simple systems.

(4) Obtain an estimate of higher-order correlation (HOC) effects, either through the additivity principle or through the multiplicative scaled higher-order correlation (SHOC) approach [23], suitable for PES studies [27].

(5) Compute the effect of core correlation, Δ(CV), using a size-extensive technique. Traditional basis sets, including (aug-)cc-pVXZ, are not designed to describe core-core and core-valence correlation, thus specially designed basis sets must be used. A popular choice is the (aug-)cc-pCVXZ series [28]. If these basis sets do not exist, customised bases can be created following well established procedures [29]. The core correlation shift is computed as $\Delta E_{\mathrm{CCSD(T)}}$(all electron) $-$ $\Delta E_{\mathrm{CCSD(T)}}$(frozen core).

(6) Compute the relativistic effect, Δ(Rel), usually through a scalar approximation to the relativistic Breit Hamiltonian, involving the one-electron Darwin and mass-velocity operators [3, 30–32] and the spin-orbit splitting, when applicable. The basis set utilized for these calculations should include core (high-exponent) Gaussian functions [3].

(7) Compute the zero-point energy contribution(s), Δ(ZPE), if necessary, at an appropriate level. While getting the harmonic contribution to ZPEs is difficult (though somewhat less difficult than getting accurate geometries), the anharmonic corrections to ZPE are reproduced accurately, with an error (usually much less) than 0.1 kJ mol^{-1}, even at low levels of theory. This favorable state of affairs can be rationalized by relatively simple arguments [33, 34].

(8) Combine all of the energy terms to give the extrapolated focal point (fp) approximation (ΔE_{fp}) to the exact answer:

$$\Delta E_{\mathrm{fp}} = \Delta E^{\infty}_{\mathrm{SCF}} + \delta(\mathrm{MP2}^{\infty}) + \delta(\mathrm{SD}) + \delta(\mathrm{T}) + \delta(\mathrm{HOC}) + \Delta(\mathrm{ZPE}) + \Delta(\mathrm{CV}) + \Delta(\mathrm{Rel}).$$

III. THERMOCHEMICAL APPLICATIONS

In a certain sense the least demanding use of the focal-point scheme is for thermochemical applications, i.e. for the determination of (temperature-dependent) enthalpies of formation, entropies, and heat capacities. This is due to the fact that the average experimental precision for, for example, enthalpies of formation, $\Delta_{\mathrm{f}}H^{\circ}_{0/298}$, is only about 2-4 kJ mol^{-1}, often times substantially less. A surprising and highly educational example about inaccuracies in experimental enthalpies of formation has been provided by Ruscic and co-workers [35, 36] for the OH radical, whereby, after careful reevaluation of the relevant experiments, the widely accepted experimental $\Delta_{\mathrm{f}}H^{\circ}_{0}$/kJ mol^{-1} of $+39.12 \pm 0.21$ had to be lowered to $+36.94 \pm 0.33$. The revised value has been fully supported by

high-level *ab initio* electronic structure computations.

We have recently completed computational investigations of $\Delta_f H^\circ_{0/298}$ of CH [37], SH [38], and CH_2 [39]. All these studies prove that if one can account for HOC effects, an accuracy of about $\pm 0.5 - 0.7$ kJ mol^{-1}, better than calibration accuracy of 1 kJ mol^{-1}, can be achieved even for radicals (better for closed-shell systems). Note, at the same time, that the usually highly successful CCSD(T) theory, almost all the time giving extremely similar results to CCSDT, is not capable of providing this accuracy; for example, for C_2, CN, and N_2 the estimated CBS HOC corrections [23] to the atomization energy are 5.8, 9.6, and 6.3 kJ mol^{-1}, respectively. This anticipates particular difficulties when the dissociation region of PESs is approached.

IV. THE METHYL INTERNAL ROTATION PROBLEM

During internal rotation a group of atoms, called the top, rotates with respect to another group, called the frame, within the molecule.

A particular internal rotation problem, that of the torsion of the methyl group in ethane, has fascinated chemists from the late 1920s [40, 41]. Therefore, it is somewhat surprising that there have remained inconsistencies in the theory of this simple molecular motion.

In particular, using symmetry analysis we have shown [42, 43] that barriers of infinite (or very large) height prevent certain rearrangements of the atoms in a molecule from occuring and therefore the complete nuclear permutation inversion (CNPI) group of the molecule should be reduced accordingly. These large barriers constrain torsional dynamics and influence how the torsional coordinates transform under the molecular symmetry (MS) group. This in turn determines the coordinate applicable for internal rotation, in the present case for the methyl problem.

Individual torsional coordinates, often emplyed in theoretical investigations of the methyl internal rotation problem, are unable to satisfy the above-mentioned symmetry requirements and thus should not be employed to describe this large-amplitude motion. Only a properly symmetrized internal rotation coordinate should be employed. If this coordinate is employed the minimum-energy torsional path exhibits the proper symmetry. In particular, all methyl torsions must show a $2\pi/3$ periodicity, irrespective of the actual geometric (point-group) symmetry of the frame and of the top.

If the focal-point approach is employed to obtain a one-dimensional effective torsional potential for the acetaldehyde molecule, CH_3CHO, not only the experimental torsional curve (V_3, V_6, and V_9) is reproduced excellently but also the available torsional transitions are within 1 cm^{-1} of experiment [43].

Computation of the proper torsional potential and subsequent analysis suggests that the conformers of the amino acid α-alanine can be distinguished based on their far-i.r. spectra [44].

V. FIRST-PRINCIPLES ROVIBRATIONAL SPECTROSCOPY

Computation of rovibrational spectra of molecules up to their dissociation limit(s) from PESs has been of central importance in physical chemistry. While first-principles computation of a PES correct up to dissociation still presents considerable difficulties, computation of semiglobal PESs able to reproduce all observed vibrational band origins (VBO) and rotational excitations with spectroscopic accuracy, i.e. within 1 cm^{-1}, is within reach.

For example, for water we have constructed [45] a mass-dependent, adiabatic PES which reproduces *all* available rovibrational levels, almost 18.000, with a mean accuracy/maximum deviation of [1.2/6.5, 0.6/1.4, 0.7/2.3, 0.7/3.0, 0.5/1.2] cm^{-1} for [$H_2{}^{16}O$, $H_2{}^{17}O$, $H_2{}^{18}O$, $D_2{}^{16}O$, $HD^{16}O$], respectively.

To achieve this accuracy for water, a 10-electrons and 3-nuclei benchmark system, it was necessary not only to approach the CBS FCI nonrelativistic limit through extrapolated MRCI calculations using basis sets up to aug-cc-pV6Z but also to treat relativistic effects beyond the usual scalar terms (in fact, we included not only corrections due to the Breit interaction but also to quantum electrodynamics (the one-electron Lamb shift), albeit through a simple scaling scheme [46]), and include adiabatic as well as nonadiabatic corrections. It will be extremely demanding to go beyond the precision achieved; nevertheless FCI computations resulting in a better HOC correction as well as use of a more dense grid, increased from the present 346 points to somewhere near 1000, should further reduce the discrepancies between theory and experiment.

The resulting compound surface gives the equilibrium structure of $H_2{}^{16}O$ as $r_e(OH) = 0.95785$ Å and $\alpha_e(HOH) = 104.501^o$, with an uncertainty of about 5 units in the final digit. This accuracy is better than that of any previous attempt to determine the equilibrium structure of water.

VI. SUMMARY

Advances in computer technology coupled with methodological developments allow us to approach all relevant limits of computational quantum chemistry. A particularly effective way of doing this is provided by the focal-point approach (Section II). When it is applied to PESs, at the present technical limits spectroscopic accuracy can be achieved for polyatomic and polyelectronic

molecules, such as water (Section V). The method can be used equally well for less demanding problems, namely the computation of accurate enthalpies of formation (Section III) and internal rotation potentials (Section IV).

Acknowledgments

Much of the work described has been sponsored by the Scientific Research Fund of Hungary (OTKA T033074). The author has the privilege to acknowledge joint work and useful discussions with Drs. W. D. Allen, M. L. Leininger, O. L. Polyansky, H. F. Schaefer III, V. Szalay, G. Tarczay, and J. Tennyson.

---

[1] M. Born and J. R. Oppenheimer, Ann. Phys. **84**, 457 (1927).
[2] A. G. Császár, W. D. Allen, Y. Yamaguchi, and H. F. Schaefer III, in *Computational Molecular Spectroscopy*, eds. P. Jensen and P. R. Bunker, Wiley, Chichester, 2000.
[3] G. Tarczay, A. G. Császár, H. M. Quiney, and W. M. Klopper, Mol. Phys. **99**, 1769 (2001).
[4] J. A. Pople, M. Head-Gordon, D. J. Fox, K. Raghavachari, and L. A. Curtiss, J. Chem. Phys. **90**, 5622 (1989).
[5] L. A. Curtiss, C. Jones, G. W. Trucks, K. Raghavachari, and J. A. Pople, J. Chem. Phys. **93**, 2537 (1990).
[6] L. A. Curtiss, K. Raghavachari, G. W. Trucks, and J. A. Pople, J. Chem. Phys. **94**, 7221 (1991).
[7] L. A. Curtiss, K. Raghavachari, P. C. Redfern, V. Rassolov, and J. A. Pople, J. Chem. Phys. **109**, 7764 (1998).
[8] L. A. Curtiss, P. C. Redfern, V. Rassolov, G. Kedziora, and J. A. Pople, J. Chem. Phys. **114**, 9287 (2001).
[9] D. J. Henry, M. B. Sullivan, and L. Radom, J. Chem. Phys. **118**, 4849 (2003).
[10] G. A. Petersson, A. Bennett, T. G. Tensfeldt, M. A. Al-Laham, W. A. Shirley, and J. Mantzaris, J. Chem. Phys. **89**, 2193 (1988).
[11] J. W. Ochterski, G. A. Petersson, and K. B. Wilberg, J. Am. Chem. Soc. **117**, 11299 (1995).
[12] J. W. Ochterski, G. A. Petersson, and J. A. Montgomery, J. Chem. Phys. **104**, 2598 (1996).
[13] P. E. M. Siegbahn, M. R. A. Blomberg, and M. Svensson, Chem. Phys. Lett. **223**, 35 (1994).
[14] P. E. M. Siegbahn, M. Svensson, and P. J. E. Boussard, J. Chem. Phys. **102**, 5377 (1995).
[15] J. M. L. Martin and G. de Oliveira, J. Chem. Phys. **111**, 1843 (1999).
[16] C. Schwartz, Phys. Rev. **126**, 1015 (1962).

[17] D. P. Carroll, H. J. Silverstone, and R. M. Metzger, J. Chem. Phys. **71**, 4142 (1979).
[18] D. Feller, J. Chem. Phys. **98**, 7059 (1993).
[19] J. M. L. Martin, Chem. Phys. Lett. **259**, 669 (1996).
[20] T. Helgaker, W. Klopper, H. Koch, and J. Noga, J. Chem. Phys. **106**, 9639 (1997).
[21] A. Halkier, T. Helgaker, P. Jørgensen, W. Klopper, H. Koch, J. Olsen, and A. K. Wilson, Chem. Phys. Lett. **286**, 243 (1998).
[1] A. G. Császár, W. D. Allen, and H. F. Schaefer III, J. Chem. Phys. **108**, 9751 (1998).
[23] A. G. Császár and M. L. Leininger, J. Chem. Phys. **114** 5491 (2001) and references therein.
[24] W. D. Allen, A. L. L. East, and A. G. Császár, in *Structures and Conformations of Non-Rigid Molecules*, Eds. J. Laane, M. Dakkouri, B. van der Veken, and H. Oberhammer, Kluwer, Dordrecht, 1993.
[25] A. L. L. East and W. D. Allen, J. Chem. Phys. **99**, 4638 (1993).
[26] T. H. Dunning, J. Chem. Phys. **90**, 1007 (1989) and subsequent papers.
[27] G. Tarczay, A. G. Császár, O. L. Polyansky, and J. Tennyson, J. Chem. Phys. **115**, 1229 (2001).
[28] D. E. Woon and T. H. Dunning, J. Chem. Phys. **103**, 4572 (1995).
[29] A. G. Császár and W. D. Allen, J. Chem. Phys. **104**, 2746 (1996).
[30] R. D. Cowan and D. C. Griffin, J. Opt. Soc. Am. **66**, 1010 (1976).
[31] S. A. Perera and R. J. Bartlett, Chem. Phys. Lett. **216**, 606 (1993).
[32] K. Balasubramanian, *Relativistic Effects in Chemistry, Part A: Theory and Techniques and Part B: Applications*, Wiley, New York, 1997.
[33] W. D. Allen and A. G. Császár, J. Chem. Phys. **98**, 2983 (1993).
[34] A. G. Császár, in *Encyclopedia for Computational Chemistry*, Eds. P. v. R. Schleyer et al., Vol. 1, pp. 13-30, Wiley, Chichester, 1998.
[35] B. Ruscic, D. Feller, D. A. Dixon, K. A. Peterson, L. B. Harding, R. L. Asher, and A. F. Wagner, J. Phys. Chem. A **105**, 2576 (2001).
[36] B. Ruscic, A. F. Wagner, L. B. Harding, R. L. Asher, D. Feller, D. A. Dixon, K. A. Peterson, Y. Song, X. Qian, C.-Y. Ng, J. Liu, W. Chen, and D. W. Schwenke, J. Phys. Chem. A **106**, 2727 (2002).
[37] A. G. Császár, P. G. Szalay, and M. L. Leininger, Mol. Phys. **100**, 3879 (2002).
[38] A. G. Császár, M. L. Leininger, and A. Burcat, J. Phys. Chem. A, in print (2003).
[39] A. G. Császár, M. L. Leininger, and V. Szalay, J. Chem. Phys. **118**, in print (2003).
[40] L. Ebert, Leipziger Vorträge, S. Hirzel Verlag, 74 (1929).
[41] C. Wagner, Z. Phys. Chem. Abt. B **14**, 166 (1931).
[42] V. Szalay, A. G. Császár, and M. L. Senent, J. Chem. Phys. **117**, 6489 (2002).
[43] A. G. Császár, V. Szalay, and M. L. Senent, J. Chem. Phys. to be submitted.
[44] A. G. Császár and V. Szalay, J. Phys. Chem. A to be submitted.
[45] O. L. Polyansky, A. G. Császár, S. V. Shirin, N. F. Zobov, P. Barletta, J. Tennyson, D. W. Schwenke, P. J. Knowles, Science **299**, 539 (2003).
[46] P. Pyykko, K. Dyall, A. G. Császár, G. Tarczay, O. L. Polyansky, and J. Tennyson, Phys. Rev. A **63**, 024502 (2001).

A. Miani, J. Tennyson and T. van Mourik (eds.)
High Accuracy Potentials for Quantum Dynamics

The Explicitly Correlated Coupled-Cluster Models CC2-R12 and CCSD(R12)

Wim Klopper

Chair of Theoretical Chemistry, Institute of Physical Chemistry, University of Karlsruhe (TH), D-76128 Karlsruhe, Germany

I. INTRODUCTION

Explicitly correlated coupled-cluster models such as the CCSD-R12 and CCSD(T)-R12 models are well suited to compute highly accurate electronic energies, enthalpies of formation, and potential energy hypersurfaces of small molecules (with up to 6 atoms) in the gas phase [1]. Such coupled-cluster calculations are, however, computationally demanding. Recently, we have started to develop explicitly correlated coupled-cluster models for much larger molecules (with up to 50 atoms), and for that purpose, we are currently exploring simplified (*i.e.*, computationally less demanding than CCSD-R12) explicitly correlated coupled-cluster models. Below, we present two such simplified models: CC2-R12 and CCSD(R12).

II. THE CLOSED-SHELL CCSD-R12 MODEL

In the closed-shell CCSD model [2], the many-electron coupled-cluster wavefunction $|\mathrm{CC}\rangle$ is obtained by operating with the exponential $\exp(\hat{S})$ onto the restricted Hartree–Fock reference determinant $|\mathrm{HF}\rangle$,

$$|\mathrm{CC}\rangle \;=\; \exp(\hat{S})|\mathrm{HF}\rangle\,. \tag{1}$$

In the standard CCSD model, r_{ij}-dependent terms are not involved and the cluster operator $\hat{S}$ contains the usual single ($\hat{T}_1$) and double ($\hat{T}_2$) excitations. In the CCSD-R12 method, however, less common double excitations (denoted $\hat{T}_{2'}$) are added, which introduce the interelectronic coordinates $r_{ij} = |\mathbf{r}_i - \mathbf{r}_j|$ into the many-electron wavefunction. Hence, in the CCSD-R12 case,

$$\hat{S} \;=\; \hat{T}_1 + \hat{T}_2 + \hat{T}_{2'}\,. \tag{2}$$

The notation $\hat{T}_{2'}$ is chosen to emphasize that this operator contains a particular form of *double* excitations, denoted R12 double excitations. Indeed, it consists of an infinite number of double excitations into the complementary orbital subspace $\{\varphi_\alpha\}$, that is, into all of those orbitals that are orthogonal to the finite basis of atomic orbitals (AOs), in which the calculation is performed,

$$\hat{T}_1 \;=\; \sum_{ai} t_a^i E_{ai}\,; \quad \hat{T}_2 \;=\; \tfrac{1}{2}\sum_{abij} t_{ab}^{ij} E_{ai}E_{bj} \tag{3}$$

$$\hat{T}_{2'} \;=\; \tfrac{1}{2}\sum_{\alpha\beta ijkl} c_{kl}^{ij} r_{\alpha k\beta l} E_{\alpha i}E_{\beta j}\,, \tag{4}$$

where E_{ai} is a singlet excitation operator and

$$r_{\alpha k\beta l} \;=\; \langle\varphi_\alpha(1)\varphi_\beta(2)|r_{12}|\varphi_k(1)\varphi_l(2)\rangle\,. \tag{5}$$

In other words, the $\hat{T}_{2'}$ operator generates all of the double excitations that otherwise would be missing in the calculation in the truncated, finite basis set. The orbital indices $p, q, r, \ldots$ denote orbitals of the finite basis and the indices $\alpha, \beta, \gamma, \ldots$ denote orbitals of the complementary basis. The finite basis and the complementary basis form together the complete basis $\{\varphi_\kappa\}$, and the orbitals $p, q, r, \ldots$ can be either occupied $(i, j, k, \ldots)$ or empty $(a, b, c, \ldots)$,

$$\{\varphi_\kappa\} \;=\; \{\varphi_p\}\cup\{\varphi_\alpha\} \;=\; \{\varphi_i\}\cup\{\varphi_a\}\cup\{\varphi_\alpha\}\,. \tag{6}$$

The similarity-transformed CCSD-R12 amplitude equations differ from their standard CCSD counterparts not only by the operator $\hat{T}_{2'}$ in the singles and doubles amplitude equations, but also by one additional equation, which represents the projection against the R12 doubles space,

$$\langle\mu_{2'}| \;=\; \sum_{\alpha\beta} r_{k\alpha l\beta} \left\langle\overline{{}^{\alpha\beta}_{ij}}\right| . \tag{7}$$

This projection is best carried out employing a biorthogonal basis [3],

$$\left\langle\overline{{}^{\alpha\beta}_{ij}}\right| \;=\; \tfrac{1}{3}\left\langle {}^{\alpha\beta}_{ij}\right| + \tfrac{1}{6}\left\langle {}^{\alpha\beta}_{ji}\right|\,; \quad \left\langle {}^{\alpha\beta}_{ij}\right| \;=\; \langle \mathrm{HF}|E_{j\beta}E_{i\alpha}\,. \tag{8}$$

Hence, the CCSD-R12 energy and amplitude equations are given by

$$E \;=\; \langle \mathrm{HF}|\hat{H}^S|\mathrm{HF}\rangle\,, \tag{9}$$

$$0 \;=\; \langle\mu|\hat{H}^S|\mathrm{HF}\rangle\,, \tag{10}$$

where $\mu \;=\; \{\mu_1, \mu_2, \mu_{2'}\}$ and

$$\hat{H}^S \;=\; \exp(-\hat{S})\hat{H}\exp(\hat{S})\,. \tag{11}$$

By assuming canonical Hartree–Fock orbitals and by partitioning the Hamiltonian into the many-electron Fock operator $\hat{f}$, the fluctuation potential $\hat{\Phi}$ and the nuclear repulsion term $h_{\rm nuc}$, we obtain

$$\hat{H} \;=\; \hat{f} + \hat{\Phi} + h_{\rm nuc}\,; \quad \hat{H}^S \;=\; \hat{f}^S + \hat{\Phi}^S + h_{\rm nuc}\,, \tag{12}$$

and

$$\hat{f}^S \;=\; \sum_{m=1,2} \varepsilon_{\mu_m} t_{\mu_m} \hat{\tau}_{\mu_m} + [\hat{f}, \hat{T}_{2'}] + \hat{f}\,; \quad \hat{\Phi}^S \;=\; \exp(-\hat{S})\hat{\Phi}\exp(\hat{S})\,, \tag{13}$$

where $\hat{\tau}_\mu$ are excitation operators, t_μ the corresponding amplitudes, and ε_μ differences between occupied and virtual orbital energies,

$$\varepsilon_{\mu_1} \equiv \varepsilon_{ai} \;=\; \varepsilon_a - \varepsilon_i\,; \quad \varepsilon_{\mu_2} \equiv \varepsilon_{aibj} \;=\; \varepsilon_a - \varepsilon_i + \varepsilon_b - \varepsilon_j\,. \tag{14}$$

The CCSD-R12 energy and the similarity-transformed coupled-cluster equations may now be written as

$$E \;=\; E_0 + \langle {\rm HF}|\hat{\Phi}^S|{\rm HF}\rangle + h_{\rm nuc}\,, \tag{15}$$

$$\varepsilon_{\mu_1} t_{\mu_1} \;=\; -\langle \mu_1|\hat{\Phi}^S|{\rm HF}\rangle\,, \tag{16}$$

$$\varepsilon_{\mu_2} t_{\mu_2} \;=\; -\langle \mu_2|\hat{\Phi}^S|{\rm HF}\rangle\,, \tag{17}$$

$$\langle \mu_{2'}|[\hat{f}, \hat{T}_{2'}]|{\rm HF}\rangle \;=\; -\langle \mu_{2'}|\hat{\Phi}^S|{\rm HF}\rangle\,, \tag{18}$$

where E_0 is the sum of the Hartree–Fock orbital energies. In this manner, the coupled-cluster CCSD-R12 eqution are written in a convenient form that is well suited to derive the simpler models CC2-R12 and CCSD(R12), as we shall see in the following.

III. THE CLOSED-SHELL CC2-R12 MODEL

Eqs. (15)–(18) define the CCSD-R12 model. As in the standard CC2 model [4], we now restrict the similarity transformation of the fluctuation potential in Eqs. (17) and (18) to *single excitations only*. Thus, in the CCSD-R12 equations, we replace the S-transformed fluctuation potential $\hat{\Phi}^S$ with the T1-transformed fluctuation potential

$$\tilde{\hat{\Phi}} = \exp(-\hat{T}_1)\hat{\Phi}\exp(\hat{T}_1)\,. \tag{19}$$

We then obtain the following equations for the CC2-R12 model:

$$\varepsilon_{\mu_1} t_{\mu_1} \;=\; -\langle \mu_1|\hat{\Phi}^S|{\rm HF}\rangle\,, \tag{20}$$

$$\varepsilon_{\mu_2} t_{\mu_2} \;=\; -\langle \mu_2|\tilde{\hat{\Phi}}|{\rm HF}\rangle\,, \tag{21}$$

$$\langle \mu_{2'}|[\hat{f}, \hat{T}_{2'}]|{\rm HF}\rangle \;=\; -\langle \mu_{2'}|\tilde{\hat{\Phi}}|{\rm HF}\rangle\,. \tag{22}$$

Eq. (22) is closely related to the R12 doubles amplitude equation of the MP2-R12 model [5], which reads

$$\langle \mu_{2'} | [\hat{f}, \hat{T}_{2'}] | \mathrm{HF} \rangle \;=\; -\langle \mu_{2'} | \hat{\Phi} | \mathrm{HF} \rangle \,. \tag{23}$$

The only difference between Eqs. (22) and (23) is that in the MP2-R12 equation Eq. (23), the fluctuation potential is *not* T1-transformed. In the CC2-R12 equation Eq. (22), on the other hand, it is. Evaluation of the corresponding term yields [5]

$$\langle \mu_{2'} | \tilde{\hat{\Phi}} | \mathrm{HF} \rangle \;=\; \sum_{\alpha\beta} r_{k\alpha l\beta} \left\langle \overline{{}^{\alpha\beta}_{ij}} \right| \tilde{\hat{\Phi}} \, | \mathrm{HF} \rangle \;=\; \sum_{\alpha\beta} r_{k\alpha l\beta} \tilde{g}_{\alpha i \beta j} \;=\; V_{kl}^{\tilde{i}\tilde{j}} \,. \tag{24}$$

The difference between the integral $V_{kl}^{\tilde{i}\tilde{j}}$ in CC2-R12 theory and its counterpart V_{kl}^{ij} in MP2-R12 theory [5] is that the coefficients of the molecular orbitals (MOs) $\varphi_{\tilde{i}}$ and $\varphi_{\tilde{j}}$ are not taken from the usual MO coefficient matrix $\mathbf{C}$, but instead from the matrix [2]

$$\mathbf{Y} \;=\; \mathbf{C}\mathbf{y}^T \;=\; \mathbf{C}(\mathbf{1} + \mathbf{t}_1) \,. \tag{25}$$

Furthermore, in comparison with the standard CC2 model, we note that in the CC2-R12 model, the term

$$\langle \mu_1 | [\tilde{\hat{\Phi}}, \hat{T}_{2'}] | \mathrm{HF} \rangle \tag{26}$$

occurs in the singles amplitude equation Eq. (20). Or course, this term also occurs in CCSD-R12 theory. It can be computed as

$$\left\langle \overline{{}^{a}_{i}} \right| [\tilde{\hat{\Phi}}, \hat{T}_{2'}] | \mathrm{HF} \Big\rangle \;=\; \sum_{klm} \left(2c_{kl}^{im} - c_{kl}^{mi}\right) \left(V^\dagger\right)_{\tilde{a}m}^{kl} \,, \tag{27}$$

where the index $\tilde{a}$ refers to a T1-transformed virtual orbital. Its MO coefficients are taken from the matrix [2]

$$\mathbf{X} \;=\; \mathbf{C}\mathbf{x}^T \;=\; \mathbf{C}(\mathbf{1} - \mathbf{t}_1^T) \,. \tag{28}$$

The integrals $\left(V^\dagger\right)_{\tilde{a}m}^{kl}$ are defined as

$$\left(V^\dagger\right)_{\tilde{a}m}^{kl} \;=\; \sum_{\alpha\beta} \tilde{g}_{a\alpha m\beta} r_{\alpha k\beta l} \,. \tag{29}$$

IV. THE CLOSED-SHELL CCSD(R12) MODEL

Motivated by the formulation of the CC2-R12 model, we proceed by proposing the following CCSD(R12) equations:

$$\varepsilon_{\mu_1} t_{\mu_1} = -\langle \mu_1 | \hat{\Phi}^S | \mathrm{HF} \rangle \,, \tag{30}$$

$$\varepsilon_{\mu_2} t_{\mu_2} = -\langle \mu_2 | \hat{\Phi}^S | \mathrm{HF} \rangle \,, \tag{31}$$

$$\langle \mu_{2'} | [\hat{f}, \hat{T}_{2'}] | \mathrm{HF} \rangle = -\langle \mu_{2'} | \tilde{\hat{\Phi}} + [\tilde{\hat{\Phi}}, \hat{T}_2] | \mathrm{HF} \rangle \,. \tag{32}$$

Eqs. (30) and (31) are the usual CCSD-R12 equations while Eq. (32) is a new R12 doubles equation in the spirit of the CC2-R12 model. This CCSD(R12) model may be viewed as a CCSD model that includes first-order R12 corrections. Note that in Eq. (32), we have used that

$$\langle \mu_{2'} | [[\tilde{\hat{\Phi}}, \hat{T}_2], \hat{T}_2] | \mathrm{HF} \rangle = 0 \,. \tag{33}$$

Thus, in the CCSD(R12) model, the right-hand side of the R12 doubles amplitude equation Eq. (32) is obtained by transforming the fluctuation potential $\hat{\Phi}$ with $\hat{T}_1$ and $\hat{T}_2$, but not with $\hat{T}_{2'}$. The essential new terms are

$$\left\langle \overline{{}^{\tilde{a}\tilde{b}}_{ij}} | [\tilde{\hat{\Phi}}, \hat{T}_{2'}] | \mathrm{HF} \right\rangle = \sum_{kl} c_{kl}^{ij} \left(V^\dagger \right)_{\tilde{a}\tilde{b}}^{kl} \tag{34}$$

$$\sum_{\alpha\beta} r_{k\alpha l\beta} \left\langle \overline{{}^{\alpha\beta}_{ij}} | [\tilde{\hat{\Phi}}, \hat{T}_2] | \mathrm{HF} \right\rangle = \sum_{ab} t_{ab}^{ij} V_{kl}^{\tilde{a}\tilde{b}} \,. \tag{35}$$

V. SUMMARY

We have presented the two explicitly correlated coupled-cluster models CC2-R12 and CCSD(R12), whose r_{ij}-dependent terms are computationally only little more involved than in the MP2-R12 model. Integrals of the type V_{kl}^{ij} are among those that occur in MP2-R12 theory. The new integrals for the models CC2-R12 and CCSD(R12) are $V_{kl}^{\tilde{i}\tilde{j}}$, $V_{kl}^{\tilde{a}m}$ and $V_{kl}^{\tilde{a}\tilde{b}}$. They are the same as in MP2-R12 theory, but with different, partly T1-transformed, indices.

Acknowledgments

Our work is supported by the DFG Research Center for Functional Nanostructures (CFN) under project number C2.3.

---

[1] W. Klopper, J. Noga, *ChemPhysChem* **4**, 32 (2003).
[2] T. Helgaker, P. Jørgensen, J. Olsen, *Molecular Electronic-Structure Theory*, Wiley, Chichester, 2000, pp. 685–698.
[3] P. Pulay, S. Sæbø, W. Meyer, *J. Chem. Phys.* **81**, 1901 (1984).
[4] O. Christiansen, H. Koch, P. Jørgensen, *Chem. Phys. Lett.* **243**, 409 (1995).
[5] W. Klopper, C.C.M. Samson, *J. Chem. Phys.* **116**, 6397 (2002).

A. Miani, J. Tennyson and T. van Mourik (eds.)
High Accuracy Potentials for Quantum Dynamics

Exploiting Systematic Basis Set Convergence for Accurate Potential Energy Surfaces

Kirk A. Peterson

Department of Chemistry, Washington State University, Pullman, Washington 99164-4630, USA

I. INTRODUCTION

In the *ab initio* calculation of potential energy surfaces (PESs), whether for spectroscopy or quantum dynamics, there are several sources of error which can greatly influence the accuracy of the resulting surface and hence the accuracy of any quantum mechanical observables calculated using this surface. The work in our group over the last several years has involved the systematic removal of one of the largest sources of error, namely the truncation of the 1-particle basis set used to describe the molecular orbitals. The foundation for this work was provided in the mid to late 1980's with the work of Ahlrichs and co-workers[1] and Almlöf and Taylor.[2] Of particular importance for the present work was the subsequent introduction of the correlation consistent (cc) family of basis sets by Dunning.[3] These latter sets were constructed such that both the Hartree-Fock and correlation energy converged systematically towards their respected basis set limits as successively larger members of the family were used. In particular, the regular convergence trends observed with these basis sets allows an accurate extrapolation to the complete basis set (CBS) limit. After this extrapolation, the remaining error in the calculation can then be attributed to the error intrinsic to the chosen electronic structure method, e.g., MP2, CCSD(T), MRCI, etc. This greatly facilitates the further improvement in the accuracy of the calculated results by systematically including other, more minor, corrections in an additive manner, e.g., effects due to core-valence correlation and relativity.

A large number of extrapolation formulas have been proposed and used in the literature with the cc basis sets. In the very first studies of this type,[4,5] a simple exponential function was used, i.e., $E(n) = E_{CBS} + Ae^{-bn}$, where n was associated with the cardinal number of the cc-pVnZ correlation consistent basis sets (n=2, 3 , 4, etc. for DZ, TZ, QZ, etc.). This was followed by the use

of the so-called "mixed" formula.[6] $E(n) = E_{CBS} + Ae^{-(n-1)} + Be^{-(n-1)^2}$. While both of these forms are only phenomenological in origin, the latter function in particular has been shown in numerous benchmark studies to lead to accurate CBS limits, particularly when basis sets of only double- through quadruple-zeta are used (c.f., Refs. [5,7-9]). In general, the simple exponential, while yielding accurate HF limits,[10] often strongly underestimates the basis set limit of the correlation energy, but can, in certain cases, yield good CBS relative energies. A second class of extrapolation formulas has its origin in the asymptotic basis set convergence characteristics of electron correlation in the He atom, which leads to extrapolations in l_{max}^{-m}, where l_{max} is the maximum angular momentum present in the basis set (c.f., Ref. [11] and references therein). Recent work[10,12] has shown that extrapolations based on $E(n) = E_{CBS} + an^{-3}$ can yield accurate estimates of the CBS limit for molecules when used in conjunction with large cc basis sets (n $\leq$ 4).

One research area that has seen widespread use of basis set extrapolations with highly correlated methods is the prediction of thermochemistry of small and medium-sized molecules. In these cases the truncation of the basis set can represent one of the largest sources of error and its removal via extrapolation leads in many cases to bond, atomization, and reaction enthalpies to within "chemical accuracy" ($<$ 1 kcal/mol) without the use of empirical parameters (after the inclusion of additional corrections due to zero-point vibrations, core-valence correlation, and relativistic effects).[13] A much less investigated area involves the use of explicit basis set extrapolations for full potential energy surfaces. A PES obtained from basis set extrapolations in conjunction with a highly correlated electronic structure method has the promise of delivering more accurate anharmonic vibrational frequencies, structures, and asymptotic energetics, as well as the full range of possible dynamical quantities, e.g., cross-sections, product state distributions, branching ratios, etc. It is also possible that by removing the possibly large errors due to basis set truncation, additional corrections to the surface, be they *ab initio* or empirical in nature, will be much more reliable. Our research group has now been involved in a number of PES studies where explicit basis set extrapolations have been used.[14-22] These can be grouped into the general categories of (i) global surfaces for chemical reactions, (ii) near-equilibrium surfaces for spectroscopy, and (iii) PESs for weakly-bound clusters.

II. GLOBAL SURFACES FOR CHEMICAL REACTIONS

The first use of explicit basis set extrapolations for large-scale potential energy surfaces was for the ground state of the HOCl molecule and its unimolecular dissociation to OH + Cl using large multireference configuration interaction wavefunctions.[14] Basis sets ranging in size from aug-cc-pVDZ to aug-cc-pVQZ were accurately extrapolated to the basis set limit at each point on the surface with the "mixed" CBS formula. In particular, basis set extrapolation improved the asymptotic energetics by more than 1 kcal/mol and only slight adjustments to this purely *ab initio* potential was required (using coordinate scaling[23]) to accurately predict the wavenumbers of all the vibrational bound states of HOCl.[24] This CBS limit surface was later extended to encompass the entire $O(^1D)$+HCl reactive surface,[15,16] and was also followed by an analogous study of the $O(^1D)$+ HBr system.[17]

The H+H_2 reaction represents a rather unique example in this area since a series of large basis sets can be used with wavefunctions of near Full CI (FCI) quality. Extrapolation to the basis set limit should then yield a potential energy surface that very closely approximates the exact Born-Oppenheimer surface. This has recently been carried out[19] using large multireference CI wavefunctions of near FCI quality (within a few μE_h) and sequences of correlation consistent basis sets for over 4000 configurations on the PES. In this work a novel basis set extrapolation technique was used, [25] whereby first a many-body decomposition was carried out on the total energy of each configuration and then the resulting 3-body energy was accurately extrapolated to the CBS limit by assuming it converged at the same rate as the sum of the 2-body terms (the basis set limit of which is very accurately known):

$$E_{CBS}^{3-body} = E_i^{3-body} + \frac{(E_i^{3-body} - E_j^{3-body})(E_{CBS}^{2-body} - E_i^{2-body})}{(E_i^{2-body} - E_j^{2-body})} \qquad (1)$$

where E^{n-body} denotes the sum of all the n-body energies, i and j denote the two basis sets used, and we require $i > j$. The estimated CBS limit for the total energy is then obtained by summing the extrapolated three-body term with the accurately known 1- and 2-body energies. Using this technique with a detailed series of convergence tests for the H_3 barrier height with basis sets as large as 7Z resulted in an estimate of 9.603 kcal/mol with a precision of about 0.003 kcal/mol.[25] This extremely accurate result could be obtained with basis sets no larger than aug-cc-pVQZ. After obtaining the CBS limits at each H_3 configuration in this manner, an analytical PES was constructed by fitting to a robust new analytical form, which yielded a mean unsigned fitting error of just 0.0023 kcal/mol. The remaining errors from fitting, correlation treatment,

and basis set incompleteness for the new CBS-limit surface were lower by over an order of magnitude compared to any prior analytic surface, and were all significantly smaller than expected non-Born-Oppenheimer effects. This surface has now been used in accurate quantum dynamics calculations for both $D+H_2$ and $H+D_2$.[26] After the inclusion of diagonal Born-Oppenheimer corrections, the calculated theoretical rate constants now agree perfectly with experiment, within experimental error, over a very large temperature range (167 – 2112 K).

III. NEAR-EQUILIBRIUM SURFACES FOR SPECTROSCOPY

Next to thermochemistry, equilibrium spectroscopic constants (r_e, ω_e, etc.) of small molecules is another area that has produced several studies involving explicit basis set extrapolations.[14,15,17,18,27-31] In most cases these involve the direct extrapolation of the properties of interest as a function of basis set. It is generally recognized, however, that the convergence with respect to basis set of properties like an equilibrium bond length or particularly a vibrational frequency is not as regular as the total energy itself. Hence, the most reliable method to obtain CBS limit spectroscopic constants is to extrapolate the energies at each point used to sample a near-equilibrium potential energy surface or analogously extrapolate the energies that are used in numerical finite difference formulas for ω_e, α_e, etc. Since our group is particularly interested in anharmonic vibrational frequencies, we have exclusively utilized the former technique. Table 1 contains some results obtained for the HOCl molecule at the MRCI+Q level of theory.[14] A total of 41 points were calculated about the experimental minimum geometry for three basis sets, which were also extrapolated to the CBS limit using the mixed formula. In each case these energies were then accurately fit to polynomials in internal displacement coordinates. The vibrational band origins were calculated using the usual 2^{nd}-order perturbation theory expressions.

One should note the smooth progression of the calculated spectroscopic constants towards their limiting CBS values. At the CBS limit, MRCI+Q slightly underestimates r_e(OH), which leads to an overestimation of ν_1 by about 16 cm^{-1}. We have also undertaken similar near-equilibrium studies of HOBr,[17] $HBBr^x$ (x=0,+1,−1),[18] and all of the related diatomic species. Recently work has been completed on highly accurate surfaces for the Na_2O and K_2O molecules,[20] which included the extrapolation of CCSD(T) all-electrons correlated calculations with new cc-pwCVnZ basis sets. The predicted spectroscopic constants arising from this latter work have expected uncertainties of less than 5 cm^{-1} in the final vibrational frequencies and about 0.002 Å in the

TABLE I: MRCI+Q spectroscopic constants calculated for HOCl as a function of basis set compared to experiment

Basis set	r_e(OH) (Å)	R_e(ClO) (Å)	θ_e(HOCl) (deg.)	ν_1 cm^{-1}	ν_2 cm^{-1}	ν_3 cm^{-1}
AVDZ	0.973	1.735	102.2	3551	1223	675
AVTZ	0.966	1.704	102.4	3608	1231	710
AVQZ	0.964	1.696	102.7	3620	1242	719
CBS	0.962	1.692	102.8	3626	1248	725
Expt.	0.964	1.689	103.0	3610	1239	724

equilibrium bond lengths. Lastly, it should be noted that for very accurate work the choice of extrapolation formula can result in CBS limit geometries that easily differ by 0.001 – 0.003 Å. Typical results[20] are shown below in Table 2 for the Na_2O molecule where all-electrons correlated CCSD(T) calculations were carried out with cc-pwCVnZ basis sets on Na and aug-cc-pwCVnZ sets on O. The CBS limits were obtained by pointwise extrapolation of 5 collinear points distributed about the equilibrium geometry.

TABLE II: Dependence on extrapolation method for the energetics and equilibrium structure of $X^1\Sigma_g^+$

Basis set	$E_e(E_h)$	$\sum D_e$(kcal/mol)	r_e(Å)
DZ	-399.057204	106.17	1.9982
TZ	-399.479668	112.26	1.9883
QZ	-399.560697	115.32	1.9825
5Z	-399.591538	116.15	1.9814
CBS(TQ,l^{-3})	-399.619844	117.56	1.9782
CBS(Q5,l^{-3})	-399.623896	117.03	1.9802
CBS(DTQ,mixed)	-399.600815	117.18	1.9788
CBS(TQ5,mixed)	-399.609498	116.64	1.9807

Taking either the CBS(Q5,l^{-3}) or CBS(DTQ, mixed) results as the best estimates for the actual CBS limit, one can see that the l^{-3} extrapolation with the smaller basis sets, CBS(TQ,l^{-3}), certainly overshoots the atomization energy and perhaps the equilibrium bond length. On the other hand, the CBS(TQ5, mixed) extrapolation yields CBS limits that are too conservative, particularly for $\sum D_e$, compared to the explicitly calculated 5Z results.

IV. SURFACES FOR WEAKLY-BOUND CLUSTERS

For the calculation of weakly-bound van der Waals species, large 1-particle basis sets are a necessary requirement to minimize basis set superposition errors (BSSE) and to accurately describe important dispersion interactions. Basis set extrapolations have been effectively used in previous studies of the binding energies of species such as rare gas dimers,[28,32] Ar-H_2, and Ar-HCl.[33] To determine if explicit basis set extrapolations could lead to accurate *surfaces* for weakly-bound systems, calculations were undertaken on the He-CO system, which has an equilibrium binding energy of less than 25 cm^{-1}. Four 3-dimensional surfaces were obtained at the CCSD(T) level of theory and ranged in quality from the doubly-augmented double zeta basis set to the extrapolated CBS limit. For each surface, over 1000 counterpoise-corrected interaction energies were accurately interpolated using a reproducing kernel Hilbert space (RKHS) approach.[34] After extrapolation to the CBS limit using the mixed formula, the residual errors inherent to the CCSD(T) method were approximately corrected by CCSDT calculations, which led to a "CBS-corr" surface. The five surfaces have well depths ranging from -14.83 cm^{-1} [CCSD(T)/d-aug-cc-pVDZ] to -22.34 cm^{-1} [CCSD(T)/CBS-corr] (the CCSDT corrections lower the well depth by just 0.32 cm^{-1}). For each of these surfaces the infrared spectrum up to dissociation has been accurately calculated. Table 3 shows the root-mean-square (RMS) errors with respect to experiment for all of the possible IR transitions (42 transitions between 28 bound ro-vibrational levels). It should be noted that several of these are very near the dissociation limit and hence provide a sensitive test of both the anisotropy and depth of the potential.

TABLE III: Errors in calculated infrared transitions for the ^{4}He-CO complex as a function of the CCSD(T) potential energy surface used (i.e., as a function of basis set). The values in parentheses are the total number of bound vibrational states present for that surface.

	DAVDZ	DAVTZ	DAVQZ	CBS	CBS-corr
	(14)	(22)	(28)	(28)	(28)
RMS error	0.15	0.17	0.09	0.04	0.03
Max. error	0.34	0.44	0.22	0.09	0.04

As can be observed in Table 3, even the d-aug-cc-pVTZ (DAVTZ) basis set does not result in a well depth that is sufficiently deep to bind all of the experimentally observed ro-vibrational levels. At the extrapolated CBS limit, the resulting RMS and maximum errors are very similar to those

obtained from the best previously reported surface, which was calculated using symmetry-adapted perturbation theory (SAPT).[35] Due to the systematics of the present work, however, the residual errors can clearly be attributed to inaccuracies correlation method, CCSD(T). After accounting for this in an approximate manner by scaling the CCSD(T) correlation energies based on a few benchmark CCSDT calculations, the resulting CBS-corr PES yields RMS and maximum errors that are nearly identical, only 0.03-0.04 cm^{-1}.

Acknowledgments

This work was supported by the Division of Chemical Sciences in the Office of Basis Energy Sciences of the U.S. DOE, as well as the National Science Foundation under a Career program award No. CHE-9501262. The author would particularly like to acknowledge the very productive collaborations that have made this work possible: Drs. Joel Bowman, David Dixon, Thom Dunning, Jr., David Feller, Bruce Garrett, Jacek Koput, George McBane, Steven Mielke, B. Ramachandran, Sergei Skokov, and David Woon.

---

[1] K. Jankowski, R. Becherer, P. S. Scharf, H. Schiffer, and R. Ahlrichs, J. Chem. Phys. **82**, 1413 (1985).
[2] J. Almlf and P. R. Taylor, J. Chem. Phys. **86**, 4070 (1987).
[3] T. H. Dunning, Jr., J. Chem. Phys. **90**, 1007 (1989).
[4] D. Feller, J. Chem. Phys. **96**, 6104 (1992).
[5] D. Feller, J. Chem. Phys. **98**, 7059 (1993).
[6] K. A. Peterson, D. E. Woon, and T. H. Dunning, Jr., J. Chem. Phys. **100**, 7410 (1994).
[7] D. A. Dixon, K. A. Peterson, and J. S. Francisco, J. Phys. Chem. A **104**, 6227 (2000).
[8] D. A. Dixon, W. A. de Jong, K. A. Peterson, and J. S. Francisco, J. Phys. Chem. A **106**, 4725 (2002).
[9] J. M. L. Martin and G. de Oliveira, J. Chem. Phys. **111**, 1843 (1999).
[10] A. Halkier, T. Helgaker, P. Jrgensen, W. Klopper, and J. Olsen, Chem. Phys. Lett. **302**, 437 (1999).
[11] W. Klopper, K. L. Bak, P. Jrgensen, J. Olsen, and T. Helgaker, J. Phys. B **32** , R103 (1999).
[12] T. Helgaker, W. Klopper, H. Koch, and J. Noga, J. Chem. Phys. **106**, 9639 (1997).
[13] D. Feller and K. A. Peterson, J. Chem. Phys. **110**, 8384 (1999).
[14] S. Skokov, K. A. Peterson, and J. M. Bowman, J. Chem. Phys. **109**, 2662 (1998).
[15] K. A. Peterson, S. Skokov, and J. M. Bowman, J. Chem. Phys. **111**, 7446 (1999).

[16] M. Bittererova, J. M. Bowman, and K. A. Peterson, J. Chem. Phys. **113**, 6186 (2000).
[17] K. A. Peterson, J. Chem. Phys. **113**, 4598 (2000).
[18] K. A. Peterson, B. A. Flowers, and J. S. Francisco, J. Chem. Phys. **115**, 7513 (2001).
[19] S. L. Mielke, B. C. Garrett, and K. A. Peterson, J. Chem. Phys. **116**, 4142, (2002).
[20] K. A. Peterson and J. Koput, in preparation, (2003).
[21] B. Ramachandran and K. A. Peterson, in preparation, (2003).
[22] K. A. Peterson and G. C. McBane, in preparation (2003).
[23] J. M. Bowman and B. Gazdy, J. Chem. Phys. **94**, 816 (1991).
[24] S. Skokov, J. Qi, J. M. Bowman, C.-Y. Yang, S. K. Gray, K. A. Peterson, and V. A. Mandelshtam, J. Chem. Phys. **109**, 10273 (1998).
[25] S. L. Mielke, B. C. Garrett, and K. A. Peterson, J. Chem. Phys. **111**, 3806 (1999).
[26] S. L. Mielke, K. A. Peterson, D. W. Schwenke, B. C. Garrett, D. G. Truhlar, J. V. Michael, M.-C. Su, and J. W. Sutherland, submitted (2003).
[27] K. A. Peterson, R. A. Kendall, and T. H. Dunning, Jr., J. Chem. Phys. **99**,9790 (1993).
[28] D. E. Woon, J. Chem. Phys. **100**, 2838 (1994).
[29] D. E. Woon and T. H. Dunning, Jr., J. Chem. Phys. **101**, 8877 (1994).
[30] T. van Mourik, T. H. Dunning, Jr., and K. A. Peterson, J. Phys. Chem. A **104**, 2287 (2000).
[31] F. Pawlowski, A. Halkier, P. Jrgensen, K. L. Bak, T. Helgaker, and W. Klopper, J. Chem. Phys. **118**, 2539 (2003).
[32] R. J. Gdanitz, J. Chem. Phys. **113**, 5145 (2000).
[33] D. E. Woon, K. A. Peterson, and T. H. Dunning, Jr., J. Chem. Phys. **109**, 2233 (1998).
[34] T.-S. Ho and H. Rabitz, J. Chem. Phys. **104**, 2584 (1996).
[35] T. G. Heijmen, R. Moszynski, P. E. S. Wormer, and A. van der Avoird, J. Chem. Phys. **107**, 9921 (1997).

A. Miani, J. Tennyson and T. van Mourik (eds.)
High Accuracy Potentials for Quantum Dynamics

Relativistic, Quantum Electrodynamic and Electroweak Effects in Molecules

H. M. Quiney

School of Chemistry, University of Melbourne,
Victoria 3010, Australia
quiney@unimelb.edu.au

I. INTRODUCTION

It is a tacit assumption of most quantum chemical investigations that relativistic and quantum electrodynamic effects are of little importance to molecular electronic structure determinations, particularly if only light elements are involved. Recent calculations have revealed, however, that the effects of special relativity play a significant role, along with the coupling of nuclear and electronic motion and core-valence correlation, in constructing accurate potential energy hypersurfaces to model the ro-vibrational spectrum of water. These investigations have evaluated the geometrical dependence of relativistic effects at both the Breit-Pauli [1] and Dirac-Hartree-Fock [2] levels of approximation, and have been extended to include leading-order quantum electrodynamical effects such as the Breit interaction [3] and estimates of the Lamb shift [4].

Of course the incidence of relativistic effects on electronic structures is most pronounced when heavy elements are involved. There are significant shifts in equilibrium geometries and spectroscopic constants caused by the interplay of several competing effects. The relativistic mass-velocity effect is mainly responsible for the radial contraction of s- and p-orbitals in heavy elements and a decrease in atomic radii, compared with non-relativistic estimates. Spin-orbit splitting of p-shells into $p_{1/2}$ and $p_{3/2}$ levels becomes increasingly important in heavy elements. The enhanced screening of the nuclear charge and the intrinsic centrifugal barrier results in a radial expansion of most d- and all f-orbitals. Many of these effects conspire to be a maximum for the coinage metals, and especially for gold, whose yellow colour in the metallic form and enhanced electron affinity in, for example CsAu, are often cited as dramatic manifestations of relativistic effects [5].

In atomic and molecular physics, the enhancement of relativistic, quantum electrodynamic and electroweak effects by strong Coulomb fields is exploited in *ab initio* investigations of fundamental processes. Recent experimental investigations into expected vibrational energy differences in the enantiomers of CHFClBr [6] has led to theoretical activity in mapping the potential energy hypersurfaces in substituted methanes using relativistic quantum chemical methods, in concert with more conventional methods for modelling many-body effects [7]. *Ab initio* relativistic quantum chemistry has also been employed in studies of effects beyond the Standard Model of the electroweak interaction, supporting interferometry studies involving the heavy diatomic systems TlF $^1\Sigma$ [8] and YbF $^2\Sigma$ [9].

II. METHODS TO CALCULATE RELATIVISTIC EFFECTS

A. Breit-Pauli equation

An authoritative source for the derivation of these operators by Pauli reduction of the Breit equation is the classic book by Bethe and Salpeter [10]. The operators may be divided into scalar spin-independent terms (H^0=Schrödinger operator; H^{MV}=mass-velocity; H^D=Darwin; H^{OO}=orbit-orbit) and spin-dependent interactions (H^{SO}=spin-orbit; H^{SoO}=Spin-other-Orbit and H^{SS}=spin-spin (which can be further divided into Fermi contact and dipole-dipole operators)).

Methods based on the Breit-Pauli scheme contain the spin-independent Schrödinger equation as the zero-order approximation, together with some (hopefully) "small" corrections. The scheme is supported in several standard quantum chemistry packages, can use existing correlated quantum chemistry methods with first-order perturbation theory for the relativistic effects, and yields satisfactory results for light elements. Against this must be weighed the need to include higher-order relativistic corrections for moderate and high values of Z, and the difficulties encountered because of the singular nature Breit-Pauli operators when used in higher-orders of perturbation theory.

B. Other two-component methods

The disadvantages inherent in the Breit-Pauli approach or the Foldy-Wouthuysen transformation [11] in its unmodified form may be avoided (and some of the advantages retained) by employing different partitionings of the pseudo-relativistic operators. The general strategy of these approaches is to

retain a wavefunction of non-relativistic form (using antisymmetric products of spin-orbitals) and to transfer all relativistic effects into a series of effective operators. Excluding methods based on relativistic pseudopotentials, the most significant and widely-employed methods in this category are (i) the "regular" approximations [12] (ii) the "direct perturbation theory" approach of Rutkowski [13] and Kutzelnigg [14] (iii) schemes devised by Hess and collaborators based on the Douglas-Kroll transformation [15] and (iv) a family of schemes formulated by Dyall [16] that include these approaches as limiting cases, designed around changes of metric or selective exclusion of effects.

The computational complexity of these approaches grows rapidly. A particular difficulty is that one must also transform electromagnetic interaction operators, leading to formidable difficulties introduced by condensing the four-component space of each electron onto a two-component space (change of picture) in evaluating molecular properties.

C. Dirac-Coulomb-Breit Hamiltonian

The direct use of relativistic quantum mechanics requires the use of a more complicated wavefunction constructed from antisymmetric products of spinors. Against this one may balance the use of simpler interactions, and greatly simplified treatment of electric and magnetic properties within QED. The Dirac-Coulomb-Breit hamiltonian, first introduced by Swirles [17] and subsequently used in second-quantized form, is

$$\begin{aligned} H_{DCB} &= \sum_i h_i + \sum_{i\rangle j} g_{ij} \\ h_i &= c\boldsymbol{\alpha}_i{\cdot}\mathbf{p}_i + \beta_i c^2 + \sum_K V_{iK} \\ g_{ij} &= \frac{1}{r_{ij}} + \frac{1}{2}\left(\frac{\boldsymbol{\alpha}_i{\cdot}\boldsymbol{\alpha}_j}{r_{ij}} + \frac{(\boldsymbol{\alpha}_i{\cdot}\mathbf{r}_{ij})(\boldsymbol{\alpha}_j{\cdot}\mathbf{r}_{ij})}{r_{ij}^3} \right) \end{aligned}$$

where h_i is the one-electron Dirac operator, and g_{ij} is the low-frequency form of the Coulomb-gauge two-body operator (instantaneous Coulomb + Breit interaction). V_{iK} is the electron-nucleus interaction, including finite nuclear size

The 4×4 Dirac matrices $\boldsymbol{\alpha}$ and β are derived from the Pauli spin matrices, and are used here in their standard form as defined in [10]. They are related to the Dirac γ-matrices through the relations $\boldsymbol{\alpha} = \gamma_0\boldsymbol{\gamma}$, $\beta = \gamma_0$, and $\gamma_0\gamma^0 = I$. The chirality matrix that appears later in the parity-violating interaction is denoted γ_5.

The relativistic wavefunctions are spinors, and the principal computational object is the charge-current four-vector, $j^\mu = (c\varrho, \mathbf{j})$. These are defined by

$$\psi_i(\mathbf{r}) = \begin{bmatrix} \psi_i^1(\mathbf{r}) \\ \psi_i^2(\mathbf{r}) \\ \psi_i^3(\mathbf{r}) \\ \psi_i^4(\mathbf{r}) \end{bmatrix} = \begin{bmatrix} \psi_i^L(\mathbf{r}) \\ \psi_i^S(\mathbf{r}) \end{bmatrix}, \quad \psi_i^\dagger(\mathbf{r}) = [\psi_i^{*1}(\mathbf{r})\ \psi_i^{*2}(\mathbf{r})\ \psi_i^{*3}(\mathbf{r})\ \psi_i^{*4}(\mathbf{r})]$$

$$\begin{array}{ll} \varrho_i(\mathbf{r}) = e\psi_i^\dagger(\mathbf{r})\psi_i(\mathbf{r}) & \textbf{Spinor charge density:} \\ \mathbf{j}_i(\mathbf{r}) = -ec\psi_i^\dagger(\mathbf{r})\boldsymbol{\alpha}_i\psi_i(\mathbf{r}) & \textbf{Spinor current density:} \\ \bar{\psi}_i(\mathbf{r}) = \mathcal{T}\psi_i(\mathbf{r}) & \textbf{Degenerate Kramers' pairs:} \end{array}$$

where $\mathcal{T}$ is the time-reversal operator, and $\langle\psi_i|\bar{\psi}_i\rangle = 0$.

Using the generalized four-vector densities, $j_{ij}^\mu = (c\varrho_{ij}, \mathbf{j}_{ij})$, where $\varrho_{ij}(\mathbf{r}) = \psi_i^\dagger(\mathbf{r})\psi_j(\mathbf{r})$ and $\mathbf{j}_{ij}(\mathbf{r}) = -c\psi_i^\dagger(\mathbf{r})\boldsymbol{\alpha}\psi_j(\mathbf{r})$, the two-body interaction matrix elements are

$$\begin{aligned} \left(ij\left|\frac{1}{r_{12}}\right|kl\right) &= \iint \varrho_{ij}(\mathbf{r}_1)\frac{1}{r_{12}}\varrho_{kl}(\mathbf{r}_2)d\mathbf{r}_1 d\mathbf{r}_2 \\ (ij|B_{12}|kl) &= \frac{1}{c^2}\iint\left(\frac{\mathbf{j}_{ij}(\mathbf{r}_1)\cdot\mathbf{j}_{kl}(\mathbf{r}_2)}{r_{12}} + \frac{(\mathbf{j}_{ij}(\mathbf{r}_1)\cdot\mathbf{r}_{12})(\mathbf{j}_{kl}(\mathbf{r}_2)\cdot\mathbf{r}_{12})}{r_{12}^3}\right)d\mathbf{r}_1 d\mathbf{r}_2. \end{aligned}$$

Note that in this form, the effective operators involved in calculations are no more complicated than $1/r_{12}$ and $x_{12}y_{12}/r_{12}^3$.

III. RELATIVISTIC QUANTUM CHEMISTRY: BERTHA

The description here is specific to BERTHA [18]. The program DIRAC [19] employs a scalar Gaussian basis set and performs quaternion transformation on a set of matrix representations to obtain the required structures.

A. Conventional integral-direct implementation

Basis sets to expand ψ_i^L and ψ_i^S must satisfy the one-to-one mapping $M[S,\mu;\mathbf{r}] \propto \boldsymbol{\sigma}\cdot\mathbf{p}M[L,\mu;\mathbf{r}]$ (strict kinetic balance). We choose the G-spinor

set

$$M[L,\mu;\mathbf{r}] = N_\mu^L \frac{1}{r_{A_\mu}} r_{A_\mu}^{\ell_\mu+1} \exp(-\lambda r_{A_\mu}^2) \chi_{\kappa_\mu,m_\mu}(\vartheta_{A_\mu},\varphi_{A_\mu})$$

$$M[S,\mu;\mathbf{r}] = iN_\mu^S \frac{1}{r_{A_\mu}} \left((\kappa_\mu+\ell_\mu+1) - 2\lambda_\mu r_{A_\mu}^2\right) r_{A_\mu}^{\ell_\mu} \exp(-\lambda r_{A_\mu}^2) \chi_{-\kappa_\mu,m_\mu}(\vartheta_{A_\mu},\varphi_{A_\mu})$$

$\mu \mapsto \{\kappa_\mu, m_\mu, A_\mu, \lambda_\mu\}$, and $\kappa_\mu \mapsto \{\ell_\mu, j_\mu, a_\mu\}$. The 2-component spin-angular functions $\chi_{\pm\kappa,m}(\vartheta,\varphi)$ are eigenfunctions of j^2, j_z, and the Lippman-Johnson operator, $K = -(1+2\boldsymbol{s}\cdot\boldsymbol{\ell})$. Determination of the basis spinors from mean-field equations is achieved by solution of a generalized matrix eigenvalue equation.

$$\mathbf{FC} = \mathbf{ESC}$$

Dirac-Hartree-Fock (DHF), Dirac-Hartree-Fock-Breit (DHFB) and Dirac-Kohn-Sham (DKS) equations [20], are solved using conventional Gaussian-based quantum-chemical methods and basis set parameters selected according to usual criteria [21].

All electronic structure integrals may be reduced to just two types of fundamental quantity:

$$M^\dagger[T,\mu;\mathbf{r}]\sigma_0 M[T,\nu;\mathbf{r}] = \sum_{ijk} E_{0,\mu\nu}^{TT;ijk} H(p,\mathbf{P};ijk)$$

$$M^\dagger[T,\mu;\mathbf{r}]\sigma_q M[\bar{T},\nu;\mathbf{r}] = \sum_{ijk} E_{q,\mu\nu}^{T\bar{T};ijk} H(p,\mathbf{P};ijk)$$

where $T = L$ or $T = S$, $\bar{T} \neq T$, $\sigma_0 = I$, σ_q (q=x,y,z) are Pauli spin matrices, and the sum over $\{i,j,k\}$ is finite. We refer to this as the relativistic McMurchie-Davidson algorithm [18]. The quantities $E_{Q,\mu\nu}^{TT';ijk}$ are the expansion coefficients of the auxiliary Hermite Gaussian functions, $H(p,\mathbf{P};i,j,k)$. The relativistic spinor structure is absorbed in the basis set, and the required Coulomb and Breit spatial integrals are evaluated analytically [23].

B. Mean-field equations based on electromagnetic energy density

The action-at-a-distance formulation that we always use is not well-suited to a relativistic Hamiltonian formulation because the interactions are always retarded.

"The use of the Hamiltonian forces one to chose the field viewpoint rather than the interaction viewpoint", R. P. Feynman, Phys. Rev, **76**, 769 (1949)

The interaction energy of two point charges, U, from the field and interaction viewpoints is

$$U = \epsilon_0 \int \mathbf{E}_1 \cdot \mathbf{E}_2 \; d\mathbf{r} = \frac{q_1 q_2}{4\pi\epsilon_0 r_{12}}$$

The generalization of this to Coulomb energy of interacting distributions is readily shown to be [22]

$$(ij|kl) \;=\; \frac{1}{4\pi} \int \mathbf{E}_{ij}(\mathbf{r}) \cdot \mathbf{E}_{kl}(\mathbf{r}) \, d\mathbf{r}, \quad \text{where} \quad \mathbf{E}_{ij}(\mathbf{r}) = -\nabla V_{ij}(\mathbf{r}),$$
$$V_{ij}(\mathbf{r}) = \iint \frac{\rho_{ij}(\mathbf{s})}{|\mathbf{r}-\mathbf{s}|} \, d\mathbf{s}.$$

leading to a new set of mean-field equations defined by

$$h_{\mu\nu} = \begin{cases} \left(\mu \left| \frac{1}{2m}\mathbf{p}^2 \right| \nu\right) & \text{Schrödinger} \\ \left(\mu \left| c\boldsymbol{\sigma}\cdot\mathbf{p} + \beta c^2 \right| \nu\right) & \text{Dirac} \end{cases}$$

$$F_{\mu\nu} = h_{\mu\nu} + \frac{1}{4\pi} \int \left\{ (\mathbf{E}_e + \mathbf{E}_N) \cdot \mathbf{E}_{\mu\nu} - \sum_a \mathbf{E}_{\mu a} \cdot \mathbf{E}_{a\nu} \right\} d\mathbf{r}$$

where $\mathbf{E}_e = \sum_a \mathbf{E}_{aa}$.

It is understood that the Schrödinger basis functions are spin-orbitals, the Dirac functions are two-spinors. The operator $\boldsymbol{\sigma}\cdot\mathbf{p}$ couples unlike (large- and small) components (odd operator), while β couples like components (even operator). The fields are evaluated using a combination of "exact" (McMurchie-Davidson) methods and multipole expansions. The integral is over field coordinates (*not particle coordinates*), and is performed using cellular quadrature methods adapted from DFT. The algorithm proves to be very well-suited for parallel execution, and eliminates most of the cost associated with the evaluation of two-electron integrals involving small-component basis functions.

The results are in complete agreement with those obtained in the interaction representation. This general approach may be extended to include the full relativistic transverse electron-electron interaction, terms that generate the frequency-dependent Breit interaction energy.

IV. PARITY VIOLATION IN CHIRAL SYSTEMS

The electroweak interaction introduces very small electronic energy differences between enantiometers:

$$H_{PV} = \frac{G_F}{2\sqrt{2}} \sum_{i,n} Q_{W,n} \gamma_i^5 \varrho_n(\mathbf{r}_i),$$

where $G_F = 2.22255 \times 10^{-14}$ a.u. is the Fermi coupling constant, $Q_{W,n} = -N_n + Z_n(1 - 4\sin^2\theta_W)$ is the electroweak charge, N_n is the number of neutrons, Z_n is the number of protons, θ_W is the Weinberg mixing angle, $\sin^2\theta_W = 0.2319$, $\varrho_n(\mathbf{r}_i)$ is the nuclear charge density, γ_i^5 is the pseudoscalar chirality operator for electron i, and the summation is over the electrons, i, and nuclei, n.

The electroweak parity violating energy, $E_{\rm PV}^G$ is calculated as

$$E_{\rm PV}^G = \langle \Psi_{\rm DHF}^G | H_{PV} | \Psi_{\rm DHF}^G \rangle = \frac{G_F}{2\sqrt{2}} \sum_n Q_{W,n} M_{\rm PV}^{G,n},$$

where,

$$M_{\rm PV}^{G,n} = \sum_i \langle \psi_i^G | \gamma_i^5 \varrho_n(\mathbf{r}_i) | \psi_i^G \rangle,$$

and the superscript G denotes dependence on nuclear geometry.

Attempts to detect the effects of H_{PV} in CHFClBr involve interferometry experiments [6] The R- and S-forms of a chiral molecule have slightly different vibrational frequencies. Given pure samples of the R- and S-systems, electroweak differences in a single vibrational mode may be investigated. The system is modelled by mapping the potential energy surface using relativistic quantum chemistry, expanding the mode-dependence as

$$E_{\rm PV}^G \simeq E_{\rm PV}^G\big|_{G_0} + \left.\frac{\partial E_{\rm PV}^G}{\partial Q_r}\right|_{G_0} Q_r + \frac{1}{2} \left.\frac{\partial^2 E_{\rm PV}^G}{\partial Q_r^2}\right|_{G_0} Q_r^2 + \cdots$$

The leading-order (harmonic) correction that causes an "in-principle" observable perturbation to the vibrational energy of mode $|n_r\rangle$ due to H_p is (for mode Q_r and effective reduced mass μ_r)

$$h\nu_{PV,r}^{\rm H} \simeq \left.\frac{\partial^2 E_{\rm PV}^R}{\partial Q_r^2}\right|_{R_0} \frac{\hbar}{2\mu_r \omega_r}.$$

The conclusions based on these calculations [7] are that the parity-violating effects in CHFClBr are currently unobservable for the C-F stretching frequency, which is the target transition in the experiments.

The more interesting outcome of the investigation is that one might be able to observe these effects in the C-Br stretching modes of chiral bromoiodomethanes, where they split the vibrational stretching modes by approximately 50Hz; this is now a detectable energy difference in interferometry experiments. Very recently parity violating electronic energies have been obtained for chiral molecules containing Bi, Re and Ir [24].

V. CALCULATION OF THE LAMB-SHIFT

Lamb-shift consists in leading order of two pieces, vacuum polarization (Uehling potential), and the electron self-energy, which requires some method of mass renormalization. Vacuum polarization energy is the renormalized sum of Coulomb integrals over vacuum states, and may be incorporated exactly within a short-range local modification of the Coulomb potential (Uehling potential).

We have devised relativistic methods for evaluating the renormalized self-energy, but these would be very demanding for molecular calculations [25]. Bethe's renormalized non-relativistic calculation for the low-energy ($k\langle k_{max}$) part of the self-energy is (in a.u.) [10]

$$\begin{aligned} E'_{a\langle} &= \frac{2}{3c}\frac{\alpha}{\pi}\int_0^{k_{max}} dk \sum_n \frac{(E_n - E_a)\langle\psi_a|\boldsymbol{\nabla}|\psi_n\rangle\langle\psi_n|\boldsymbol{\nabla}|\psi_a\rangle}{E_n - E_a + ck} \\ &= \frac{2}{3c^2}\frac{\alpha}{\pi}\sum_n \langle\psi_a|\boldsymbol{\nabla}|\psi_n\rangle\langle\psi_n|\boldsymbol{\nabla}|\psi_a\rangle \ln\left|\frac{E_n - E_a + ck_{max}}{|E_n - E_a|}\right| \end{aligned}$$

This is matched to the Feynman-Schwinger relativistic formulae for ($k\langle k_{max}$), $E_{a\rangle}$, the dependence on k_{max} is eliminated. The non-relativistic Lamb-shift can be estimated by rescaling the one-body Darwin operator, $(Z\pi/2c^2)\langle\delta\mathbf{r}\rangle$, or by fitting to the relativistic hydrogenic calculations of Mohr [4].

Here, we suggest a possible (and computationally feasible) refinement, based on our earlier investigations [26]:

Step 1: Calculate the modified k-dependent logarithmic sum-rule

$$E'_{a\langle} = \frac{2}{3c^2}\frac{\alpha}{\pi}\sum_n \langle\psi_a|\boldsymbol{\nabla}|\psi_n\rangle\langle\psi_n|\boldsymbol{\nabla}|\psi_a\rangle \ln\left|\frac{E_n - E_a + ck_{max}}{|E_n - E_a|}\right|$$

for selected, finite values of $k_{max} \simeq c$ using a large Gaussian basis set.

Step 2: Match this numerically to the analytic value of $E'_{a\rangle}$ (including vacuum polarization)

$$E'_{a\rangle} = \frac{4\pi}{3c^2}\frac{\alpha}{\pi}\left[\ln\frac{mc}{\lambda_{min}} - \ln 2 - \frac{3}{8} + \frac{5}{6} - \frac{1}{5}\right][\langle\delta(\mathbf{r})\rangle]$$

The modified Darwin correction is then used only in the high-energy region. Low-energy interactions are handled explicitly, and require only that $k_{max} \simeq 100$. Perform matching using $\ln 2k_{max} - 5/6 = \ln \lambda_{min}$, noting carefully the comments in [27].

Acknowledgments

I gratefully acknowledge many fruitful years of collaboration with Ian Grant and Haakon Skaane (Oxford) and Stephen Wilson (DRAL), and more recent collaborations with Paola Belanzoni and Antonio Sgamellotti (Perugia), Jon Laerdahl (Oslo and Auckland) and Peter Schwerdfeger (Auckland), Knut Fægri jr and Trond Saue (Oslo) Jonathan Tennyson, Paolo Barletta, Oleg Polyansky (UCL) and Attila Császár and György Tarczay (Budapest). This research has been supported by the Australian Research Council, the Victorian Partnership for Advanced Computing, CNR (Italia), The University of Melbourne, and Wadham College, Oxford.

---

[1] A. G. Császár, J. S. Kain, O. L. Polyansky, N. F. Zobov, J. Tennyson, Chem. Phys. Lett., **293**, 317 (1998); **312**, 613 (1998).

[2] H. M. Quiney, H. Skaane, I. P. Grant, Chem. Phys. Lett., **290**, 473 (1998).

[3] G. Tarczay, A. G. Császár, W. Klopper, H. M. Quiney, Mol. Phys., **99**, 1769 (2001); H. M. Quiney, P. Barletta, G. Tarczay, A. G. Császár, O. L. Polyansky, J. Tennyson, Chem. Phys. Lett., **344**, 413 (2001).

[4] P. Pyykkö, K. G. Dyall, A. G. Császár, G. Tarczay, O. L. Polyansky, J. Tennyson, Phys. Rev. A, **63** 024502 (2001).

[5] P. Pyykkö, Ang. Chem. Int. Ed., **41**, 3573 (2003).

[6] Ch Daussy, T. Marrel, A. Amy-Klein, C. T. Nguyen, Ch. J. Bordé, Ch. Chardonnet, Phys. Rev. Lett., **83**, 1554 (1999).

[7] J. K Laerdahl, P. Schwerdtfeger, Phys. Rev. A **60**, 4439 (1999); J. K Laerdahl, P. Schwerdtfeger, H. M. Quiney, Phys. Rev. Lett, **84**, 3811 (2000), J. Thyssen, J. K Laerdahl, P. Schwerdtfeger, Phys. Rev. Lett., **84**, 3811 (2000).

[8] J. K Laerdahl, T. Saue, K. Fægri jr., H. M. Quiney, **79**, 1642 (1997); H. M. Quiney, J. K Laerdahl, K. Fægri jr., Phys. Rev. A **57** 920 (1998).

[9] H. M. Quiney, H. Skaane and I. P. Grant, J. Phys. B. :Atom. Molec. Opt. Phys., **31**, L85 (1998).

[10] H. A. Bethe, and E. E. Salpeter, Quantum mechanics of one- and two-electron systems, Springer-Verlag, Berlin-Göttingen-Heidelberg (1957).

[11] L. L. Foldy and S. Wouthuysen, *Phys. Rev.* **78**, 29 (1950).

[12] Ch. Chang, M. Pellisier, Ph. Durand, Phys. Scripta, **34**, 394 (1986); E. van Lenthe, E. J., Baerends, and J. G. Snijders, *J. Chem. Phys.*, **99**, 4597 (1993).

[13] A. Rutkowski, *J. Phys. B*, **19**, 149 (1986); A. Rutkowski,*J. Phys. B*, **19**, 3431 (1986); A. Rutkowski, *J. Phys. B*, **19**, 3443 (1986).

[14] W. Kutzelnigg, *Phys. Rev. A*, **54**, 1183 (1996).
[15] B. A. Hess, *Phys. Rev. A*, **32**, 756 (1985); B. A. Hess, *Phys. Rev. A*, **33**, 3742 (1986).
[16] K. G. Dyall, *J. Chem. Phys.*, **106**, 9618 (1996); K. G. Dyall, *J. Chem. Phys.*, **109**, 4201 (1997).
[17] B. Swirles, *Proc. Royal Soc. (London) Series A*, **152**, 625 (1935).
[18] H. M. Quiney, H. Skaane and I. P. Grant, Adv. Quant. Chem., **32**, 1–49 (1999); I. P. Grant and H. M. Quiney, Int. J. Quantum Chem., **80**, 283 (2000).
[19] T. Saue, K. Fægri jr, T. Helgaker and O. Gropen, *Mol. Phys.*, **91**, 937 (1997).
[20] I. P. Grant and H. M. Quiney, in "Relativistic Electronic Structure Theory", ed. P. Schwerdtfeger , pp107-202, Elsevier Amsterdam (2002).
[21] K. Fægri and K. G. Dyall, in "Relativistic Electronic Structure Theory", ed. P. Schwerdtfeger, pp259-290, Elsevier Amsterdam (2002).
[22] J. C. Slater, Quantum Theory of Atomic Structure: I, pp 486-487 McGraw-Hill New York (1960); R. P. Feynman, R. Leighton, M. Sands, Lectures on Physics: II, Chapter 19, Addison-Wesley Massachusetts (1964).
[23] H. M. Quiney, in Handbook of Molecular Physics and Quantum Chemistry, vol 2, pp696-716, ed S. Wilson, John Wiley and Sons, Chichester (2003).
[24] P. Schwerdtfeger, J. Gierlich and T. Bollwein, Ang. Chem. Int Ed., **42**, 1293 (2003).
[25] H. M. Quiney and I. P. Grant, J Phys. B: At. Mol. Opt. Phys., **27**, L199 (1994).
[26] H. M. Quiney, in The Effects of Relativity in Atoms, Molecules and the Solid State, eds S. Wilson, I. P. Grant, B. Gyorffy, pp 83-123, Plenum Press, New York (1991).
[27] J. B. French and V. Weisskopf, Phys. Rev., **75**, 1240 (1949); R. P. Feynman, Phys. Rev., **76**, 749 (1949); R. P. Feynman, Phys. Rev., **76**, 769 (1949).

A. Miani, J. Tennyson and T. van Mourik (eds.)
High Accuracy Potentials for Quantum Dynamics

The Role of Born-Oppenheimer Breakdown Terms in the Prediction of Accurate Transition Frequencies for Ordinary Molecules

David W. Schwenke

Mail Stop T27B-1 NASA Ames Research Center Moffett Field, CA 94035-1000, USA

When one thinks of the breakdown of the Born-Oppenheimer approximation (BOA), the picture of catastrophic failure in the vicinity of nearly degenerate potential energy curves probably comes to mind. For the ground electronic states of the ordinary molecules we consider in the present work, H_2^+, H_2, H_2O, and CO, there are no electronic states nearly degenerate with the ground state in the vicinity of the potential minimum, thus text book arguments would indicate that the BOA would be exceedingly accurate. Now all approximations eventually break down, thus the pertinent question is whether or not corrections to the BOA are required in practical calculations. In this work we show that at the 1 cm^{-1} level, these corrections are important even for ordinary molecules.

We consider three levels of refinement:

0: The Born-Oppenheimer approximation [1] - set the nuclear masses to ∞ when solving the electronic Schrödinger equation (SE) to obtain the electronic wavefunctions and eigenvalues, then reset the nuclear masses and solve the nuclear SE with the nuclei moving on the potential energy surface (PES) which is the geometry dependence of the electronic eigenvalue.

1: The adiabatic or Born-Huang approximation [2] - follow the same procedure as above, except the PES is the expectation value of the full Hamiltation operator computed using the Born-Oppenheimer electronic wavefunction.

2: Full electron-nuclear coupling. Compared to the BOA, the Born-Huang approximation (BHA) differs by the addition of a nuclear mass dependent term to the PES, the Born-Oppenheimer diagonal correction (BODC),

but the solution of the nuclear SE is exactly the same. In contrast, the accurate introduction of full electron-nuclear coupling is much more difficult, and has been done only for the one electron molecule H_2^+.[3] Fortunately, since the BOA is quite accurate, the problem of electron-nuclear coupling can be treated reliably with perturbation theory. The work of Bunker and Moss[4] (BM) shows formally how this can be done, and in their theory the first order correction to the BOA is the BODC, while a second order correction is required to mix in other electronic wavefucntions. The non-adiabatic, or second order correction is more complicated than the BODC in that additional derivative terms are introduced into the nuclear SE. Nonetheless, the solution of the nuclear SE including the second order correction is not significately more expensive than when making the BOA.

In spite of the formal development, it is surprising that more than 20 years elapsed before the BM formalism was implemented in an *ab initio* calculation.[5] In that work we compared the results of the BM method to accurate calculations for H_2^+ [3] and HD^+.[6] The agreement was very good: the root-mean-square (rms) difference between our calculations of ro-vibrational energy levels and the accurate results was only 0.0006 cm-1 for H_2^+. This meant we computed the non-adiabatic correction to an accuracy of about 1 part in 10^3. For HD^+, the agreement was similar except near the dissociation limit where some interesting non-adiabatic effects took place, leading to the breakdown of the perturbation expansion. Nonetheless , this work paved the way for the reliable prediction of non-adiabatic effects for systems with more than one electron.

When applying the BM formalism, one has two choices to make, firstly how accurately to represent the ground electronic state, and secondly, how to represent the excited electronic states. For the H_2^+ molecule, there is only one electron, thus one can relatively easily achieve high accuracy for the ground electronic state. For excited electronic states, the situation is more complex, because continuum electronic states contribute. Our strategy for H_2^+ was to expand the ground electronic state wavefunction in terms of nuclear centered gaussian basis functions, then compute the excited electronic states as higher eigenvalues of the electronic Hamiltonian in that basis. We tested that this procedure converged with respect to using larger basis sets, and the results indicated that the continuum states are adequately represented.[5] We next turned to the H_2 molecule.[7] As with the H_2^+ molecule, very accurate BOA PES and BODC are available, and Wolniewicz [8] has computed non-adiabatic corrections using an alternate perturbation theory. However that theory is not easily extended to more complicated molecules, in contrast to the BM formalism. We first computed the BODC using the self consistent field method (SCF), the

simplest *ab initio* wavefunction, and found that it was not even in qualitative agreement with accurate results. Using the two orbital complete active space SCF which gives proper dissociation to generate the ground state electronic wavefunction, and then using this wavefunction to compute the BODC gave much improved results, however the agreement with accurate results was still not quantitative. To obtain quantitative results for the BODC it is necessary to use accurate electronic wavefunctions. In our accurate work, we compute the BODC from internally contracted multi-reference configuration interaction (icMRCI) wavefunctions obtained from a modified version of MOLPRO 2000.1.[9].

For the second order correction for H_2, we also started with the simplest *ab initio* treatment, namely we used an SCF wavefunction for the ground electronic state, and for excited states, we only considered single excitations out of the SCF wavefunction. We call this the SCF/CIS method. However, in contrast to the case with the BODC, we found that the SCF/CIS method gave quite reasonable results for vibrational levels all the way up to the dissociation limit. For low lying vibrational levels, scaling the non-adiabatic correction function obtained from the SCF/CIS method by 1.1 gave results of great accuracy. This factor of 1.1 is very similar to the amount the electronic contribution to the rotational g factor is underestimated, thus our model for the non-adiabatic corrections is to compute the non-adiabatic correction functions by the SCF/CIS method, then scale them by the factor required to bring the computed rotational g factor into agreement with the experimental value.

We now turn to H_2O.[10] Here we are primarily interested in the question of accurately predicting vibrational frequencies for isotopically substituted water. This provides a very stringent test, for the BODC brings explicit mass dependence to the PES and the non-adiabatic correction brings additional mass dependence to the derivative operators in the nuclear SE. In these calculations, we re-optimized our PES for the principle isotopomer of water now including the non-adiabatic correction. This PES is called V_{nemp}, as compared to V_{emp},[11] which was our original refined PES. We then carried out calculations for HDO, HTO, D_2O, and T_2O using V_{emp} + our accurate BODC, not including non-adiabatic effects, V_{nemp} + our accurate BODC including non-adiabatic effects, and V_emp + our empirical mass dependence, [11] which was optimized to simultaneously fit experimental data for HDO and D_2O. We find that both the BODC and non-adiabatic corrections are significant at the 1 cm^{-1} level, and when both are included, they give results of equal accuracy as the empirical mass dependent PES for fundamental vibrations. However this *ab initio* correction should be much more accurate than the empirical one for higher overtones.

We finally consider the CO molecule, or rather the isoelectronic sequence CO, N_2, and NO^+. Here we are interested in making very accurate *ab initio*

predictions of vibrational energy levels. We write our PES as

$$V = V_{TZ}^{CORR} + \Delta V^{Basis} + \Delta V^{CV} + \Delta V^{Rel} \quad (1)$$

where ΔV_{TZ}^{CORR} is the result of either a CCSD(T) calculation, an icMRCI calculation, an icMRCI+Q calculation, or an ACPF calculation using the cc-pVTZ basis,[12] and the remaining terms are corrections.
The term ΔV^{Basis} is computed as the difference between CCSD(T) computed using an infinite basis and CCSD(T) computed using the cc-pVTZ basis. The infinite basis results are obtained by decomposing the energy into the SCF energy, the singlet pair contribution to the CCSD energy, the triplet pair contribution to the CCSD energy, and the (T) energy, and extrapolating the results of cc-pVXZ basis sets with extrapolation coefficients determined from comparisons to accurate calculations.[13, 14]
The next term, ΔV^{CV} accounts for the error incurred by not correlating the core electrons. This is determined as the difference between a CCSD(T) calculation correlating all electrons and a CCSD(T) calculation correlating only the valence electrons. The calculations are carried out using the cc-pCVXZ basis sets, [15] and the results are extrapolated to the basis set limit with extrapolation coefficients determined from comparisons to accurate calculations.[13, 14]

The final term, ΔV^{Rel}, includes corrections due to the finite speed of light. This includes scalar relativity computed as the difference between a CCSD(T) calculation using the Douglas-Kroll-Hess method [16, 17] using the appropriately re-contracted cc-pVTZ basis and the non-relativistic CCSD(T) calculation using the cc-pVTZ basis. Also included is the Lamb shift[18] computed at the icMRCI level using the cc-pVTZ basis.

To this PES we add the accurate BODC and solve the nuclear SE including non-adiabatic effects.

Our results indicate that the icMRCI+Q method is the most reliable for treating electron correlation, as this method gives the best systematic agreement with experimental values for the isoelectronic sequence CO, N_2, and NO^+. The errors are all much less than 1 cm$-$1 , and both the BODC and non-adiabatic corrections are significant, with the non-adiabatic correction being much larger. This is contrary to ones expectations based on text book arguments that the accuracy of the BOA is primarily dependent on the ratio of the nuclear to electron mass. One clearly sees from the structure of the correction functions in the BM formalism that that is only one factor. Another is the relative density of electronic states. Due to the complex electronic structure arising from the triple bound in these molecules, the density of electronic states is very high and

hence the non-adiabatic correction is significant.

---

[1] M. Born and J.R. Oppenheimer, Ann. Phys. (Leipzig) **84**, 457 (1927).
[2] M. Born, Nackr. Akad. Wiss. Gttingen 1, (1951); M. Born and K. Huang, "Dynamical Theory of Crystal Lattices" (Oxford University Press, New York, 1956)
[3] R. E. Moss, Mol. Phys. **80**, 1541 (1993).
[4] P. R. Bunker and R. E. Moss, Mol. Phys. **33**, 417 (1977).
[5] D. W. Schwenke, J. Chem. Phys. **114**, 1693 (2001).
[6] R. E. Moss, Mol. Phys. **78**, 371 (1993).
[7] D. W. Schwenke, J. Phys. Chem. A **105**, 2352 (2001).
[8] L. Wolniewicz, J. Chem. Phys. **78**,673 (1983).
[9] MOLPRO is a package of ab initio programs written by H.-J. Werner and P. J. Knowles, with contributions from J. Almlf, R. D. Amos, A. Berning, D. L. Cooper, M. J. O. Deegan, A. J. Dobby, F. Eckert, S. T. Elbert, C. Hampel, R. Lindh, A. W. Lloyd, W. Meyer, A. Nicklass, K. Peterson, R. Pitzer, A. J. Stone, P. R. Taylor, M. E. Mura, P. Pular, M. Schitz, H. Stoll, and T. Thorsteinsson.
[10] D. W. Schwenke, J. Chem. Phys. **118**, 6898 (2003).
[11] H. Partridge and D. W. Schwenke, J. Chem. Phys. **106**, 4618 (1997).
[12] T. Dunning, J. Chem. Phys. **90**, 1007 (1989).
[13] W. Klopper, Mol. Phys. **99**, 481 (2001).
[14] D. W. Schwenke, to be published.
[15] D. E. Woon and T. H. Dunning, J. Chem. Phys. **103**, 4572 (1995).
[16] M. Douglas and N. M. Kroll, Ann. Phys. **89**, 82 (1974).
[17] B. A. Hess, Phys. Rev. A **32**, 756 (1985); G. Jansen, B.A. Hess, Phys. Rev. A **39**, 6016 (1989)
[18] P. Pyykkö, K. G. Dyall, A. G. Császár, G. Tarczay, O. L. Polyansky, and J. Tennyson, Phys. Ref. A **63**, 24502 (2001).

A. Miani, J. Tennyson and T. van Mourik (eds.)
High Accuracy Potentials for Quantum Dynamics

The Asymptotic Regions of the Potential Energy Surfaces Relevant for the $O(^3P) + O_2(X^3\Sigma_g^-) \rightleftharpoons O_3$ and $O(^3P) + OH(X^2\Pi) \rightleftharpoons O_2(X^3\Sigma_g^-) + H(^2S)$ Reactions

Claire Gillery and Pavel Rosmus

Laboratoire de Chimie Théorique, Université Marne-la-Vallée
F-77454 Champs-sur-Marne, France

The potential energy functions and the spin-orbit couplings for all states of ozone correlating with the lowest $O(^3P) + O_2(X^3\Sigma_g^-)$ asymptote have been calculated in the asymptotic region employing correlated electronic wavefunctions and valence coordinates [1]. For linear ozone, the $^s\Sigma$ states ($s = 1, 3$, and 5) lie above the corresponding $^s\Pi$ states (Figure 1).

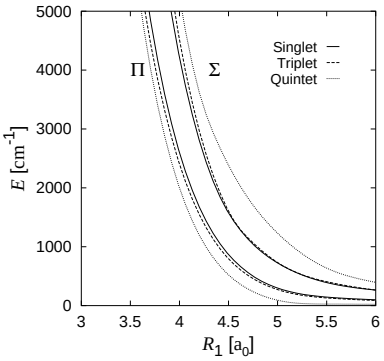

FIG. 1: One-dimensional potential cuts for linear ozone relative to the supramolecule energy of the $^1\Pi$ state at $R_1 = 10\ a_0$ ($R_2 = 2.288\ a_0$), MRCI + Davidson correction.

For bent geometries the Π states split into Renner-Teller components with A' and A'' symmetry, respectively. While the $^3\Pi$ and $^1\Pi$ states lead to bent-bent Renner-Teller pairs, the $^5\Pi$ state gives rise to a linear/linear pair of states. The different Π spin multiplets cross for valence angles around 160° and the $^1A'$ component becomes the lowest one (Figure 2).

For intermediate $O - O_2$ distances the preferential path for the formation of singlet ozone in its open structure goes through bond angles between 110°

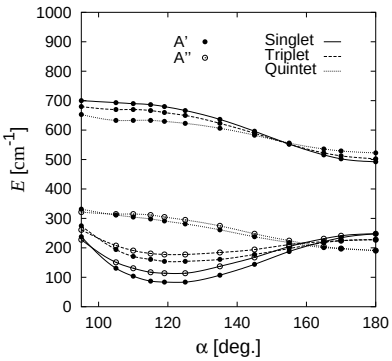

FIG. 2: Angular dependence of the nine lowest potential energy surfaces of ozone ($R_1 = 5.2\ a_0$, $R_2 = 2.288\ a_0$) obtained from full valence CASSCF calculations.

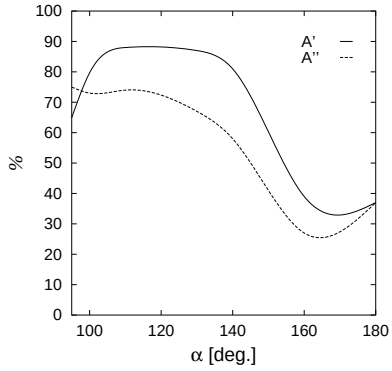

FIG. 3: Percentage of the $S = S_z = 0$ spin components of the eigenfunctions after diagonalization of the spin-orbit matrix for the 27 spin states correlating with the lowest dissociation asymptote as a function of the valence angle for the $^1A'$ and $^1A''$ components of the $^1\Pi$ state ($R_1 = 4.9\ a_0$ and $R_2 = 2.288\ a_0$)

to 130° where the potentials of the singlet and triplet Renner-Teller pairs are minimal. The matrix elements of the spin-orbit operator have also been calculated. They are dominated by the atomic ^3P contributions and their dependence on the mutual orientation of the O_2 molecule and the O atom is small. In the regions where the states correlating to the linear $^{1,3,5}\Pi$ cross, i.e. for valence angles between 150° and 180°, and close to 90° the mixing among the singlet, triplet, and quintet states is strong and the electron spin quantum

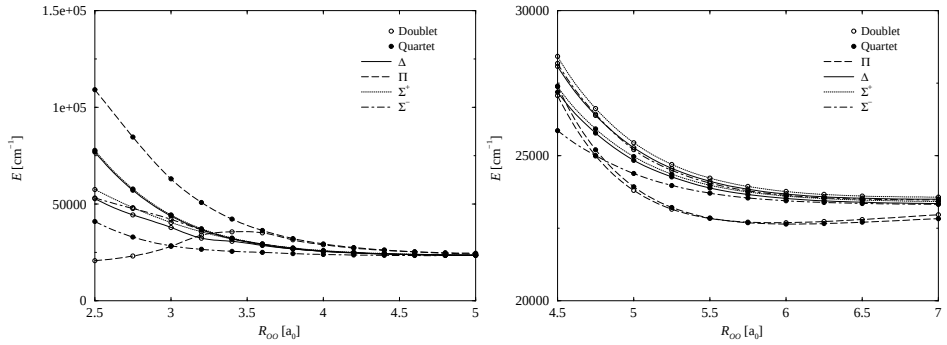

FIG. 4: One-dimensional potential cuts for linear OOH and OHO relative to the equilibrium energy of the X^2A" state for $R_{OH} = 1.835\ a_0$, MRCI + Davidson correction.

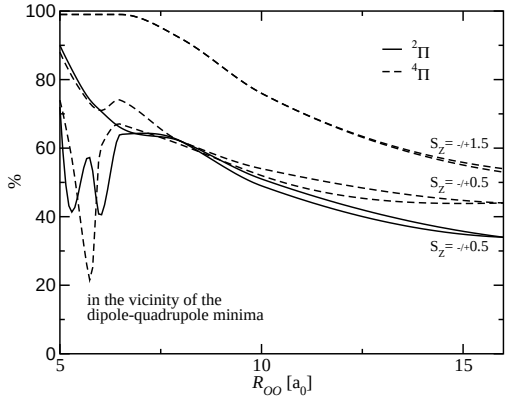

FIG. 5: Percentage of the $S_z = 0.5$ and 1.5 of the Π states spin components of the eigenfunctions of the spin-orbit matrix as a function of the OO distance in the OHO structure, with $R_{OH} = 1.835\ a_0$, CASSCF.

number is no longer a good quantum number(Figure 3).

The potential energy functions and the spin-orbit couplings for all states correlating with the lowest asymptotes of the $O(^3P) + OH(X^2\Pi) \rightleftharpoons O_2(X^3\Sigma_g^-) + H(^2S)$ reaction have been calculated in the asymptotic regions employing similar approach as for ozone. The starting point of our study was the

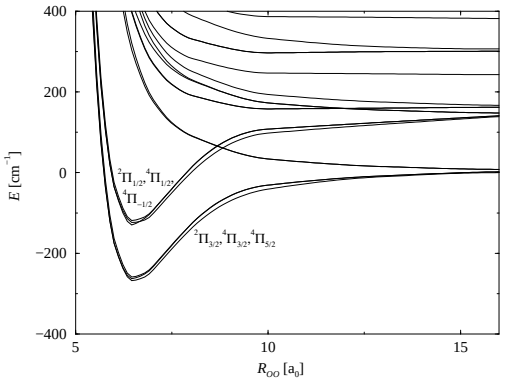

FIG. 6: 18 CASSCF adiabatic potential energy surfaces obtained from the diagonalisation of the spin-orbit matrix for the 36 spin states correlating with the lowest dissociation asymptote OH + O as a function of the OO distance, with R_{OH} = 1.835 a_0.

treatment of all states resulting from the O(^3P) + OH($X^2\Pi$) asymptote (s = 2,4; $^s\Sigma^+$,$^s\Sigma^-$,$^s\Pi$,$^s\Delta$) for any orientation of the atom and diatom. In the most recent works only the lowest energy path for the formation of OOH has been reported [2,3].

The bent X^2A" and A^2A' states of OOH can correlate at linearity with the doublets of Σ^+, Σ^-, Π and Δ symmetry. In contrast to the bond formation regions, the A^2A' and X^2A" states for near equilibrium OH and OO distances correlate at linearity with a $^2\Pi$ state. The corresponding MRCI barrier to linearity has been calculated to lie only about 2800 cm^{-1} below the O + OH asymptote calculated at 23400 cm^{-1}. In Figure 4 (left) the potential energy surfaces for collinear approach O...OH are shown. For long OO distances the lowest state is $^4\Sigma^-$. Both Renner-Teller bent/bent components of the $^2\Delta$ state cross around R_{OO} = 4.2 a_0 and an apex angle of 140^o this quartet state, and for R_{OO} between 3.2 and 3.3 a_0 the $^2\Delta$ state components cross the $^2\Pi$ state leading to the two lowest bent electronic states of OOH. For the other collinear orientation OH...O the lowest states are $^{2,4}\Pi$, which are energetically well separated from the remaining 6 electronic states (Figure 4, right). In the region of the linear dipole-quadrupole minima the quartet and doublet Π states lie very close in energy and cross between R_{OO} = 5.5 and 5.8 a_0. Figure 5 shows that in the van der Waals minima the mixing of the spin states renders the assignment with the electron spin quantum numbers impossible. In the Figure 6 the CASSCF adiabatic potential energy surfaces for the collinear OH...O

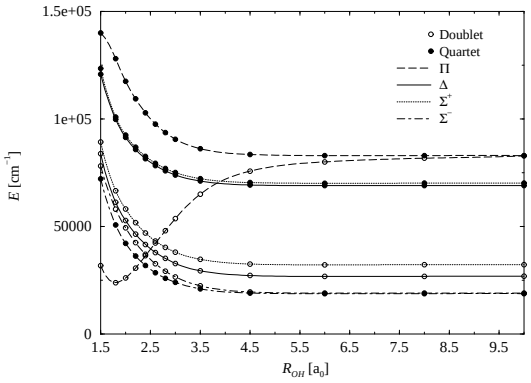

FIG. 7: One-dimensional potential cuts for linear OOH relative to the equilibrium energy of the $X^2A"$ state for $R_{OO} = 2.283\ a_0$, MRCI + Davidson correction.

approach for 18 (each of the 36 states is doubly degenerate, some of the states lie very close together and are not distinguishable in the drawing) spin-orbit coupled states are displayed.

Previously, this long range part of the surfaces has been studied by employing the dipole-quadrupole potential expansion[4], i.e. the region of the van der Waals minima could not be treated. The present results show that six states of $(^{2,4}\Pi)$ possesses a dipole-qudrupole OH..O van der Waals minimum, the second group of states has repulsive potentials. The $^{2,4}\Pi$ states form linear/linear Renner-Teller pairs.

For the collinear approach O_2...H (Figure 7) the lowest state is $^4\Sigma^-$ which crosses the $^2\Pi$ for R_{OH} of about 2.4 a_0. The same electronic states treated for the other asymptote now correlate with other electronic states of the oxygen molecule. The dissociation energy for the lowest O_2 + H asymptote has been calculated to be 18800 cm^{-1}. The $^2\Pi$ for the orientation OOH is a bent/bent, for the OHO orientation a linear/linear Renner-Teller case. The $^2\Delta$ state for OOH forms a linear/bent and OHO bent/bent pairs.

As shown in this brief note vibronic and complicated angular momenta coupling effects are of crucial importance for the dynamics of the O_2 + O, O + OH and

O_2 + H atmospheric reactions.

---

[1] P. Rosmus, P. Palmieri and R. Schinke, *J. Chem. Phys.*, **117**, 4871 (2002) (cf. references therein).

[2] L. B. Harding, A.I. Maergoiz, J. Troe and V.G. Ushakov, *J. Chem. Phys.* **113**, 11019 (2000) (cf. references therein).

[3] L.B. Harding, J. Troe and V.G. Ushakov, *Phys. Chem. Chem. Phys.* **2**, 631 (2000).

[4] M.M. Graff and A.F. Wagner, *J. Chem. Phys.* **92**, 2423 (1990).

A. Miani, J. Tennyson and T. van Mourik (eds.)
High Accuracy Potentials for Quantum Dynamics

Two Exothermic Reactions in the "Lithium Chemistry" Network: $LiH + H \rightarrow Li + H_2$ and $LiH^+ + H \rightarrow Li^+ + H_2$. A Comparison of Computed Potential Energy Surfaces.

E. Bodo, R. Martinazzo† and F. A. Gianturco

Department of Chemistry, University "La Sapienza", P.le A. Moro 5, 00185 Rome, Italy
†*Department of Physical Chemistry and Electrochemistry, CNR Center CSRSRC, V. Golgi 19, 20133 Milan, Italy.*

The two typical alkali-hydrogen processes given by

$$LiH(X^1\Sigma^+) + H(^2S) \rightarrow Li(^2S) + H_2(X^1\Sigma^+) \quad (1)$$
$$LiH^+(X^2\Sigma^+) + H(^2S) \rightarrow Li^+(^1S) + H_2(X^1\Sigma^+) \quad (2)$$

are important reactions for the modeling of the lithium chemistry in the primordial Universe[1], but only recently high quality ab-initio calculations of the full 3D interaction potential have been produced. The two Potential Energy Surfaces (PES's) for the reactions are very similar and show highly exothermic profiles. The main difference is that while in 1 the LiH molecule is strongly bound, in 2 the LiH^+ moiety has a much smaller binding energy. Furthermore, the ionic interaction extends over a larger region of coordinate space in comparison to its neutral counterpart. A simple pictorial view of the topological properties of the two types of reactive interactions could be obtained by looking at the two collinear cuts of the surfaces reported in fig.1 where the two PES's are plotted in 3D for two different orientational views and where the energy of $Li + H + H$ break-up pieces has been chosen to be the zero of the energy scales (coordinates in Å and energies in eV). The upper ionic surface originates from our analytical fitting of the data computed in Refs. [2, 3], while the lower neutral one comes from the fitting of the CI calculations reported by Ref. [4]. The analytical fitting for the ionic system uses Aguado-Paniagua (AG) type functions to fit the 3-body contribution to the ab-initio energy computed in 11,341 different geometries. Since the charge is mainly localized on the Li atom, the 3-body interaction was calculated by subtracting the energies of two isolated LiH^+ and that of H_2. Since the AG functions die exponentially at long range while in a ionic system the main contribution to

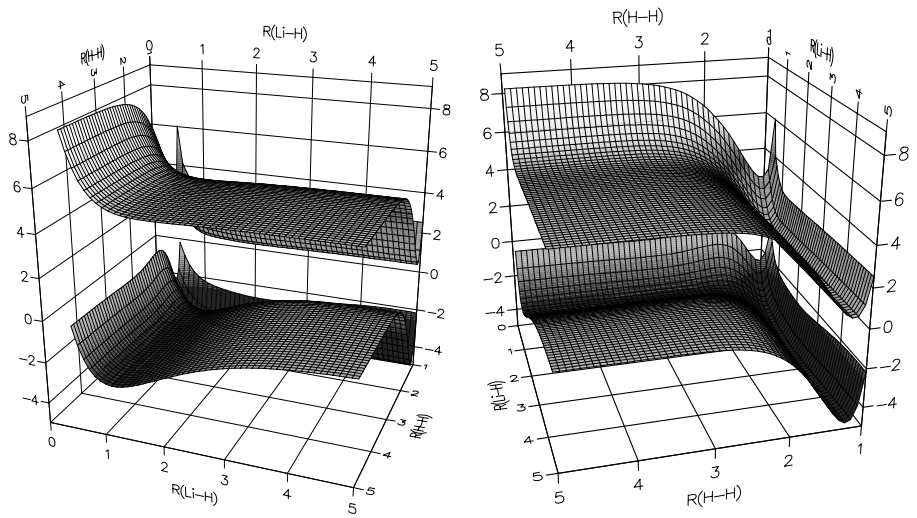

FIG. 1: Two different orientation views for the LiH + H and LiH^++H reactions

the long range 3-body potential comes from electrostatic interactions (charge-polarizability and quadrupole-charge in this case), a non-linear optimization procedure was employed to determine a switching function which smoothly joined the long range analytic expression (a simple multipolar expansion) to the AG functions.

Although the two potential energy surfaces turn out to be very similar, one expects the dynamical behavior of the initial LiH/LiH^+ partner to be extremely different, at least for what we know from the studies performed so far: classical trajectories and quantum wavepacket dynamics, the latter only for collinear geometries. As it was suggested before, most of the differences in the two PES shapes occur in the entrance channel that appears as a flat energy region in the case of the ionic surface. It is the difference between the two entrance channels that affects the dynamical behavior of the two systems, as we shall show more in detail below. The minimum energy paths for different approaching angles (defined by the small inset at the top of the left panel in the figure) are reported in fig. 2. For each of the two panels the reference level of the potentials has been taken at the bottom of the outgoing valley of the products. Reaction

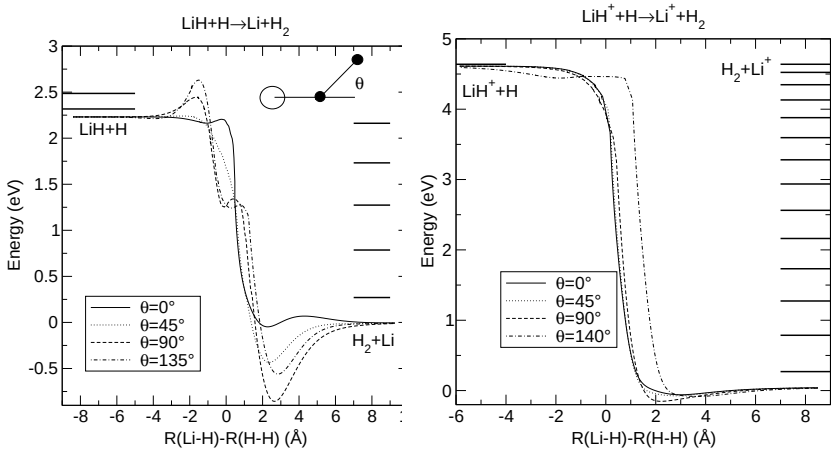

FIG. 2: Minimum energy paths for different approaching angles

2 shows a higher exothermicity (4.5 eV) as it is to be expected for an ionic reaction. Moreover it seems not hindered by any activation barrier even when the approaching angle moves away from the collinear shape. On the other hand the neutral reaction paths show the appearance of an activation barrier of $\sim 11\,\mathrm{kcal}\cdot\mathrm{mol}^{-1}$ for $\theta = 90$. Another marked difference between the two surfaces is the presence, for the neutral system, of a significant well in the outgoing product channel that is clearly visible at all angles, with the exclusion of $\theta = 0$. The smaller well that can also be seen in the H_2 channel of the ionic reaction, as mentioned above, is due there to the electrostatic interaction between the quadrupole of H_2 and the Li^+ charge.

A first attempt at modeling the reactive dynamics of 1 has been carried out some time ago by Clarke et al. [5] using a collinear Spin Coupled Valence Bond (VB) calculation. The VB surface in the collinear arrangement is very similar to the newest one of Ref. [4] although the more recent results show no barrier unless the angle is larger than 75 degrees. Classical and time dependent quantum wavepacket dynamics has been explored for collinear geometries and the relevant results can be summarized as follows: the two sets of results, classical and quantum, are in good agreement in the energy range considered. For all the initial vibrational states the probability increases sharply at the low energy, reaching its maximum around 0.2 eV. With a further increase in the collision energy the reaction probability shows a slow monotonic increase which remains smaller for higher ν states. Below 0.1 eV both calculations show oscillations probably due to resonances. An additional important feature is

that the vibrational energy content of the initial LiH has a very small effect on the reaction probabilities. After the above study, there have been a series of additional computations for the potential energy surface of the LiH_2 neutral system[4, 6, 7]. Ref. [6], although mainly focused on the reaction that begins with and excited Li atom $Li(2p)+H_2 \rightarrow LiH + H$, is the only one that reports the behavior of the first and second electronic excited states. It is interesting to note that the asymptote $Li(2p) + H_2$ is always energetically open with respect to the $LiH + H$ entrance channel. The two reactions that form $Li(2s)$ and $Li(2p)$ are exothermic of about 2.04 eV and 0.2 eV respectively. Very recently, the high quality CI calculation of Ref. [4] were used by the same authors to perform a series of quasi-classical reactive calculations and the total reactive rate constant turned out to be of the order of $2 - 6 \times 10^{-10}$ cm^3s^{-1} and its dependency on temperature was reasonably well represented by the functional form $k(T) = 8.4 \times 10^{-13} T\, exp(-0.0004T)$.

The LiH_2^+ system has been studied by us in some detail in a series of recent papers [2, 8–11]. In its electronic ground state it is known to form a weak complex between H_2 and the Li^+ ion in C_{2v} symmetry[12] whose binding energy should be of the order of $20 - 25\,KJ\,mol^{-1}$ with respect to $Li^+ + H_2$. Here we are interested in the ground state electronic potential that connects the $LiH^+ + H$ asymptote with the minimum corresponding to the stable $[Li^+ - H_2]$ complex. Since the energy difference between the asymptotic system containing the weakly bound molecule LiH^+ and the triatomic dissociation threshold is small, the break-up process of LiH^+ due to collision with H is important also at low temperature. We intentionally do not mention the triplet manifold of the $LiH^+(^2\Sigma^+) + H(^2S)$ complex, because we expect that the spin-orbit coupling that triggers the triplet-singlet inter-system crossing is quite small for such light atoms. The ground-state surface represents the interaction potential relevant for the study of the adiabatic processes: $LiH^+ + H \rightarrow Li^+ + H_2$ and $LiH^+ + H \rightarrow Li^+ + H + H$; where the latter has been considered because of the very low binding energy of the LiH^+ molecule (0.11 eV). A collinear study of the dynamics taking place on this surface has been carried out [10] using the two collinear approaches $Li - H - H$ and $H - Li - H$ and the time dependent formulation of quantum dynamics. For a wavepacket prepared in the ground vibrational state the non-reactive outcome (unreacted LiH^+) is dominant although an increase in energy tends to also increase the amount of dissociation products. The most striking result of the calculations is given by the almost complete absence of reaction even when the energy is just above the threshold (0.1-0.5 eV). The highest reaction probabilities are observed for the $n = 2$ initial vibrational level, but they still do not exceed 20% of the total and decrease rapidly with increasing total energy.

The comparative analysis of accurately computed potential energy surfaces and the corresponding effort in generating an analytical fitting of the raw ab-initio points described above, indicate that we are now in a position to produce reliable computational estimates of the two processes involved in the network of reactions relevant to the modeling of the "Lithium chemistry". This paradig system involves networks of light atoms, strong quantum effects and is also of relevance for the studies of the early universe chemistry[1]. Moreover Li (as other alkali metals) is among those employed in atomic Bose-Einstein condensation studies as a possible candidate for the achievement of ultra-cold molecules via photo-association experiments[13]. LiH molecules are also highly polar and thus may be taken up as likely candidates for Stark deceleration experiments[13]. Beams of ultra cold molecules might be used to explore the chemistry in the ultra cold temperature range where quantum effects become dominant and where both theoretical and experimental interest has certainly been mounting in recent years[14, 15].

---

[1] S. Lepp, P. C. Stancil, and A. Dalgarno, J. Phys. B **35**, R57 (2002).
[2] E. Bodo, F. A. Gianturco, and R. Martinazzo, J. Phys. Chem. A **105**, 10986 (2001).
[3] R. Martinazzo, E. Bodo, F. A. Gianturco, and M. Raimondi, Chem. Phys. **287**, 335 (2003).
[4] L. J. Dunne, J. N. Murrel, and P. Jemmer, Chem. Phys. Lett. **336**, 1 (2001).
[5] N. J. Clarke, M. Sironi, M. Raimondi, S. Kumar, F. Gianturco, E. Buonomo, and D. Cooper, Chem. Phys. **233**, 9 (1998).
[6] H. S. Lee, Y. S. Lee, and G. Jeung, J. Phys. Chem. A **103**, 11080 (1999).
[7] E. Bodo, F. A. Gianturco, R. Martinazzo, and M. Raimondi, Eur. Phys. J. D **15**, 321 (2000).
[8] E. Bodo, F. A. Gianturco, R. Martinazzo, A. Forni, A. Famulari, and M. Raimondi, J. Phys. Chem. A **104**, 11972 (2000).
[9] E. Bodo, F. A. Gianturco, and R. Martinazzo, Chem. Phys. **271**, 309 (2001).
[10] E. Bodo, F. Gianturco, and R. Martinazzo, J. Phys. Chem. A **105**, 10994 (2001).
[11] M. Satta, E. Bodo, R. Martinazzo, and F. A. Gianturco, J. Chem. Phys. **117**, 2587 (2002).
[12] D. J. Searles and E. I. von Nagy-Felsobuki, Phys. Rev. A **43**, 3365 (1991).
[13] G. Meijer, ChemPhysChem **3**, 495 (2002).
[14] E. Bodo, F. A. Gianturco, and A. Dalgarno, Chem. Phys. Lett. **353**, 1 (2002).
[15] E. Bodo, F. A. Gianturco, and A. Dalgarno, J. Chem. Phys. **116** (2002).

A. Miani, J. Tennyson and T. van Mourik (eds.)
High Accuracy Potentials for Quantum Dynamics

Spectroscopic Determination of Ground and Excited State Potential Energy Surfaces.

K. Ahmed, G. G. Balint-Kurti and C. M .Western

School of Chemistry, University of Bristol, Cantock's Close, Bristol BS8 1TS UK

I. INTRODUCTION

The combination of the recent development of methods for accurate calculation of energy levels from potential energy surfaces and experimental advances in techniques have made very high quality potential energy surfaces available that are firmly based on experimental data. A selection of these is shown in table 1.

TABLE I: Selected Determinations of Potential Energy Surfaces

	Levels fitted	Average Error/cm^{-1}	Highest Level	Lowest ω cm^{-1}	Data Source[a]	Ref.
H_2O	105	0.1	25000	1595	FT	[1]
N_2O	71	0.52	15000	596	FT, IC	[2]
H_2S	73	0.03	14300	1183	FT, IC	[3]
CO_2	65	0.099	9627	667	FT	[4]
SO_2	125	2.9	6886	518	DF, SEP	[5]
O_3	60	0.025	5783	701	FT	[6]
C_2H_2	287[b]	1.2	10000	612	FT,DR	[7]

[a] Key to Data Source: FT = Fourier Trnsform infrared; IC= Intracavity Absorption; DF = Dispersed Fluorescence; SEP = Stimulated Emission Pumping; DR: Double Resonance.

[b] Using an Effective Hamiltonian.

C_2H_2 is the only tetra-atomic molecule and is the only one on the list for which an effective rather than an exact Hamiltonian was used, illustrating the demands of the calculations involved. H_2O is also unusual in that extensive coverage has

been achieved entirely though absorption spectroscopy; this required the use of very hot sources (including flames and the sun) and is only practical for a hydride with large rotational and vibrational spacings. For any other molecule a flexible and selective method of populating high vibrational states is required, typically based on one or more of the many forms of laser spectroscopy. In this respect the SO_2 is a particularly nice example as dispersed fluorescence and stimulated emission pumping measurements via the state have yielded information on levels up to 21600 cm^{-1} in the ground state, far above the range of data fitted. This paper concentrates on C_3 which has several interesting features, is experimentally tractable and has a similar mismatch between the data available and the theoretical modelling.

II. THE $\tilde{A}^1\Pi_u - \tilde{X}^1\Sigma_g^+$ TRANSITION IN C_3

The spectroscopy of the C_3 radical has a remarkably long history, dating back to 1881 when the ultraviolet emission was first seen by Huggins [8] in the spectra of comets. The same complex spectrum has subsequently been observed in many places; C_3 is a relatively stable radical and the spectrum shows strongly in almost any low temperature carbon rich radical source. It was first observed in the laboratory by Herzberg [9] in a discharge in methane, though the carrier of the spectrum was not identified until 1951 by Douglas [10]. The first detailed analysis of the spectrum was by Gausset et al [11] in 1965 who identified the transition as $\tilde{A}^1\Pi_u - \tilde{X}^1\Sigma_g^+$. They explained some of the reasons for the complexity of the spectrum: the ground state bending frequency is only 63 cm^{-1} and the excited state shows a strong Renner-Teller splitting. The Renner-Teller parameter, ϵ, was estimated at 0.537 giving a 350 cm^{-1} splitting of the bending levels, comparable to the bending frequency of 307 cm^{-1}. The system thus became of considerable theoretical interest as a prototype for Renner-Teller interactions. Despite all the interest in the system, the basic analysis was only completed in 1995 by Izuha and Yamanouchi [12] when the asymmetric stretch, ν_3, in the excited state was determined. This mode was found to be very anharmonic implying a double minimum in the asymmetric stretching co-ordinate.

The interest in the molecule has meant that a great wealth of experimental data is available. For the ground state dispersed fluorescence (at 10 cm^{-1} resolution) and stimulated emission pumping studies [13] (0.08 cm^{-1} resolution) have covered levels with up to 17000 cm^{-1} of vibrational energy with $v_1 \leq 8$, $v_2 \leq 37$ and $v_3 \leq 4$. Accurate theoretical modelling has not yet made full use of this data; high level *ab initio* calculations [14] of 108 points on the ground state surface were able to reproduce levels below 3000 cm^{-1} to better than 15

cm^{-1}. A partial fit to the surface was also performed by Spirko et al [15] using the MORBID method, giving a similar quality of fit as the ab initio work.
The excited state has a similar wealth of data available; coverage has been extended from T_0 + 1100 cm^{-1} in the original work [11] to [16] T_0 + 2500 cm^{-1} and then [17] T_0 + 5400 cm^{-1} in addition to the asymmetric stretch work [18]. As for the ground state, accurate theoretical has been somewhat limited; the most detailed work was by Jungen and Merer [19] who modelled the Renner-Teller interaction allowing for wide amplitude bending motion, but not coupling to the other modes.
Given this background, it seems that the time is ripe for extending the accurate theoretical modelling in both the ground and excited state, and using this as a lever to extend the range of assigned transitions in the ultraviolet spectrum.

III. EXPERIMENTAL AND RESULTS

C_3 radicals are generated in a molecular beam using an electric discharge mounted within the molecular beam source [20]. The normal gas mixture used is 1% C_2H_2 in atmospheric pressure argon, though most organic compounds give strong C_3 signals. Typical rotational temperatures are 10-20 K, with vibrational temperatures rather higher. Laser induced fluorescence spectra are taken using a Nd:YAG pumped pulsed dye laser with a resolution of 0.15 cm^{-1} and with a higher resolution (0.01 cm^{-1}) laser system developed in our laboratory [21]. The latter system uses a tuneable diode laser to seed an optical parametric oscillator (OPO) pumped by an injection seeded 355 nm Nd:YAG laser. The OPO consists of two β-Barium Borate crystals in a ring cavity locked to the seeding wavelength. Both the signal and idler outputs are narrow bandwidth, within a factor of two of the Fourier transform limit of the 10 ns pump pulse. By using frequency doubling and/or mixing with harmonics of the pumping Nd:YAG laser the coverage of the system is extended to include most of the visible and ultraviolet. A strong dense spectrum was found throughout the 24000 - 30000 cm^{-1} region. A typical spectrum is shown in figure 1.

Individual bands were fitted to the standard expression for rotational energy levels:

$$E_{rot} = T_v + B[J(J+1) - (l+\Lambda)^2] \pm \frac{1}{2}qJ(J+1) \qquad (1)$$

where the Λ or l doubling parameter q gives the difference between the effective rotational constants for e or f parity levels. The fits were in general good though, as has been observed by previous workers, several bands showed localised perturbations with typically just one or two rotational lines out of position. These probably reflect localised interactions with the ground state or lower lying

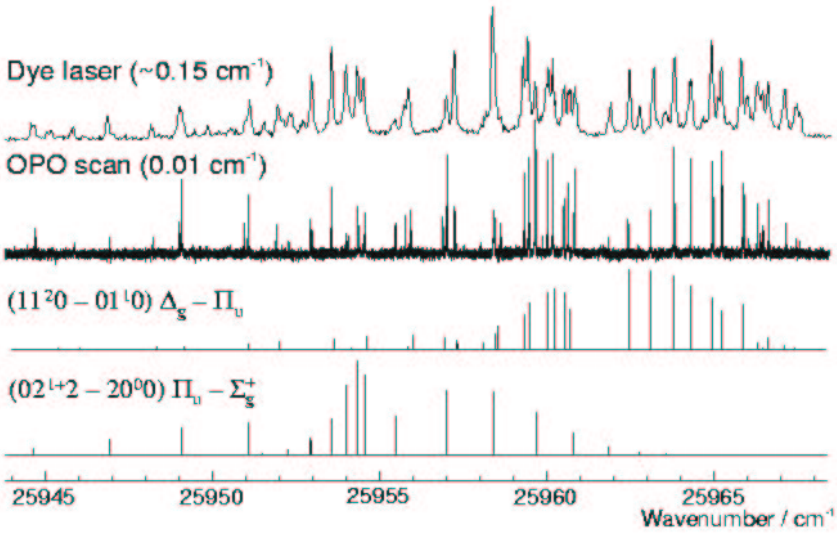

FIG. 1: Laser Induced Fluorescence spectrum of part of the $\tilde{A}^1\Pi_u - \tilde{X}^1\Sigma_g^+$ Transition in C_3.

triplet states. Good agreement was found in general with previous work, and more than 50 new bands have been observed.

IV. CALCULATIONS

To assign the new bands, and to refine the potential energy surface for both states exact calculations of the vibronic levels are being undertaken. A grid based method using Jacobi co-ordinates is used; for the basic method see [22] and references therein. To take account of the two surfaces in the excited state the angular kinetic energy operator must be modified to allow for both vibrational and electronic angular momentum:

$$\hat{T}_{rot} = \left(\frac{1}{2\mu R^2} + \frac{1}{2\mu_{BC} r^2}\right)\hat{j}^2 + \frac{1}{2\mu R^2}\left(\hat{J}^2 - \hat{J}_z^2 - \hat{j}_z^2 - \hat{J}_+\hat{j}_- - \hat{J}_-\hat{j}_+\right) \quad (2)$$

as the projections and of the total and diatomic fragment angular momentum now differ by $\hat{L}_z$; see for example ref [23]. For our basis functions we use

electronic wavefunctions that are eigenfunctions of the electronic L_z operator:

$$L_z|\Lambda = \pm 1\rangle = \pm 1|\Lambda = \pm 1\rangle \tag{3}$$

With this formulation the average of the two potentials gives diagonal matrix elements, and the difference between the two potentials mixes the two states. The potential surfaces are expressed in a simple power series in symmetrised valence co-ordinates [14]:

$$S_1 = \frac{1}{2}(\Delta r_1 + \Delta r_2); S_2 = \gamma; S_3 = \frac{1}{2}(\Delta r_1 - \Delta r_2) \tag{4}$$

$$V = \sum_{ijk} \left(C_{ijk} + sC'_{ijk} \right) S_1^i \gamma^j S_3^k \tag{5}$$

where γ is the bond angle and s is 1 for the upper surface and 0 for the lower surface.
Calculations are performed on a Beowulf cluster of Intel Pentium dual CPU systems with either fast (Myrinet) or slow (100 Mbps ethernet) interconnection. The grid based method allows each row of the Hamiltonian matrix to be calculated independently and thus easily split over computational nodes. The matrix is diagonalised using the ScaLAPACK library [24]; perhaps surprisingly (as this involves a significant amount of communication) this gives good results even when using slow interconnects. To fit to experimental data, a standard non-linear least squares fit method was used, with numerical calculation of the derivatives of the energies with respect to the parameters.

V. RESULTS

Preliminary fits to both the ground and excited state potentials have been undertaken. Using the *ab initio* surface of Mladenovic et al [14] as a starting point a fit to 80 ground state J = 0 and J = 1 (- parity) levels below 7500 cm^{-1} yielded an average error of 5 cm^{-1} when floating 18 parameters. The excited state surface was fitted using only quadratic and quartic terms in the potential and was able to fit 54 levels for J = 1 (both parities) below T_0 + 2500 cm^{-1} to 10 cm^{-1} using only 8 parameters. These fits were to vibrational origins only; for future fits as well as extending the range of the fit we plan to include the rotational constants and l doubling parameters as these are also available from

our calculations.

---

[1] S. V. Shirin, O. L. Polyansky, N. F. Zobov, P. Barletta and J. Tennyson, *J. Chem. Phys.* **118**, 2124 (2003).

[2] J. Zúñiga, M. Alacid, A. Bastida, F. J. Carvajal, and A. Requena, *J. Chem. Phys.* **110**, 6339 (1999).

[3] V. G. Tyuterev, S. A. Tashkun, D. W. Schwenke, *Chem. Phys. Lett.* **348**, 223 (2001).

[4] J. Zúñiga, M. Alacid, A. Bastida, F. J. Carvajal, and A. Requena, *J. Mol. Spectroscop.* **195**, 137 (1999).

[5] A. J. C. Varandas, S. P. J. Rodrigues, *Spec. Act A* **58**, 629 (2002).

[6] Vl. G. Tyuterev, S. Tashkun, P. Jensen, A. Barbe and T. Cours, *J. Mol. Spectrosc.* **198**, 57 (1999).

[7] K. Hoshina, A. Iwasaki, K. Yamanouchi, M. P. Jacobson and R. W. Field, *J. Chem. Phys.* **114**, 7424 (2001).

[8] W. Huggins, *Proc. Roy. Soc. (London)* **33**, 1 (1882).

[9] G. Herzberg, *Astrophys. J.* **96**, 314 (1942).

[10] A. E. Douglas, *Astrophys. J.* **114**, 466 (1951).

[11] L. Gausset, G. Herzberg, A. Lagerqvist and B. Rosen, *Astrophys. J.* **142**, 45 (1965).

[12] M. Izuha and K. Yamanouchi, *Chem. Phys. Lett.* **242**, 435 (1995).

[13] E. A. Rohlfing and J. E. M. Goldsmith, *J. Opt. Soc. Am. B* **7**, 1915 (1990); F. J. Northrup and T. J. Sears, *J. Opt. Soc. Am. B* **7**, 1924 (1990).

[14] M. Mladenovic, S. Schmatz and P. Botschwina, *J. Chem. Phys.* **101**, 5891 (1994).

[15] V. Spirko, M. Mengel and Per Jensen, *J. Mol. Spectrosc.* **183**, 129 (1997).

[16] W. J. Balfour, J. Cao, C. V. V. Prasad, and C. X. W. Qian, *J. Chem. Phys.* **101**, 10343 (1994).

[17] J. Baker, S. K. Bramble and P. A. Hamilton, *J. Molec Spectrosc.* **183**6, (1997).

[18] M. Izuha and K. Yamanouchi, *J. Chem. Phys.* **109**, 1810 (1998).

[19] Ch. Jungen and A. J. Merer, *Mol. Phys.* **40**, 95 (1980).

[20] K.N. Rosser, Q.-Y. Wang and C.M. Western, *J. Chem. Soc. Farad. Trans.* **89**, 391 (1993).

[21] J.A.J. Fitzpatrick, O.V. Chekhlov, J.M.F. Elks, C.M. Western and S.H. Ashworth, *J. Chem. Phys.* **115**, 6920 (2001).

[22] A. R. Offer and G. G. Balint-Kurti, *J. Chem. Phys.* **101**, 10416 (1994).

[23] C. Petrolongo, *J. Chem. Phys.* **89**, 1297 (1988).

[24] *http://www.netlib.org/scalapack*

A. Miani, J. Tennyson and T. van Mourik (eds.)
High Accuracy Potentials for Quantum Dynamics

From Single- to Multi-Sheeted Potential Energy Surfaces: a Dual Strategy for Accurate Global Forms

A.J.C. Varandas
Departamento de Qumica, Universidade de Coimbra
3004-535 Coimbra, Portugal

I. INTRODUCTION

The representation of molecular potential energy surfaces has long been a major stumbling block in both reactive and non-reactive dynamics (Refs. [1–4], and references therein). The least unbiased starting point is to presume that the electronic Schrödinger equation is solved at sufficiently many nuclear configurations to characterize the relevant electronic manifold. This is a formidable undertaking since *ab initio* energies are calculated by pointwise solution of the electronic Schrödinger equation while the dynamics requires a quick and efficient method to evaluate the potential energy surface(s) for any geometry of the nuclei. In favorable cases, the *ab initio* calculations (often after inclusion of some semiempirical correction [5–7]) can reach sufficient accuracy for direct use in the solution of the nuclear equations of motion. Unfortunately, direct dynamics approaches or hybrid schemes utilizing direct dynamics/local interpolation methods get unaffordable if the computational effort per point is far too demanding to calculate more than a thousand points or so.

In this report, we focus on global forms that may be useful both for spectroscopic and reaction dynamics studies. Since vibrational-rotational spectra and kinetics data cannot generally be inverted to yield the adiabatic potential energy surface(s), the only practical way available to obtain them with the required accuracy is via a comparison of the calculated and experimental results, and minimization of the difference between the two. For spectroscopic purposes, one usually resorts to some effective Taylor-series expansion whose coefficients are optimized via a least-squares fitting procedure. However, such expansions miss important topological features due to conical intersections, and even fail to describe the dissociation channels in an acceptable way. We suggest here a dual approach [4] to this problem. In its most complete though computationally expensive format, a global form is adopted and accurate vibrational-rotational data is included in the calibration procedure. The approach involves an iterative process with the parameters being determined from a multiproperty fit to *ab initio* data, vibrational-rotational levels, and

eventually other information. An *ab initio* based potential usually offers an excellent starting point for the fitting procedure [8]. The alternative approach consists of merging a spectroscopically determined Taylor-series expansion with a global form via an *energy-switching* [9, 10] (ES) scheme. Both strategies are illustrated below.

II. GLOBAL VERSUS LOCAL METHODS

In the global methods, the potential energy surface is determined at each point by all the data that are used as input for the calibration procedure. They include various sub-categories depending on whether they employ functional forms obtained from: (i) quantum chemistry such as those based on semiempirical valence-bond type theories [11, 12] and many-body expansion type developments [2–4]; (ii) other motivations such as standard cubic-spline [13] methods, Morse-spline [14] and rotated Morse-spline [15] interpolation methods, reproducing kernel Hilbert space [16] interpolation methods, distributed approximating functionals [17], and hybrid methods combining spline fits with simple empirical functions [18]; (iii) merging functions that are reliable for different energy regimes by using the ES [9, 10] approach. In the local methods, the potential energy surface at each point depends only on the *ab initio* data for geometries close to that point. They include Shepard interpolation methods [19, 20], moving least-squares methods [21], and interpolation on the fly [21] using force field data obtained when doing direct dynamics [22]. We focus here on recent applications of the double many-body expansion [2, 4] (DMBE) and ES [9, 10] methods.

III. CASE STUDIES

A. Single-sheeted DMBE forms: ground-state SO_2

The vibrational quantum numbers were assigned automatically and calculated by using [23]

$$n_i = \frac{1}{2}\left(\frac{\langle n|\Delta Q_i^2|n\rangle}{\langle 0|\Delta Q_i^2|0\rangle} - 1\right) \tag{1}$$

where $\Delta Q_i^2 = Q_i^2 - \langle Q_i\rangle^2$, and Q_i is the i-th normal mode eigenvector at the equilibrium geometry. Counterchecks were done by using the Dunham expansion

$$E_n = \sum_{i=1}^{3}\left(n_i + \frac{1}{2}\right)\omega_i + \sum_{i=1}^{3}\sum_{j=1}^{3}\left(n_i + \frac{1}{2}\right)\left(n_j + \frac{1}{2}\right)x_{ij}$$

$$+\sum_{i=1}^{3}\sum_{j=i}^{3}\sum_{k=j}^{3}\left(n_i+\frac{1}{2}\right)\left(n_j+\frac{1}{2}\right)\left(n_k+\frac{1}{2}\right)x_{ijk} \qquad (2)$$

and occasionally through eye-inspection of sample wave function plots. Except for a few levels above the 150 working ones (up to 7500 cm^{-1}), no assignment problems occurred. For a few higher levels, incorrect assignments happened although the problems could be overcome through the following procedure. First, the first 150 levels were assigned to a Dunham expansion. This was then used to check and/or reassign the higher levels: if the difference between the calculated and Dunham energies were less than a threshold of 20 cm^{-1} or quantum numbers differed at most by one unity (with the energy criterion satisfied), the quantum numbers in the Dunham expansion were accepted and the level considered as assigned. Otherwise, the Dunham expansion was refitted up to the last assigned level, and the procedure repeated. The quality of the final assignment was checked by recalculating the Dunham expansion.

Starting with a DMBE form [24] (I) calibrated from extensive CASPT2 energies suitably corrected by scaling the dynamical correlation, the above procedure has been used to fit the vibrational levels up to 6886 cm^{-1} above the SO_2 minimum; see Ref. [8] for details on the DMBE-II surface. Thermal rate coefficients for the reaction $S + O_2 \rightarrow SO + O$ and its reverse calculated by running trajectories [25] on the DMBE-II surface show a satisfactory agreement with experiment. This may not be surprising due to the large scatter of the experimental data, and neglect of crossings with upper electronic states.

B. Multi-sheeted forms

1. H_3^+: *a direct fit to accurate* ab initio *data*

A global DMBE potential energy surface has been reported [26] for the lowest adiabatic sheet of triplet H_3^+ which shows a conical intersection with the upper adiabatic sheet along geometries with D_{3h} symmetry. Only *ab initio* energies of cc − pV5Z quality have been used for the calibration procedure. Using a distributed $n-$body polynomial approach [27] and an integrity basis that includes the Jahn-Teller coordinate [28], all points could be represented with a root mean square deviation of 3.46 cm^{-1} in the energy region below the $H_2^+(X^2\Sigma_g^+) + H(^2S)$ dissociation threshold and with less than 15 cm^{-1} up to the three-particle breakup energy. The energy levels of the vibronic states have been calculated together with the splitting between the A' and E' components and proposed assignments. Although the vibrational spectroscopic quantum numbers are only approximate [26], the smallness of the splitting between

corresponding A' and E' states indicates that they remain good quantum numbers even above the potential barriers. Some of the assignments made by Sanz *et al.* [29] have been corrected. A comparison with the splittings calculated from their data show a nearly exact agreement with ours for the lower vibronic states, and a good agreement for the higher ones. Such splittings may provide a key feature to identifying the unassigned transitions that have been observed in hydrogen plasmas [29]. In turn, the highly excited vibronic states can play a crucial role in probing the longe range regions of the potential energy surface.

2. $\mathbf{NO_2(^2A')}$: *a challenging triatomic system*

Modelling the NO_2 electronic manifold with $^2A'$ symmetry provides a remarkable challenge. We focus here on a multi-sheeted DMBE form for $NO_2(^2A')$ that has recently [10] been calibrated to reproduce its known topological features. Starting with a multi-sheeted [2, 4, 30] DMBE form, near spectroscopic accuracy has been achieved for the $\tilde{X}\,^2A_1$ ($1\,^2A'$) adiabatic sheet in the vicinity of the spectroscopically characterized minimum by using a multiple-ES scheme. It shows a high-energy ridge for C_{2v} insertion of $N(^4S)$ into $O_2(X\,^3\Sigma_g^-)$ in agreement with accurate CASPT2 calculations that were carried out for such geometries. However, it smooths out for geometries with C_s symmetry yielding a barrier height for the $N + O_2$ reaction of 0.30 eV at a bent N−O−O structure, in good agreement with previous *ab initio* calculations and the recommended data. Another salient feature of the novel 8×8 DMBE/ES potential energy surface is a shallow minimum on the $\tilde{A}\,^2B_2$ adiabatic sheet that is separated from the $\tilde{X}\,^2A_1$ absolute minimum by a conical intersection. Such a feature is accurately predicted by the *ab initio* calculations [10] and well mimicked by the DMBE/ES potential energy surface. Based on the ES results, a tentative assessment of the accuracy of spectroscopically determined effective single-valued forms is also done. In turn, preliminary trajectory results for the $N(^4S) + O_2$ reaction have shown excellent agreement with available thermal rate coefficient data once accounting to the contribution [31] from the lowest quartet state surface.

Acknowledgments

This work has the financial support of Fundao para a Ciência e a Tecnologia, Portugal. It has also been supported in part by the European Community's

Human Potential Programme under contract HPRN-CT-2002-00170.

[1] G. C. Schatz, *Lecture Notes in Chemistry*, Springer, Berlin, **75**, 15 (2000).
[2] A. J. C. Varandas, *Lecture Notes in Chemistry*, Springer, Berlin, **75**, 33 (2000).
[3] A. J. C. Varandas,*Int. Rev. Phys. Chem.*,**19**, 199 (2000).
[4] A. J. C. Varandas, in *Conical Intersections: Electronic Structure, Dynamics and Spectroscopy*, eds. D. Yarkony, H. Köppel, and W. Domcke. World Scientific Publishing, Singapore, (in press).
[5] F. B. Brown and D. G. Truhlar, *Chem. Phys. Lett.*, **117**, 307 (1985).
[6] A. J. C. Varandas,*J. Chem. Phys.*,**90**, 4379, (1989).
[7] A. J. C. Varandas, *J. Chem. Phys.*,**113**, 8880 (2000).
[8] A. J. C. Varandas and S. J. P. Rodrigues,*Spectrochim. Acta Part A*, **58**, 629 (2002).
[9] A. J. C. Varandas,*J. Chem. Phys.*,**105**, 3524 (1996).
[10] A. J. C. Varandas, (to be submitted for publication).
[11] J. C. Tully, *Adv. Chem. Phys.*, **42**, 63 (1980).
[12] P. J. Kuntz, *Atom-Molecule Collision Theory*, ed. R. Bernstein. Plenum, New York, 79 (1979).
[13] N. Sathyamurthy and L. M. Raff, *J. Chem. Phys.*, **63**, 464–473 (1975).
[14] H. Koizumi, G. C. Schatz, and S. P. Walch,*J. Chem. Phys.*, **95**, 4130 (1991).
[15] J. S. Wright and S. K. Gray,*J. Chem. Phys.*,**69**, 67 (1978).
[16] T.-S. Ho and H. Rabitz,*J. Chem. Phys.*,**104**, 2584 (1996).
[17] A. Frishman, D. K. Koffman, and D. J. Kouri,*J. Chem. Phys.*, **107**, 804 (1997).
[18] G. s. Wu, G. C. Schatz, G. Lendvay, D.-C. Fang, and L. B. Harding,*J. Chem. Phys.*, **113**, 3150 (2000).
[19] K. C. Thompson, M. J. T. Jordan, and M. A. Collins,*J. Chem. Phys.*, **108**, 564 (1998).
[20] T. Ishida and G. C. Schatz,*Chem. Phys. Lett.*, **298**, 285 (1998).
[21] T. Ishida and G. C. Schatz, *Chem. Phys. Lett.*, **314**, 369 (1999).
[22] A. J. C. Varandas and P. E. Abreu, *Chem. Phys. Lett.*, **293**, 261 (1998).
[23] M. Menou and C. Leforestier,*Chem. Phys. Lett.*, **210**, 294 (1993).
[24] S. P. J. Rodrigues, J. A. Sabn, and A. J. C. Varandas, *J. Phys. Chem. A*, **106**, 556 (2002).
[25] S. P. J. Rodrigues and A. J. C. Varandas, *J. Phys. Chem. A*, (submitted).
[26] M. Cernei, A. Alijah, and A. Varandas, *J. Chem. Phys.*, **118**, 2637 (2003).
[27] E. Martínez-Nuñez and A. J. C. Varandas,*J. Phys. Chem.*, **105**, 5923 (2001).
[28] A. J. C. Varandas and J. N. Murrell,*Faraday Discuss. Chem. Soc.*, **62**, 92 (1977).
[29] C. Sanz, O. Roncero, C. Tablero, A. Aguado, and M. Paniagua, *J. Chem. Phys.*, **114**, 2182 (2001).
[30] A. J. C. Varandas and A. I. Voronin,*Mol. Phys.*, **95**, 497 (1995).
[31] R. Says, C. Oliva, and M. Gonzlez,*J. Chem. Phys.*, **117**, 670 (2002).

A. Miani, J. Tennyson and T. van Mourik (eds.)
High Accuracy Potentials for Quantum Dynamics

Adiabatic and diabatic intermolecular potentials for open-shell complexes and their applications.

J. Kłos, W. B. Zeimen, V. Lotrich, G. C. Groenenboom, and A. van der Avoird

Institute of Theoretical Chemistry, NSRIM, University of Nijmegen
Toernooiveld 1, 6525 ED Nijmegen, The Netherlands

I. INTRODUCTION

In the more familiar case of two interacting closed-shell molecules the intermolecular potential obtained by solving the first step of the Born-Oppenheimer (BO) or adiabatic approximation is a scalar function. That is, it is invariant under rotations of the whole system, as well as under space-inversion. When the anisotropy of the potential is expressed by expansion in a basis of angular functions—a generalization of the well known Legendre expansion for atom-diatom complexes—also these functions should be invariant under overall rotations [1]. For open-shell systems the situation is more complicated. The electronic states of open-shell atoms and molecules are often degenerate, and for a given electronic state of the interacting species there exist multiple adiabatic intermolecular potential surfaces that are asymptotically degenerate. Nonadiabatic coupling between the electronic states involved becomes important and for specific geometries of the complex one finds phenomena that resemble Renner-Teller and Jahn-Teller coupling. In dynamical calculations it is useful to define a "generalized BO model" which includes the nonadiabatic coupling, but only between the set of electronic states that are asymptotically degenerate. This model works well when the energy separation between the electronic states included in the model and all other states is large with respect to the intermolecular interactions that split the model states.

Formulas for atom-diatom potentials when either the atom or the diatom is an open-shell system have been presented by Alexander [2, 3] and by Dubernet and Hutson [4–6]. The same formulas, and their extension to more complex systems, can be obtained in a very general way [7, 8] by defining an effective

potential energy operator

$$\widehat{V} = \sum_{i',i=1}^{N} |i'\rangle \, V_{i',i} \, \langle i| \tag{1}$$

acting on the space spanned by all N dimer states $|i\rangle$ that asymptotically correlate with the degenerate states of the interacting open-shell species and using merely the property that this operator is invariant under rotations, inversion, and Hermitian conjugation. We assume that $|i\rangle$ correlates with monomer states that are independent of the intermolecular coordinates. Therefore, the states $|i\rangle$ may be called diabatic states and the elements $V_{i',i}$ of the matrix $\boldsymbol{V}^{\rm diab}$ are diabatic interaction potentials. The adiabatic potentials are formally given by diagonalization of this matrix

$$\boldsymbol{V}^{\rm adiab} = \begin{pmatrix} V_1^{\rm adiab} & 0 & \cdots & 0 \\ 0 & V_2^{\rm adiab} & \cdots & 0 \\ \vdots & \vdots & \ddots & \vdots \\ 0 & 0 & \cdots & V_N^{\rm adiab} \end{pmatrix} = \boldsymbol{U}^{\dagger} \boldsymbol{V}^{\rm diab} \boldsymbol{U}, \tag{2}$$

but the potentials that are actually provided by electronic structure calculations are the adiabatic ones and the reverse transformation is required to obtain the diabatic potentials $V_{i',i}$. Also the appropriate transformation matrix $\boldsymbol{U}$ must be extracted from electronic structure calculations, see Sec. II.

Take, for example, an open-shell atom with electronic angular momentum λ interacting with a closed-shell diatom. A set of asymptotically degenerate diabatic dimer states $|\lambda, \mu\rangle$ with $\mu = -\lambda, \ldots, \lambda$ correlate with atomic states labeled by the same quantum numbers and the diabatic potentials are

$$V_{\mu',\mu}(R, r, \theta) = \langle \lambda, \mu' | \, \widehat{V} \, | \lambda, \mu \rangle = \sum_{l} v_l^{\mu',\mu}(R, r) \, C_{l,\mu-\mu'}(\theta, 0), \tag{3}$$

where θ is the angle between the diatom axis $\boldsymbol{r}$ and the vector $\boldsymbol{R}$ from the atom to the center of mass of the diatom. It was shown in Ref. [8] that it follows from rotational invariance of $\widehat{V}$ that only spherical harmonics $C_{l,m}(\theta, 0)$ with $m = \mu - \mu'$ occur in the expansion of the diabatic potential $V_{\mu',\mu}$. These functions $C_{l,m}(\theta, 0)$ are equal to associated Legendre functions $P_{l,m}(\theta)$, apart from a normalization factor. Furthermore, it follows from inversion invariance, $\widehat{i} \, \widehat{V} \, \widehat{i}^{\dagger} = \widehat{V}$, and from Hermiticity, $\widehat{V}^{\dagger} = \widehat{V}$, that the expansion coefficients obey the relations

$$v_l^{-\mu',-\mu}(R, r) = v_l^{\mu',\mu}(R, r) \tag{4}$$

and

$$v_l^{\mu',\mu}(R,r)^* = (-1)^{\mu'-\mu} v_l^{\mu,\mu'}(R,r). \tag{5}$$

When these formulas are used in the analytic fits of *ab initio* calculated potential surfaces (see below) it is very helpful that for large R the expansion coefficients can be expressed in closed form. For the open-shell atom - diatom system chosen here as an example, we find in first order that [8]

$$\begin{aligned} v_l^{\mu',\mu}(R,r) \;=\; & \sum_{l'} \left[\frac{(2l'+2l+1)!}{(2l')!(2l)!}\right]^{\frac{1}{2}} (-1)^{l'-\mu'} \begin{pmatrix} l' & l & l'+l \\ \mu'-\mu & \mu-\mu' & 0 \end{pmatrix} \\ & \times \begin{pmatrix} \lambda & l' & \lambda \\ -\mu' & \mu'-\mu & \mu \end{pmatrix} \begin{pmatrix} \lambda & l' & \lambda \\ 0 & 0 & 0 \end{pmatrix}^{-1} Q_0^{(l')}\, Q_0^{(l)}(r)\, R^{-l'-l-1} \end{aligned} \tag{6}$$

in terms of the atomic and molecular multipole moments $Q_0^{(l')} = \langle \lambda, 0 |\, \widehat{Q}_0^{(l')} \,| \lambda, 0 \rangle$ and $Q_0^{(l)}(r)$. The quantities in large round brackets are 3-j symbols. For the atom in a P level, such as the halogens F, Cl, and Br in their ground ^2P state, the only nonvanishing multipole moment is the quadrupole $Q_0^{(2)}$ and the summation in Eq. (6) is restricted to $l' = 2$.

II. *AB INITIO* CALCULATIONS; METHOD FOR CATIONIC COMPLEXES

For quite a few weakly interacting open-shell species the intermolecular potential surfaces were recently obtained from *ab initio* calculations. The most accurate results are nowadays computed with the RCCSD(T) method, a spin-restricted coupled cluster method including single, double, and non-iterative triple excitations. By definition, electronic structure computations with clamped nuclei produce adiabatic potentials. The nonadiabatic coupling matrix elements contain derivatives of the electronic wavefunctions with respect to the nuclear coordinates. The RCCSD(T) method does not explicitly provide wavefunctions and, in order to compute the nonadiabatic coupling, one uses MRCI (multi-reference configuration interaction) methods, for example, with orbitals from preliminary RHF (restricted Hartree-Fock) or CASSCF (complete interacting space self-consistent field) calculations.

In dynamical calculations and also for the analytic representation of intermolecular potential surfaces it is convenient to define a set of diabatic states and use diabatic potentials, instead of using the adiabatic ones and considering explicitly the nonadiabatic coupling. The nonadiabatic coupling originates

from the nuclear kinetic operator acting on the electronic wavefunctions. The transformation $\boldsymbol{U}$ to diabatic potentials $V_{i',i}$ removes this kinetic coupling, but the price one pays is that the matrix $\boldsymbol{V}^{\mathrm{diab}}$ is nondiagonal. The adiabatic states are automatically adapted to the point group symmetry of the complex and the transformation from adiabatic to diabatic states is facilitated when the latter are symmetry adapted also. In the case of a closed-shell atom interacting with an open-shell Π state diatom one finds, for example, that taking the sum and difference of the two diabatic states that correlate with the $\Pi_{\pm 1}$ states of the diatom produces states adapted to reflection in the plane through the nuclei. One of those is symmetric, A', the other is antisymmetric, A''. Also the two adiabatic potential surfaces resulting from *ab initio* calculations correspond to A' and A'' symmetry, and the diabatic potentials are simply the sum and difference of the adiabatic potentials. In general, there are multiple states of the same symmetry that mix and the matrix $\boldsymbol{U}$ that transforms the adiabatic states to the diabatic ones must be determined numerically from the properties of the computed adiabatic wavefunctions. For some examples, we refer to recent work of Alexander [9] on Ar–NO($^2\Pi$) and of Kłos *et al.* on He–NO($^2\Pi$) [10], X(^2P)–H_2, with X = F, Cl, Br [8, 11–13], Cl(^2P)–HCl [14, 15], Cl(^2P)–CH_4 [16], as well as on OH($^2\Pi$)–HCl [17].

For cationic open-shell complexes we developed a special method [18]. The interaction energy of a cationic complex A–B^+ is computed as

$$E^{+}_{\mathrm{int}} = E^{0}_{\mathrm{int}} + \Delta_{\mathrm{int}}, \tag{7}$$

where $E^{0}_{\mathrm{int}} = E^{0}_{AB} - E^{0}_{A} - E^{0}_{B}$ is the interaction energy of the neutral complex A–B and

$$\Delta_{\mathrm{int}} = IP_{AB} - IP_{B}. \tag{8}$$

The geometry dependent ionization potential IP_{AB} of the complex A–B and the ionization potential IP_B of molecule B are calculated by the outer valence Green's function (OVGF) method [19]. This method is very attractive and efficient since:

1. The calculation of an accurate interaction potential for a neutral closed-shell complex is considerably easier than for a cationic open-shell complex. Neutral interaction potentials are already available for many systems.

2. The calculation of ionization energies by the OVGF method is implemented in the GAUSSIAN program package [20] and converges much faster with the basis size than the calculation of the interaction energy of the ionic complex by the RCCSD(T) method.

3. The simultaneous computation of the multiple asymptotically degenerate potential surfaces that one finds in many open-shell complexes is relatively easy because the computation of multiple ionization energies of a closed-shell molecule by the OVGF method is quite simple.

These advantages make the method applicable to obtain full potential energy surfaces for larger systems.

We tested this method by computing the intermolecular potential of the complexes Rg–$CO^+(^2\Sigma)$, with Rg = He, Ne, Ar, and the two asymptotically degenerate potentials for the ground state of the He–$HF^+(^2\Pi)$ complex, which are actually degenerate in all linear geometries. Results from Eq. (7) were compared with the results of a direct calculation of the interaction energy in the ionic complex. All interaction energies were obtained from supermolecule calculations with the CCSD(T) and RCCSD(T) methods for the neutral and ionic complexes, respectively, and all quantities (including Δ_{int}) were corrected for the basis set superposition error [21] by the Boys-Bernardi counterpoise procedure [22]. In these tests we found one problem, however. The major contribution to the geometry dependent ionization energy difference Δ_{int} originates from induction effects which are determined by the polarizability of the neutral molecule A and the charge and multipole moments of the molecular ion B^+. Although the OVGF method includes the effects of electron correlation to a certain extent it was designed for regular molecules, not for weakly interacting complexes. Apparently, the amount of electron correlation in OVGF is not sufficient to provide an induction energy corresponding to fully correlated polarizabilities and multipole moments of the interacting species. An analysis of this defect showed that it is, in particular, the long range behavior of Δ_{int} that is deficient. This can be easily remedied by a simple correction procedure: subtract the deficient long range induction contributions from the cationic interaction potentials and replace them with the corresponding terms computed from accurate correlated monomer multipole moments and polarizabilities. After this rescaling the interaction potentials of Rg–$CO^+(^2\Sigma)$ and He–$HF^+(^2\Pi)$ from Eq. (7) agree with supermolecule RCCSD(T) results within a few percent for all intermolecular separations [18].

An application of this procedure that is presently pursued is the study of the lowest five electronic states of the Ar–benzene$^+$ complex [23]. The lowest two potential surfaces are degenerate when Ar is on the sixfold symmetry axis of the $C_6H_6^+$ cation and correlate with the twofold degenerate ground E_{1g} state of this cation (D_{6h} symmetry). The three higher ones correlate with the E_{2g} and A_{2u} excited states. Direct RCCSD(T) calculations of the interaction potentials for all these states would not have been practically possible. All of these states of $C_6H_6^+$ display interesting Jahn-Teller and pseudo Jahn-Teller effects [24–28]. Additional nonadiabatic effects originating from the intermolecular interaction

might be expected in the rovibronic states of the Ar–benzene$^+$ complex [28–30].

III. APPLICATIONS

Applications of these interaction potentials in our group are the calculation of bound levels, elastic and inelastic scattering and photodissociation cross sections, and spectra of several open-shell complexes. The X(^2P)–H_2 complex, with X = F, Cl, Br, the Cl(^2P)–HCl complex, the He–HF$^+$($^2\Pi$) complex, and the Ar–benzene$^+$ complex were already mentioned. In addition, we studied the Rg–NO($^2\Pi$) complex with Rg = He, Xe, and the He–CO($^3\Pi$) complex. The X(^2P)–H_2 and Cl(^2P)–HCl complexes are entrance and exit channel complexes in chemical reactions. The He–HF$^+$($^2\Pi$) complex is important for the study of Renner-Teller coupling [31]. The He–CO($^3\Pi$) complex is of interest because CO($^3\Pi$) is a long-lived metastable species which is a candidate for being cooled to ultralow temperatures by electrostatic deceleration [32]. The complex with He can be formed by singlet-triplet excitation of ground state He–CO, but is found to dissociate rapidly by spin-orbit predissociation [7, 33]. The same mechanism is responsible for spin-orbit inelastic collisions that will play a role in evaporative cooling of CO($^3\Pi$) by He.

Acknowledgments

This research has been financially supported by the Council for Chemical Sciences of the Netherlands Organization for Scientific Research (CW-NWO). We also acknowledge support from the European Research Training Network THEONET II. We thank Dr. Paul E. S. Wormer for many useful comments.

[1] A. van der Avoird, P. E. S. Wormer, F. Mulder, and R. M. Berns, Topics in Current Chemistry **93**, 1 (1980).
[2] M. H. Alexander, Chem. Phys. **92**, 337 (1985).
[3] M. H. Alexander, J. Chem. Phys. **99**, 6014 (1993).
[4] M.-L. Dubernet, D. Flower, and J. M. Hutson, J. Chem. Phys. **94**, 7602 (1991).
[5] M.-L. Dubernet and J. Hutson, J. Chem. Phys. **101**, 1939 (1994).
[6] M.-L. Dubernet and J. Hutson, J. Phys. Chem. **98**, 5844 (1994).
[7] W. B. Zeimen, G. C. Groenenboom, and A. van der Avoird, J. Chem. Phys. (2003), submitted.
[8] W. B. Zeimen, J. A. Kłos, G. C. Groenenboom, and A. van der Avoird, J. Chem. Phys. (2003), accepted.

[9] M. H. Alexander, J. Chem. Phys. **111**, 7426 (1999).
[10] J. Kłos, G. Chałasiński, M. T. Berry, R. Bukowski, and S. M. Cybulski, J. Chem. Phys. **112**, 2195 (2000).
[11] J. Kłos, G. Chałasiński, and M. M. Szczęśniak, Int. J. Quant. Chem. **90**, 1038 (2002).
[12] J. Kłos, G. Chałasiński, and M. M. Szczęśniak, J. Chem. Phys. **117**, 4709 (2002).
[13] J. Kłos, G. Chałasiński, and M. M. Szczęśniak, J. Phys. Chem. A **106**, 7362 (2002).
[14] J. Kłos, G. Chałasiński, M. M. Szczęśniak, and H.-J. Werner, J. Chem. Phys. **115**, 3085 (2001).
[15] W. B. Zeimen, J. A. Kłos, G. C. Groenenboom, and A. van der Avoird, J. Phys. Chem. (2003), submitted.
[16] J. Kłos, Chem. Phys. Lett. **359**, 309 (2002).
[17] J. Kłos, G. C. Groenenboom, and A. van der Avoird, (2003), in preparation.
[18] V. F. Lotrich and A. van der Avoird, J. Chem. Phys. **118**, 1110 (2003).
[19] L. S. Cederbaum, W. Domcke, and W. von Niessen, J. Phys. B **10**, 2963 (1977).
[20] M. J. Frisch, G. W. Trucks, H. B. Schlegel et al., GAUSSIAN 98, Revision A.7, Gaussian, Inc., Pittsburg PA, 1998.
[21] F. B. van Duijneveldt, J. G. C. M. van Duijneveldt-van der Rijdt, and J. H. van Lenthe, Chem. Rev. **94**, 1873 (1994).
[22] S. F. Boys and F. Bernardi, Mol. Phys. **19**, 553 (1970).
[23] V. F. Lotrich and A. van der Avoird, (2003), in preparation.
[24] H. Köppel, L. S. Cederbaum, and W. Domcke, J. Chem. Phys. **89**, 2023 (1988).
[25] J. Eiding, R. Schneider, W. Domcke, H. Köppel, and W. von Niessen, Chem. Phys. Lett. **177**, 345 (1991).
[26] R. Lindner, K. Müller-Dethlefs, E. Wedum, K. Haber, and E. R. Grant, Science **271**, 1698 (1996).
[27] J. G. Goode, J. D. Hofstein, and P. M. Johnson, J. Chem. Phys. **107**, 1703 (1997).
[28] B. E. Applegate and T. A. Miller, J. Chem. Phys. **117**, 10654 (2002).
[29] H. Krause and H. J. Neusser, Chem. Phys. Lett. **213**, 603 (1993).
[30] J. M. Bakker, R. G. Satink, H. Piest, G. von Helden, and G. Meijer, Phys. Chem. Chem. Phys. **4**, 24 (2002).
[31] T. Schmelz and P. Rosmus, Chem. Phys. Lett. **220**, 117 (1994).
[32] H. Bethlem, G. Berden, and G. Meijer, Phys. Rev. Lett. **83**, 1558 (1999).
[33] W. B. Zeimen, G. C. Groenenboom, and A. van der Avoird, J. Chem. Phys. (2003), submitted.

A. Miani, J. Tennyson and T. van Mourik (eds.)
High Accuracy Potentials for Quantum Dynamics

Intermolecular Interaction Potentials

Krzysztof Szalewicz

Department of Physics and Astronomy, University of Delaware, Newark, DE 19716, USA
Department of Chemistry, Princeton University, Princeton, NJ 08544, USA

I. INTRODUCTION

Intermolecular interaction potentials (or force fields) are used in a vast area of modern science. In the simplest cases, i.e., for interactions between atoms and small linear molecules, the potentials are now usually computed *ab initio* or fitted to spectroscopic data. These potentials can be accurate to within a few percent. For larger molecules, whose condensed phase is often investigated by molecular dynamics or Monte Carlo simulations, only empirical interaction potentials—fitted within such simulations to reproduce a subset of experimental data—are used. Such potentials can be qualitatively incorrect in various regions of coordinate space despite reproducing experimental observations in the simulations [1, 2]. For most biomolecular simulations even more crude potentials are used, assembled as a sum of standarized atom-atom interactions, disregarding actual molecular environment. Clearly, if *ab initio* potentials for such systems were available, these would put this field on a much more certain footing.

Unfortunately, *ab initio* calculations of intermolecular potentials for larger monomers encounter several steep difficulties as the sizes of the monomers increase above two atoms:

(a) Even a single-point calculation becomes very time-consuming. Reliable intermolecular interaction energies require inclusion of electron correlation effects at least at the level of the second-order many-body perturbation theory (MBPT2), but preferably at the coupled-cluster singles and doubles plus noniterative triples level [CCSD(T)]. The former method scales as the fifth and the latter method as the seventh power of system size. Furthermore, such potentials require about triple-zeta quality basis sets with diffuse and bond functions [3] in order for basis set truncation

errors to be of comparable size to theory level truncation errors. As a consequence, even for triatomic monomers a single-point calculation takes on the order of one hour on modern processors.

(b) The number of grid points that need to be computed for a potential is large even if monomers are assumed rigid. In this case the pair potentials are at most six-dimensional. It was found that to determine the water dimer potential with accuracy of about 5% one needs to compute about two thousand grid points [4]. With accuracy goals relaxed, the number of points can be somewhat reduced, but at least several hundred points will be needed. For example, the interaction potential for the largest system computed to date, the dimethylnitramine dimer [5] containing 24 atoms, required above four hundred grid points.

(c) If the rigidity restriction is removed, the dimer potential for a system containing N atoms becomes $3N-6$ dimensional. Since the number of grid points needed to determine a potential grows exponentially with the number of degrees of freedom, the $3N-6$ dimensionality makes calculations of such potentials impossible at present, except for diatomic monomers or atom-triatom interactions. Whereas the rigid-monomer approximation appears to work reasonably well, flexible-monomer potentials are needed for high-accuracy work on clusters and to investigate observables depending explicitly on intramonomer coordinates such as bond lengths in solid phase or infrared spectra of condensed phase and molecular clusters.

(d) Pair potentials are insufficient for most systems and nonadditive effects have to be taken into account, i.e., the total potential has to be build as a sum of many-body potentials. Even if the inclusion of three-body nonadditive effects appears to be sufficient [2], the three-body potential is 12-dimensional already for rigid monomers.

As the power of computers increases, larger and larger systems will be accessible. However, it is clear that with brute force approaches the size of the systems that can be handled will increase extremely slowly. Fortunately, some recently developed methods for computations of intermolecular potentials bring hopes for a faster progress.

After a potential is computed on a grid of points, an analytic function has to be fitted to these points in order to be used in various types of simulations. Many forms of such functions have been proposed in literature and we are far from a consensus which of them is most effective.

II. THEORY OF INTERMOLECULAR INTERACTIONS

The conceptual framework for describing the phenomenon of intermolecular forces is provided by symmetry-adapted perturbation theory (SAPT) [6–8]. In two-body SAPT one uses the following partitioning of the total Hamiltonian: $H = H_A + H_B + V = F + V + W$, where H_X is the exact Hamiltonian for monomer X, X = A or B, V is the intermolecular interaction operator collecting all Coulomb repulsion and attraction terms between all particles of monomer A and those of monomer B, $F = F_A + F_B$ is the sum of the Fock operators for monomers A and B, and $W = W_A + W_B$ is the intramonomer correlation operator with $W_X = H_X - F_X$. The interaction energy can then be represented as a double-perturbation series

$$E_{\rm int} = \sum_{n=1}^{\infty} \sum_{j=0}^{\infty} E^{(nj)} \tag{1}$$

with the consecutive superscripts referring to the operators V and W, respectively. Each SAPT correction is naturally separated into several components, related to the physical picture of intermolecular interactions, such as the electrostatic, induction, dispersion, and exchange energies. For three-body interactions, the overall form of the expansion is the same, however, the operator V now contains interaction between each pair of monomers and $W = W_A + W_B + W_C$ [9, 10].

III. COMPUTATIONAL METHODS

The SAPT approach outlined above provides not only the conceptual framework for describing intermolecular interactions, but it has been developed into a robust computational tool [11]. It can be used at various levels of theory, starting from terms appearing in the Hartree-Fock (HF) interaction energy. At the highest currently available level, the most time-consuming quantity to compute is the triple excitations contribution contained in the dispersion energy correction $E^{(22)}_{\rm disp}$. For a dimer consisting of identical molecules, the computational cost of this quantity scales roughly as $n_{\rm o}^3 n_{\rm v}^4$ where $n_{\rm o}$ and $n_{\rm v}$ are, respectively, the numbers of occupied and virtual orbitals in a monomer [12]. This overall seventh power scaling is the same as in many-body perturbation theory at the fourth-order level (MBPT4) or in the CCSD(T) method, however, the calculation of triples contribution in SAPT is faster due to summation ranges extending only over orbitals of monomers rather than over orbitals of the

dimer. The dispersion energy can also be computed with selected intramonomer correlation effects summed up to infinity, see Refs. [13–15].

Whereas the use of the SAPT approach to calculate interaction potentials offers the advantage of a physical insight into the computed quantity, any electronic structure method that is size-consistent, i.e., dissociates to the sum of energies of monomers, can be used for this purpose. As mentioned in the Introduction, intermolecular interaction potentials require taking into account electron correlation effects, at least at the MBPT2 level. If the accuracy goal is to reproduce the potential to within a few percent, higher-order methods such as MBPT4 or the coupled cluster approaches [16] have to be used. The computer resources required by such methods make applications to monomers with more than a few atoms not practical at the present time even if monomers are assumed rigid.

Density functional theory (DFT) is much less time consuming and would allow treatment of much larger systems. Unfortunately, this method fails when used in the supermolecular approach to compute interaction potentials for systems where dispersion is a significant component. Thus, DFT is not appropriate for studies of intermolecular interactions except for the cases of strongly, electrostatically bound systems. Numerous papers have been devoted to this problem and the reader is sent to Ref. [17] for a review and a quantitative analysis.

Williams and Chabalowski [18] have proposed a perturbational approach where the interaction energies are obtained using only the lowest-order, computationally least demanding SAPT expressions, but replacing the HF orbitals and orbital energies by the Kohn-Sham (KS) counterparts. This approach will be referred to as SAPT(KS). For medium-size monomers, SAPT(KS) is about three orders of magnitude faster than the regular SAPT with high-order treatment of electron correlation. However, the accuracy of the SAPT(KS) predictions was found to be disappointing [18] even for the electrostatic energy which is potentially exact in this approach. In a recent paper, Misquitta and the present author have demonstrated [19] that some deficiencies of SAPT(KS) stem from an incorrect asymptotic behavior of exchange-correlation potentials (see also Ref. [20]). Upon applying an asymptotic correction in monomer DFT calculations, the SAPT(KS) approach was not only able to accurately recover the electrostatic energy, but also the first-order exchange and second-order induction and exchange-induction energies. For example, for He_2 the sum of these corrections has been recovered with errors of 2-5% (relative to the nearly exact values from Ref. [21]) for a range of functionals. Dispersion was reproduced less accurately, with errors of 5-17% for the same functionals. For other systems, the deviations of SAPT(KS) dispersion energies from benchmark results are still larger (12-16% for neon, 19-22% for water, and 33-37% for carbon

dioxide dimers [22]), too large to enable computations of quantitatively correct interaction potentials.

Very recently Misquitta *et al.* [23] proposed a new method for computing the dispersion energy that utilizes frequency-dependent density susceptibilities (FDDS's) predicted by time-dependent DFT in an expression which is a generalization of the asymptotic Casimir-Polder formula (see also Ref. [24]). This generalization was derived by Dmitriev and Peinel [25] and by McWeeny [26] and applied with coupled Hartree-Fock (CHF) FDDS's (polarization propagators) by Jaszunski and McWeeny [27] and by Knowles and Meath [28]. The CHF and DFT FDDS's are closely related to the frequency-dependent polarizabilities and can be directly computed using the methodologies developed for the latter case [29, 30]. Similarly as for the dispersionless part of the interaction energy, application of an asymptotic correction is critical. It was found [23] that the correction of the Fermi-Amaldi form applied as prescribed by Tozer and Handy [31] is the most robust. The method recovers the dispersion energies of He, Ne, and H_2O dimers to within 3% or better. Since the computational effort of the new algorithm scales approximately as the third power of system size, the method is much more efficient than standard wave-function methods capable of predicting the dispersion energy at a similarly high level of accuracy.

The development of Refs. [19, 20, 23, 24] paves the road for theoretical predictions of accurate intermolecular potentials for much larger systems than it has been possible so far. One can soon expect to see routine calculations of interactions potentials for rigid monomers with a few dozens atoms. This will open exciting opportunities to investigate molecules of biological interest.

IV. DIMENSIONALITY PROBLEM

Whereas with the DFT-based SAPT method one should be able to compute rigid-monomer potentials for molecules much larger than presently possible, even this very fast method will not be sufficient to evercome the very steep scaling of difficulty with system size in the case of flexible monomers. With k points per dimension, calculation of a flexible-monomer potential energy surface for a dimer would require k^{3N-6} grid points. The difficulty can be illustrated by the example of the water dimer potential, whose dimensionality increases from 6D to 12D if the monomers are allowed to flex. Thus, to generate a flexible potential comparable in accuracy to the existing rigid-water SAPT-5s potential [4] (fitted to 2510 *ab initio* points, i.e., k equal to about 4) would require the calculation of over 16 million points. Even if a single-point calculation were to take only about one minute, the whole potential would take dozens of CPU years.

Most of the published flexible-monomer potentials were obtained from rigid-monomer potentials by using the "atom-following" approach. If a rigid-monomer potential is in the form of a site-site fit, changes of internal geometry of a monomer naturally modify the interaction energy. However, it has been shown [32] that the atom-following approach performs poorly and in fact may predict changes opposite to actual ones. Murdachaew *et al.* [32, 33] have recently developed a new method of extrapolating the rigid-monomer potentials to flexible-monomer potentials based on limiting the expensive *ab initio* calculations to individual monomers only. Such calculations result in only $k^{3N_A-6} + k^{3N_B-6}$ scaling, where N_X is the number of atoms in monomer X. Thus, for the water dimer only 128 points are needed in this step. The flexible-monomer properties computed in this step—such as electron densities and van der Waals asymptotic coefficients—are used together with the rigid-monomer potential and density overlap integrals to predict the values of the flexible-monomer potential. The density overlap integrals have to be computed for all k^{3N-6} grid points, however, a single calculation of this type takes very little of CPU time compared to any *ab initio* calculation of the interaction energy, even at the HF level. The method has been first tested on the simple example of Ar-HF [33] showing that, in contrast to the atom-following approach, it does recover a major fraction of the nonrigidity effect for deformations corresponding to the ground and lowest excited vibrational states of monomers. Only for very small intermonomer separation the predictions of the method were not accurate enough. In this region the interaction energy is small in magnitude compared to the magnitudes of its individual components. This leads to fairly large errors in the interaction energy computed as the sum of the components, despite of the fact that the relative errors of individual components remain small. At this point the only solution to this problem is to compute a number of *ab initio* points in this region. The method has recently been applied to the water dimer [34]. The root means square error of the flexible-monomer potential computed in this way is several times smaller than the error of the potential obtained from the atom-following approach.

V. MANY-BODY POTENTIALS

The interaction energy of N monomers can be expressed as a sum of terms involving interactions of 2, 3, ... monomers

$$E_{\rm int} = E_{\rm int}[2,N] + E_{\rm int}[3,N] + ... + E_{\rm int}[N,N], \qquad (2)$$

where K-body contributions to the N-mer energy, $E_{\rm int}[K,N]$, can be written as the following sums

$$E_{\rm int}[2,N] = \sum_{i<j} E_{\rm int}(\boldsymbol{Q}_i, \boldsymbol{Q}_j)[2,2], \tag{3}$$

$$E_{\rm int}[3,N] = \sum_{i<j<k} E_{\rm int}(\boldsymbol{Q}_i, \boldsymbol{Q}_j, \boldsymbol{Q}_k)[3,3], \tag{4}$$

etc., where $\boldsymbol{Q}_i = (\boldsymbol{R}_i, \boldsymbol{\omega}_i, \boldsymbol{\xi}_i)$ stands for the set of all coordinates needed to specify the spatial position $\boldsymbol{R}_i$, orientation $\boldsymbol{\omega}_i$, and the internal geometry $\boldsymbol{\xi}_i$ of the ith monomer. The two-body or *pairwise-additive* interaction energies $E_{\rm int}[2,2]$ are just the regular dimer interaction energies. Their sum, $E_{\rm int}[2,N]$, is the (pairwise) additive component of the interaction energy of an N-mer. The higher-body terms, i.e., the *nonadditive* contributions to the N-mer interaction energy, are defined recursively. For example, the three-body contribution to a trimer interaction energy, $E_{\rm int}[3,3]$, is the difference between the total interaction energy of a given trimer and the sum of all pair energies.

Three-body SAPT [9, 10, 35, 36] allows direct calculations of the $E_{\rm int}[3,N]$ component. Applications of this method to a number of systems allowed to shed light on the importance of this component of the N-body interaction potential. For rare gas trimers the nonadditive contribution is dominated by the first-order exchange and third-order dispersion energies, although for Ar_3 the exchange-dispersion contribution is quite large. This contribution is critical for predicting the correct crystal structure of argon [37]. For Ar_2–HF all these components are still important but a very significant role is played also by the induction and exchange-induction nonadditive contributions. The situation changes completely in the water trimer. The dispersion contributions are dwarfed by the very significant induction effects. Even the third-order induction nonadditivity is very important here. The first-order exchange nonadditivity is important for all systems.

The overall importance of three-body effects varies from almost negligible for helium [35] to major for water [1, 2]. For equilibrium structures, the ratio of the three-body component to the sum of two-body interactions changes from 0.4% for He_3 to 16% for the water trimer. The nonadditive contribution can be of either sign at the equilibrium and frequently changes the sign as the trimer geometry is changed. When the three-body SAPT potential for water developed in Ref. [1] was applied to simulations of liquid water, it contributed 14.5% to the internal energy of water at ambient conditions [2], a similar contribution as for the equilibrium water trimer. In some cases, however, the three-body effects can be amplified, like in the case of solid argon [37], or may cancel to a large extent, as for acetonitril [38].

One might expect that for clusters larger than trimers and for condensed phase, four- and higher-body interactions may become important. However, this does not appear to be the case. When the four- and higher-body effects were approximated by a polarization model, these contributed 1.4% to the internal energy of liquid water [2]. Calculations on small clusters also indicate that these contributions should be fairly small. *Ab initio* calculations of Refs. [39, 40] have found that the 4-body contribution to interaction energies varied between -1.2% and 2.3% for tetramers and between 1.2% and 3.6% for pentamers. The 5-body contribution to the interaction energy of pentamers was completely negligible as it ranged between -0.11% and 0.25%. These percentage contributions are likely to be even smaller if basis sets of sizes larger than double-zeta are used since small basis sets underestimate pair contributions while giving more saturated values of nonadditive terms [1].

VI. FITS OF POTENTIALS

Once the interaction energies are computed on a set of grid points, for most consecutive applications these energies have to be fitted by an analytic potential. Three-body potentials are a largely unexplored territory [2, 41]. Therefore, the discussion here will be limited to pair potentials of rigid monomers. The fits are usually performed by the standard least-squares method. For a large number of grid points and a large number of nonlinear parameters this procedure is far from trivial.

There are several possible forms of the fitting functions. These forms can be divided into two major categories, the center of mass (COM) and site-site fits. The COM fits are expressed in terms of the distance R between the COM's of monomers and a set of Euler angles determining the mutual orientation of the two monomers. Usually this function is written as a sum of products of angular functions and radial functions [8]. The angular functions are built from Wigner functions and form a complete set in the space spanned by the Euler angles. The radial functions typically contain an exponential factor possibly multiplied by a polynomial in R plus a sum of $1/R$ terms, usually multiplied by a damping function restricting their divergence at small R. An example of such a fit for the case of the water dimer can be found in Ref. [42]. The advantage of this fitting form is its elegant mathematical structure, close relation to the formalism used in the theory of molecular scattering, and a direct connection with the van der Waals constants [43]. The major disadvantage of COM fits compared to site-site fits is their larger complexity at the same level of fit accuracy. For example, the COM fit for the water dimer from Ref. [42] is 1400 times more time consuming to compute than the site-site fit from Ref. [4]. For larger monomers one may

expect the convergence of the COM expansion to get gradually worse, for the same reasons for which COM asymptotic expansions quickly diverge [8] in such cases.

The simplest site-site expansion builds the interaction potential from functions depending only on distances r_{ab} between the pairs of sites from different monomers. The sites are usually put on all atoms and in addition a number of off-atomic sites may be introduced. The total potential can be built as a sum of site-site functions or may include also the products of these functions or some functions depending on more than one site-site coordinate. More complicated site-site potentials are anisotropic, i.e., depend not only r_{ab}'s but also on the mutual orientation of the monomers. The latter form is firmly based in the so-called distributed multipole expansion [8].

For small molecules, the sum of isotropic site-site terms with sites limited to atoms is known to result in poor quality fits, no matter how flexible the individual site-site functions are. There is no real evidence that the performance of this type fits gets better for larger molecules, although such functional forms are used almost exclusively in simulations for biomolecules. If a few off-atomic sites are added, such a fitting form can provide very high accuracy, as shown for example in Ref. [4] where five off-atomic sites were used for the water monomer (three symmetry-distinct off-atomic sites). It should perhaps be mentioned that the values of the individual site-site functions in such fits are often far from the physical range of interaction energies and the total potential results from significant cancellations between the individual site-site functions. This becomes an issue for applications in path integral Monte Carlo simulations which apply propagation to individual isotropic site-site functions. Potentials with a more balanced set of site-site functions can be obtained using least-squares fitting with constraints [44].

Not much is known about the importance of inclusion, in addition to the sum of isotropic site-site functions, of the product terms. Fits containing a large number of product terms have recently been used by Koch *et al.* [45], but the role of the products terms has not been analyzed. Presumably if enough off-atomic sites are included, the product terms are not needed, as evidenced by the high accuracy of the water dimer fit from Ref. [4].

The individual site-site functions can be assumed in various forms. The classical Lennard-Jones 12-6 form is still sometimes used, although an exponential plus a sum of (possibly damped) powers of $1/r_{ab}$ is now a more common choice. The exponential term may be multiplied by a polynomial of r_{ab}, as in Ref. [4].

The anisotropic site-site potentials have the significant advantage that if sites are limited to atoms, their asymptotics can be obtained directly from distributed multipoles and polarizabilities [8, 46]. One may expect that the individual atom-atom contributions will be physically interpretable and perhaps allow for

some transferability between different systems. Such fits are somewhat more complicated than the fits with isotropic sites only, but if the angular components are restricted to low-order terms, the computational cost may be reasonable.

Acknowledgments

This research was supported by the NSF grant CHE-0239611. The author is grateful to Professor Giacinto Scoles for numerous discussions of this subject.

---

[1] E. M. Mas, R. Bukowski, and K. Szalewicz, J. Chem. Phys. **118**, 4404 (2003).
[2] E. M. Mas, R. Bukowski, and K. Szalewicz, J. Chem. Phys. **118**, 4386 (2003).
[3] H. L. Williams, E. M. Mas, K. Szalewicz, and B. Jeziorski, J. Chem. Phys. **103**, 7374 (1995).
[4] E.M. Mas, R. Bukowski, K. Szalewicz, G. Groenenboom, P.E.S. Wormer, and A. van der Avoird, J. Chem. Phys. **113**, 6687 (2000).
[5] R. Bukowski, K. Szalewicz, and C. Chabalowski J. Phys. Chem. A **103**, 7322 (1999).
[6] B. Jeziorski, R. Moszynski, and K. Szalewicz, Chem. Rev. **94**, 1887 (1994).
[7] B. Jeziorski and K. Szalewicz, in *Handbook of Molecular Physics and Quantum Chemistry*, edited by S. Wilson, Wiley, 2002, Vol. 3, Part 2, Chap. 9, p. 232.
[8] A.J. Stone *The Theory of Intermolecular Forces*, Clarendon, Oxford, 1996.
[9] V. F. Lotrich and K. Szalewicz, J. Chem. Phys. **106**, 9668 (1997).
[10] R. Moszynski, P. E. S. Wormer, B. Jeziorski, and A. van der Avoird, J. Chem. Phys. **103**, 8058 (1995); Erratum: **107**, 672 (1997).
[11] *SAPT2002: An Ab Initio Program for Many-Body Symmetry-Adapted Perturbation Theory Calculations of Intermolecular Interaction Energies* by R. Bukowski *et al.*, University of Delaware and University of Warsaw.
[12] S. Rybak, B. Jeziorski, and K. Szalewicz, J. Chem. Phys. **95**, 6576 (1991).
[13] S. Rybak, K. Szalewicz, B. Jeziorski, and M. Jaszunski, J. Chem. Phys. **86**, 5652 (1987).
[14] R. Moszynski, B. Jeziorski, and K. Szalewicz, Int. J. Quantum Chem. **45**, 409 (1993).
[15] H.L. Williams, K. Szalewicz, B. Jeziorski, and R. Moszynski, J. Chem. Phys. **103**, 4586 (1995).
[16] J. Paldus and J. Cizek, Adv. Quantum Chem. **9**, 105 (1975); R.J. Bartlett, J. Phys. Chem. **93**, 1697 (1989).
[17] X. Wu, M.C. Vargas, S. Nayak, V. Lotrich, and G. Scoles, J. Chem. Phys. **115**, 8748 (2001).
[18] H.L. Williams and C.F. Chabalowski, J. Phys. Chem. A **105**, 646 (2001).
[19] A.J. Misquitta and K. Szalewicz, Chem. Phys. Lett. **357**, 301 (2002).
[20] A. Hesselmann and G. Jansen, Chem. Phys. Lett. **357**, 464 (2002); *ibid.* **362**, 319 (2002).

[21] T. Korona, H.L. Williams, R. Bukowski, B. Jeziorski, and K. Szalewicz, J. Chem. Phys. **106**, 5109 (1997).
[22] A.J. Misquitta and K. Szalewicz, manuscript in preparation.
[23] A.J. Misquitta, B. Jeziorski, and K. Szalewicz, submitted for publication.
[24] A. Hesselmann and G. Jansen, Chem. Phys. Lett. **367**, 778 (2003).
[25] Y. Dmitriev and G. Peinel, Int. J. Quantum. Chem. **19**, 763 (1981).
[26] R. McWeeny, Croat. Chem. Acta **57**, 865 (1984).
[27] M. Jaszunski and R. McWeeny, Mol. Phys. **55**, 1275 (1985); Errata: **57**, 1317 (1986).
[28] P.J. Knowles and W.J. Meath, Chem. Phys. Lett. **124**, 164 (1986); Mol. Phys. **59**, 965 (1986).
[29] S.M. Colwell, N.C. Handy, and A.M. Lee, Phys. Rev. A **53**, 1316 (1996).
[30] A.G. Ioannou, S.M. Colwell, and R.D. Amos, Chem. Phys. Lett. **278**, 278 (1997).
[31] D.J. Tozer and N.C. Handy, J. Chem. Phys. **109**, 10180 (1998).
[32] G. Murdachaew and K. Szalewicz, Faraday Discuss. **118**, 121 (2001).
[33] G. Murdachaew, K. Szalewicz, and R. Bukowski, Phys. Rev. Lett. **88**, eid. 123202 (2002).
[34] G. Murdachaew, R. Bukowski, and K. Szalewicz, manuscript in preparation.
[35] V.F. Lotrich and K. Szalewicz, J. Chem. Phys. **112**, 112 (2000).
[36] P.E.S. Wormer, R. Moszyński, and A. van der Avoird, J. Chem. Phys. **112**, 3159 (2000).
[37] V.F. Lotrich and K. Szalewicz, Phys. Rev. Lett. **79**, 1301 (1997).
[38] A.K. Sum, S.I. Sandler, R. Bukowski, and K. Szalewicz, J. Chem. Phys. **116**, 7627 (2002); A.K. Sum, S.I. Sandler, R. Bukowski, and K. Szalewicz, J. Chem. Phys. **116**, 7637 (2002).
[39] M.P. Hodges, A.J. Stone, and S.S. Xantheas, J. Phys. Chem. A **101**, 9163 (1997).
[40] A. Milet, R. Moszynski, P.E.S. Wormer, and A. van der Avoird, J. Phys. Chem. A **103**, 6811 (1999).
[41] V.F. Lotrich and K. Szalewicz, J. Chem. Phys. **106**, 9688 (1997).
[42] E.M. Mas, K. Szalewicz, R. Bukowski, and B. Jeziorski, J. Chem. Phys. **107**, 4207 (1997).
[43] P.E.S. Wormer and H. Hettema, J. Chem. Phys. **97**, 5592 (1992); P.E.S. Wormer and H. Hettema, POLCOR package, University of Nijmegen, The Netherlands, 1992.
[44] O. Akin-Ojo *et al.*, work in progress.
[45] H. Koch, B. Fernandez, and J Makarewicz, J. Chem. Phys. **111**, 198 (1999).
[46] C. Hättig, G. Jansen, B.A. Hess, and J.G. Ángyán, Mol. Phys. **91**, 145 (1997).

A. Miani, J. Tennyson and T. van Mourik (eds.)
High Accuracy Potentials for Quantum Dynamics

Accurate Coupled-Cluster Potential Energy Surfaces: Large Calculations on Cyclopropenylidene Anharmonicities

Timothy J. Lee[a] and Christopher E. Dateo[b]

[a] *MST27B-1, NASA Ames Research Center, Moffett Field, CA 94035-1000, USA*

[b] *Eloret Corporation, MST27B-1, NASA Ames Research Center, Moffett Field, CA 94035-1000, USA*

I. INTRODUCTION

The singles and doubles coupled-cluster method that includes a perturbational correction for connected triple excitations, CCSD(T), has been used extensively in recent years to compute accurate potential energy surfaces (PESs) for use in dynamics calculations, especially determination of vibrational or rovibrational energy levels (for example, see Refs. 1-4, and references therein). However, CCSD(T) calculations become prohibitively expensive, especially when considering the number of points needed for a potential energy surface, once the one-particle basis set approaches 250 to 300 basis functions. For calculations of this size or larger, researchers have generally performed a few calculations that are then used to modify or improve a PES computed with a smaller one-particle basis set.

The reason that large basis set CCSD(T) calculations become prohibitively expensive is largely due to the amount of data manipulation and/or I/O that must be done. For accurate CCSD(T) calculations, large one-particle basis sets are used, beginning with at the very least a basis similar in quality to Dunning's cc-pVTZ basis. In this case, the number of $(vv|vv)$ integrals will far exceed the number of all other types of integrals, were v refers to a virtual molecular orbital in the reference function. In addition, the number of $(ov|vv)$ molecular orbital integrals will far exceed the remaining types, specifically $(ov|ov)$, $(oo|vv)$, $(oo|ov)$, and $(oo|oo)$, where o refers to an occupied molecular orbital in the reference function.

It is possible to use integral direct coupled-cluster methods to avoid the I/O, but this does not reduce the amount of data manipulation, and significantly

increases the CPU time of a CCSD calculation due to recomputation of the atomic orbital integrals during each iteration of the coupled-cluster procedure (for example, see Ref. [4]). In addition, the (T) perturbative correction is not as amenable to integral direct techniques. We point out that reduction of the amount of data to be used is important, not just to make single processor calculations run more efficiently, but even more so that distributed memory parallel coupled-cluster calculations will run efficiently.

In 1994, Rendell and Lee [5] proposed a method in which the $(vv|vv)$ and $(ov|vv)$ classes of integrals would be approximated by use of a resolution of the identity (RI) in the form of the "V" approximation defined by Vahtras et al. [6]

$$(ab|cd) = \sum (ab|m)(m|cd) \quad (1)$$

$$(ia|cd) = \sum (ia|m)(m|cd) \quad (2)$$

Equations (1) and (2) assume that the two-center V matrix has been included according to the form given in Ref. 5. The interested reader is referred to Ref. 5 for complete details. In 1994, the performance of computers was somewhat different to that of today, and thus Rendell and Lee proposed using this approximation to eliminate storage and I/O bottlenecks. However, disc storage has become inexpensive, such that it is usually not a bottleneck in CCSD(T) calculations today, although I/O remains a bottleneck, especially for PCs. Currently, high performance computing is almost entirely defined as distributed memory parallel computing, and in spite of considerable effort (see Ref. 7 and references therein), CCSD(T) codes do not generally scale well in a distributed memory parallel environment.

It is our contention that the method proposed by Rendell and Lee holds the most promise in allowing large, accurate CCSD(T) calculations to be run efficiently in both single processor and distributed memory parallel environments. Incorporation of Equations (1) and (2) into the coupled-cluster procedure significantly reduces the amount of data that must be either read from disc (i.e., I/O) or distributed through message passing in a parallel environment. Hence the use of approximate $(vv|vv)$ and $(ov|vv)$ integrals not only benefits serial CCSD(T) calculations, but it makes development of a distributed memory parallel code simpler due to the significant reduction in data. We point out that use of approximate integrals for the $(vv|vv)$ and $(ov|vv)$ classes of integrals may be performed in conjunction with local correlation CCSD(T) techniques, thereby reducing the amount of data manipulation necessary in those calculations as well, although for purposes of determining a PES for dynamics calculations, the local correlation technique must be sufficiently reliable and not lead to a "bumpy" surface. The one remaining question is to what extent the use of

approximate $(vv|vv)$ and $(ov|vv)$ integrals affects the accuracy of a CCSD(T) PES. Below we discuss a benchmark study on the fundamental vibrational frequencies of cyclopropenylidene.

II. RESULTS AND DISCUSSION

We have studied the fundamental vibrational frequencies of cyclopropenylidene previously [8]. In Ref. 8, we used the CCSD(T) method in conjunction with the cc-pVTZ one-particle basis set to compute a quartic force field for cyclopropenylidene. Second-order rovibrational perturbation theory was then used to compute fundamental vibrational frequencies and other spectroscopic constants. In the present study we have computed a CCSD(T)/cc-pVTZ quartic force field using approximate $(vv|vv)$ and $(ov|vv)$ integrals as outlined above. We will also present results for geometry optimizations and harmonic frequencies determined with the cc-pVQZ basis set and for basis sets that allow for correlation of the carbon $1s$ core electrons. For all of the calculations involving approximate integrals, the RI basis was taken simply as the full atomic orbital basis.

The errors in the CCSD(T) calculations when using approximate $(vv|vv)$ and $(ov|vv)$ integrals are small and become smaller as the basis set is improved. For the cc-pVTZ basis set, the average absolute error in the C-C and C-H bond distances is only 0.00025 Å while for the cc-pVQZ basis set the average absolute error reduces to only 0.00003 Å. The average absolute error for the two unique bond angles in cyclopropenylidene is also very small: 0.009 degrees for the cc-pVTZ basis set and 0.0015 degrees for the cc-pVQZ basis set. For the harmonic frequencies the average absolute errors are also acceptably small: 0.76 cm^{-1} for the cc-pVTZ basis set and 0.20 cm^{-1}. For the cc-pVTZ fundamental frequencies, the average absolute error is 1.66 cm^{-1}, which is somewhat larger than that for the harmonic frequencies, but still acceptably small. Further investigations of the effect of the use of approximate $(vv|vv)$ and $(ov|vv)$ integrals on the anharmonic corrections and other spectroscopic constants will be discussed. The reduction in data is significant for these calculations. For the cc-pVTZ basis set (C_1 symmetry calculation), the $(vv|vv)$ integrals use 0.523 Gb of disc space, while the $(ov|vv)$ integrals use 0.069 Gb. The next largest class of integrals use only 0.019 Gb. In contrast, the $(vv|m)$ integrals would use only 0.005 Gb of file space. For larger basis sets, the savings are even more significant, while the error becomes even smaller! For example, the $(vv|vv)$, $(ov|vv)$, and $(vv|m)$ integrals use 8.053 Gb, 0.523 Gb, and 0.039 Gb, respectively, for a C_1 symmetry calculation with the cc-pVQZ basis set. The core-correlation basis set is even larger, and results for this basis set will also be presented and discussed.

III. CONCLUDING REMARKS

The use of approximate $(vv|vv)$ and $(ov|vv)$ integrals in CCSD(T) calculations leads to a significant reduction in data that must be either read from disk or stored in memory and accessed through message passing in a distributed memory parallel implementation. Through our benchmark study on the anharmonicities and spectroscopic constants of cyclopropenylidene, we show that approximating these integrals leads to very small errors relative to the exact integral CCSD(T) results. In fact, the error is significantly less than the residual one-particle basis set error. Based on these results, it is our assertion that the use of approximate $(vv|vv)$ and $(ov|vv)$ integrals is cost-effective when evaluating an accurate CCSD(T) PES for use in dynamics calculations, especially when using a one-particle basis set of at least cc-pVTZ quality, and the effectiveness increases with larger one-particle basis sets. An analysis of timings will be presented in order to demonstrate this assertion. We will discuss strategies for when this approach should be used. We will also discuss our efforts for development of a production level code for approximate integral CCSD(T) calculations.

Acknowledgments

Christopher E. Dateo gratefully acknowledges support from the NASA prime contract NAS2-00062.

---

[1] J. M. L. Martin, T. J. Lee, and P. R. Taylor, J. Chem. Phys. **108**, 676 (1998).
[2] T. J. Lee and C. E. Dateo, Spectrochim. Acta **55A**, 739 (1999).
[3] T. J. Lee and J. M. L. Martin, Chem. Phys. Lett. **357**, 319 (2002).
[4] H. Koch, A. Sanchez de Meras, T. Helgaker, and O. Christiansen, J. Chem. Phys. **104**,4157 (1996).
[5] A. P. Rendell and T. J. Lee, J. Chem. Phys. **101**, 400 (1994).
[6] O. Vahtras, J. Almlf, and M. Feyereisen, Chem. Phys. Lett. **213**, 514 (1993).
[7] R. Kobayashi and A. P. Rendell, Chem. Phys. Lett. **265**, 1 (1997).
[8] C. E. Dateo and T. J. Lee, Spectrochim. Acta **53A**, 1065 (1997).

A. Miani, J. Tennyson and T. van Mourik (eds.)
High Accuracy Potentials for Quantum Dynamics

Vibrational Effects on Molecular Properties: the Dalton Approach

Trygve Helgaker and Torgeir A. Ruden,[a] Dan Jonsson,[b] Kenneth Ruud,[c] Peter R. Taylor[d] and Per-Olof Åstrand[e]

[a] *Department of Chemistry,University of Oslo,Box 1033 Blindern, N-0315 Oslo, Norway*
[b] *Department of Physics, Stockholm University, AlbaNova University Centre, SE-106 91 Stockholm, Sweden*
[c] *Department of Chemistry, University of Tromsø, N-9037 Tromsø, Norway*
[d] *Department of Chemistry, University of Warwick, Coventry CV4 7AL, UK*
[e] *Department of Chemistry, NTNU, N-7491 Trondheim, Norway*

I. INTRODUCTION

Quantum chemistry is now capable of calculating numerous molecular properties to high accuracy. Comparing these calculations with experimental measurements requires more than performing a single calculation at a particular nuclear geometry, however. In the real world the nuclei are moving, giving rise to various nuclear-motion contributions to properties. Perhaps the most obvious is vibrational averaging — the property of interest must be averaged over a given vibrational state or states (most commonly the zero-point level). For some properties there may be a contribution purely from the nuclear motion, such as the dipole moment in HD, or the so-called "pure vibrational" contributions to electric and magnetic properties. In addition, rotational motion may play a role, for example via centrifugal distortion. In this paper we will look at different methods for accounting for vibrational contributions to properties in the Dalton quantum chemistry program [1].

Dalton is a freely available program for calculating molecular properties at the SCF, DFT, MP2, MCSCF and CC levels. There is a particular emphasis on electric (static and frequency-dependent) and magnetic properties, response methods, and potential energy surfaces. Rather than include a laundry list here we refer the interested reader to the Dalton website [2] for full details on the capabilities of the program, and how to obtain a copy. In what follows

we will concentrate exclusively on the treatment of nuclear motion. We first discuss manual and automatic methods for generating a property surface (the variation of a given property with geometry), and then methods for carrying out vibrational averaging of properties very efficiently. Finally, we will briefly mention pure vibrational contributions to electric and magnetic properties.

II. PROPERTY SURFACES BY HAND

The most obvious way to calculate the geometry dependence of a property is simply to run the program multiple times at a range of geometries, computing the property on a grid. This is an obvious, if somewhat ad hoc, tactic, used with all programs for more than forty years, and we mention it here only for completeness and to remind the reader of its weaknesses. Namely, a large number of calculations must be performed, even if we are interested only in low-lying vibrational levels, unless the molecule is very small (say, four atoms or fewer). Further, the resulting points must be fitted to some sort of multidimensional surface, itself often a time-consuming step, especially when large variations in geometry are considered.

III. PROPERTY SURFACES AUTOMATICALLY

Often, a more elegant approach is to write the property dependence on geometry as a Taylor expansion around a minimum in the energy. This is particularly useful where over the region of interest the property can be well approximated by rather low-order derivatives like fourth or fifth. We then face the perennial dilemma of quantum chemistry: do we implement analytical formulas for the various derivatives, or compute them by finite differences? And if the latter, do we compute higher derivatives as finite differences of energies, or as finite differences of lower derivatives? The analytical approach is always to be preferred on the grounds of efficiency and precision, so the answers to these questions are determined primarily by the effort required to program the analytical derivatives. Dalton can calculate analytical nuclear-motion gradients for almost all methods and nuclear-motion Hessians for many, although not for CC methods (ACES II offers that capability [3]). Dalton does, however, offer analytical derivatives with respect to other perturbations, such as electric and magnetic fields (external and internal) through fourth order.

Finite difference estimates have been programmed automatically [4], using a

general recursive finite difference formula

$$\left.\frac{d^n P}{dx_1^{n_1}\, dx_2^{n_2} \cdots dx_m^{n_m}}\right|_{\mathbf{X}=\mathbf{X}_0} = \delta^{-n} \sum_{k_1,k_2,\ldots k_m} b_{k_1}^{n_1} b_{k_2}^{n_2} \cdots b_{k_m}^{n_m} P\left(x_1^0 + k_1\delta, x_2^0 + k_2\delta, \cdots, x_m^0 + k_m\delta\right) \quad (1)$$

for the property P and displacements δ, where the summation ranges are $-\lfloor (n_l+1)/2 \rfloor \leq k_l \leq \lfloor (n_l+1)/2 \rfloor$. The factors b_k^n are given by

$$b_k^{n=2i} = a_{2k}^{2i}; \quad b_k^{n=2i+1} = \frac{1}{2}\left(a_{2k-2}^{2i} - a_{2k+2}^{2i}\right), \quad (2)$$

where the auxiliary coefficients a_i^n are given by

$$a_0^0 = 1; \quad a_i^n = a_{i-1}^{n-1} - a_{i+1}^{n-1}, \quad (3)$$

noting that $a_i^n = 0$ for $i \rangle n$. Eq. 1 allows us to compute any derivative desired of a given property. The property may itself be an energy derivative, so for example in principle we could calculate an eighth derivative of the energy by numerically calculating the fourth derivative with respect to nuclear motion of an analytically computed second hyperpolarizability.

In practice, of course, there are numerical issues to contend with in the use of Eq. 1. One would like to keep the displacements δ as small as possible to minimize the error from contamination of the finite difference estimates by higher derivative contributions. On the other hand, the smaller the δ, the more precision is needed in the calculation to ensure meaningful results. A simple analysis [4] leads to an estimate for the optimum displacement for calculating the nth-order derivative as

$$\delta = \left(\frac{\epsilon}{\alpha}\right)^{\frac{1}{n+2}}, \quad (4)$$

where the property P is determined to within an accuracy ϵ and α is an order-of-magnitude estimate of the $(n+2)$th derivative of P.

For higher derivatives or many nuclei, the finite-difference approach still requires many calculations and it is therefore desirable to use additional means to reduce this number. Accordingly, Dalton uses the full symmetry of the molecule (including groups with higher-order axes, although currently cubic groups are not accommodated) to determine which derivatives are symmetry-independent and non-zero [4]. Only these are computed, after which the nonzero symmetry-dependent derivatives are generated from the appropriate formulas. The actual property calculations within Dalton use at most D_{2h} and its subgroups. Where

there are different possible choices of independent and dependent derivatives, Dalton automatically chooses as the independent values those that will retain the highest symmetry after the nuclei are displaced, leading to the fastest property calculations.

Once all the desired derivatives are computed, the Taylor expansion can be used to calculate the vibrational averages of the property, spectroscopic constants, etc. In addition to harmonic frequencies, Dalton can calculate vibrationally averaged geometries [4] and vibrationally averaged spin–spin coupling constants [5] using second-order perturbation theory to treat vibrational motion. Another possibility is to use the derivatives as input into a suitable vibrational wave function program. We have made much use of the program SPECTRO [6], which also employs second-order perturbation theory to treat vibrations. Once again, for many atoms in the molecule this can require considerable work. For vibrationally averaged molecular properties, at least over low-lying vibrational levels, another approach based on a slightly different Taylor expansion can be used.

IV. PROPERTY SURFACES EXPANDED AROUND AN EFFECTIVE GEOMETRY

As we noted in the previous section, the usual Taylor expansion of a property is performed around a minimum in the potential energy surface, at which the nuclear-motion gradient is of course zero. If the property of interest is expanded around the same point, a perturbation-theoretic analysis can be used to derive approximate formulas for the corrections to the property for, e.g., zero-point motion [7]. A knowledge of at least the cubic terms in the potential, as well as the second derivative of the property with respect to nuclear displacements, is required. We can recast the calculation of vibrational corrections to properties in the following way.

Instead of expanding the potential and the property surface around a minimum (the equilibrium geometry, designated r_e, and characterized by $E_j^{(1)} = 0$, where $E_j^{(1)}$ is an element of the nuclear-motion gradient vector), we expand around a new point r_{eff} by minimizing not the electronic energy E but $E + \frac{1}{2}\sum_i \omega_i$: the sum of the electronic energy and the zero-point vibrational energy [8]. It is straightforward to show that at r_{eff} we have

$$E_j^{(1)} + \frac{1}{4}\sum_i \frac{E_{iij}^{(3)}}{\omega_i} = 0, \tag{5}$$

which is a relationship between the nuclear-motion gradient and the third derivatives [9]. This can in fact be used to develop a method for a single-step

calculation of $r_{\rm eff}$, starting from r_e, since some simple manipulations give

$$r_{{\rm eff},j} = r_{e,j} - \frac{1}{4\omega_j^2} \sum_i \frac{E^{(3)}_{e,jii}}{\omega_i}, \tag{6}$$

where the third derivatives are evaluated at r_e.

What are the advantages of this reformulation? First, the $r_{\rm eff}$ geometry is easily shown to be the geometry averaged over the zero-point vibrational level [9]: this is often denoted r_0, although strictly speaking an experimental r_0 geometry would be derived from the zero-point-averaged rotational constant B_0, which is not quite the same thing. Second, in the perturbation-theoretic expressions for the vibrationally averaged property, the contribution from the leading term in the anharmonicity of the potential vanishes. We can expect much better convergence of the perturbation series under these circumstances. This modified expansion point was originally suggested for use in, e.g., hydrogen-bonded complexes, where the intermolecular potential is very anharmonic, and it performs very well there. In the calculation of vibrationally averaged properties, its use means that we require only the property evaluated at the new expansion point, and the diagonal second derivatives of that property with respect to normal coordinates, evaluated again at $r_{\rm eff}$ [10].

The calculation of the expansion point $r_{\rm eff}$ and vibrationally averaged properties is completely automated in Dalton [10]. The user first calculates the r_e geometry at the desired level of computation. Dalton then determines the $r_{\rm eff}$ geometry, a step which requires evaluation of the Hessian and $2(3N-6)+1$ gradient evaluations for an N-atom molecule. Finally, at the $r_{\rm eff}$ geometry the second derivatives of the property are calculated and used in the perturbation-theoretic expressions for the vibrationally averaged properties. This requires an additional Hessian evaluation and $2(3N-6)+1$ property evaluations. The program uses normal coordinates — since the expansion point is not the minimum of the potential a projection operator is applied to eliminate translational and rotational motion from the Hessian. We note also that Eckart axes are used to ensure that property tensors behave continuously as the geometry changes from r_e to $r_{\rm eff}$.

We may note finally here that for some properties it may be possible to construct empirical rules for the effects of vibration. For example, for proton NMR shieldings (chemical shifts) it has been possible to devise a table of additive functional-group contributions which when added to chemical shifts calculated at r_e provide a rather accurate estimate of the effects of zero-point vibration [11]. Unfortunately it is not always possible to do this: we were unable to estimate useful functional-group vibrational corrections for ^{13}C or ^{17}O chemical shifts, for instance. Other applications of this approach are described in a forthcoming review [12].

V. PURE VIBRATIONAL CONTRIBUTION TO PROPERTIES

In addition to the vibrational contributions to properties obtained by averaging over zero-point motion, there is another possible contribution from vibration (see, e.g., Ref. [13]). We denote vibronic states of the system by $|Kk\rangle$, where K labels electronic states and k vibrational levels within those states, and as a simple illustration, we consider the ground state and a static second-order property given by

$$P_{00} = \sum_{Kk \neq 00} \frac{\langle 00|\mathscr{O}_1|Kk\rangle\langle Kk|\mathscr{O}_2|00\rangle}{E_{Kk} - E_0}, \tag{7}$$

where $\mathscr{O}_1$ and $\mathscr{O}_2$ are appropriate operators (dipole operators for P the polarizability, for example).

We can distinguish two cases of interest here: $K = 0$ (in which case $k \neq 0$), and $K \neq 0$. The former involves contributions from the excited vibrational levels of the ground electronic state to the property of interest. It is this contribution that constitutes the "pure vibrational" contribution to P: it can be seen to involve vibrational transition moments over the operators $\mathscr{O}_1$ and $\mathscr{O}_2$. Conversely, terms in Eq. 7 in which $K \neq 0$ but $k = 0$ comprise the zero-point averaged property value discussed in the previous section. Obviously there may also be contributions from terms in which both $K \neq 0$ and $k \neq 0$, but this is beyond the scope of our analysis here.

Eq. 7 is, as noted, a simplified example for illustration. In practice we may be interested in higher-order properties, such as hyperpolarizabilities, and frequency-dependent as well as static values. General expressions for pure vibrational frequency-dependent higher polarizabilities were given by Bishop and Kirtman [13], and similar formulas for the hypermagnetizability (a fourth-order property involving two electric and two magnetic perturbations) were given by Ruud et al [14]. These formulas involve products of frequency-dependent property derivatives, which are computed in Dalton using analytical linear, quadratic and cubic response functions. An auxiliary program is used to calculate the necessary property derivatives and to combine them, giving the pure vibrational contributions.

VI. CONCLUSIONS

We have reviewed here, rather superficially, various approaches available within the Dalton quantum chemistry program for calculating the contributions molecular vibrations make to molecular properties. In the space available it is

impossible to discuss numerical results, for which the reader is referred to the original literature. We emphasize here, however, that if the goal is to perform accurate calculations that can be compared with experiment, the treatment of vibrational effects is indispensable.

Acknowledgments

Part of this work was performed when some of the authors were at the University of California, San Diego, where the work was supported by the National Science Foundation through Grant No. CHE-9700627 and Cooperative Agreement No. DACI-9619020, and by a grant of computer time from the San Diego Supercomputer Center. The work was also supported by the Wolfson Foundation through the Royal Society.

---

[1] T. Helgaker, H. J. A. Jensen, P. Jørgensen, J. Olsen, K. Ruud, H. Ågren, A. A. Auer, K. L. Bak, V. Bakken, O. Christiansen, S. Coriani, P. Dahle, E. K. Dalskov, T. Enevoldsen, B. Fernandez, C. Hättig, K. Hald, A. Halkier, H. Heiberg, H. Hettema, D. Jonsson, S. Kirpekar, R. Kobayashi, H. Koch, K. V. Mikkelsen, P. Norman, M. J. Packer, T. B. Pedersen, T. A. Ruden, A. Sanchez, T. Saue, S. P. A. Sauer, B. Schimmelpfennig, K. Sylvester-Hvid, P. R. Taylor and O. Vahtras, Dalton, an ab initio electronic structure program, Release 1.2.

[2] `http://www.kjemi.uio.no/software/dalton/dalton.html`.

[3] J. F. Stanton and J. Gauss, *Int. Rev. Phys. Chem.* **19**, 61 (2000).

[4] T. A. Ruden, P. R. Taylor, and T. Helgaker, *J. Chem. Phys.* (submitted for publication).

[5] T. A. Ruden, O. B. Lutnæs, T. Helgaker and K. Ruud, *J. Chem. Phys.* (in press).

[6] SPECTRO v7.0 (1999), written by J.F. Gaw, A. Willets, W.H. Green, and N.C. Handy.

[7] C. W. Kern and R. L. Matcha, *J. Chem. Phys.* **49**, 2081 (1968).

[8] P.-O. Åstrand, G. Karlström, A. Engdahl, and B. Nelander, *J. Chem. Phys.* **102**, 3534 (1995).

[9] P.-O. Åstrand, K. Ruud, and P. R. Taylor, *J. Chem. Phys.* **112**, 2655 (2000).

[10] K. Ruud, P.-O. Åstrand, and P. R. Taylor, *J. Chem. Phys.* **112**, 2668 (2000).

[11] K. Ruud, P.-O. Åstrand, and P. R. Taylor, *J. Am. Chem. Soc.* **123**, 4826 (2001).

[12] K. Ruud, P.-O. Åstrand, and P. R. Taylor, *J. Comp Meth. Sci. Eng.* (in press).

[13] D. M. Bishop and B. Kirtman, *J. Chem. Phys* **95**, 2646 (1991).

[14] K. Ruud, D. Jonsson, and P. R. Taylor, *Phys. Chem. Chem. Phys.* **2**, 2161 (2000).

A. Miani, J. Tennyson and T. van Mourik (eds.)
High Accuracy Potentials for Quantum Dynamics

Subwavenumber Accuracy for the *Ab Initio* Rotation-Vibration Transitions of Water.

Oleg Polyansky

Department of Physics and Astronomy, University College London, Gower Street, WC1E 6BT, London, UK

In this paper I would like to present the results of extensive efforts of a big group of researchers [1] to increase the accuracy of *ab initio* calculations of water monomer molecular spectrum. Why anyone would bother to do that? There are many reasons. The description of motivation falls naturally into two parts – first – the reason for the precise *ab initio* calculations of any molecule – and second - the particular interest in water.

The development of high resolution molecular spectroscopy started with the microwave spectra of small molecules - like ammonia. The experimental observations of the molecular lines were very accurate - with kHz accuracy and were limited in the spectral region. Moreover they were limited to the mostly ground vibrational state of molecules, as the room temperature Boltzmann factor allowed only strong lines in the ground state to be observed. The vibrational spectra of molecules were observed with much less accurate experimental tools. Thus the theory of calculation of high resolution molecular spectra was concentrated in the very accurate knowledge of the energy levels in the isolated vibrational state (primarily ground state). Very accurate phenomenological theory of effective Hamiltonians was developed based on the perturbation theory.

The experimental developments in the last two decades have required a drastic change of viewpoint. The observation of infrared and optical spectra started to catch up with the microwave in its sophistication and accuracy mostly due to the developments of the lasers. The sensitivity of the spectrometers went up and up so that the line density became higher and higher. Warming the cell produced spectra at hundreds and even thousands of degrees. Spectra with a density of lines up to 50 per wavenumber began to appear. The culmination of this process was the observation of the predissociation spectrum of H_3^+ by Carrington and coworkers [2] which resulted in the line density of 300 per wavenumber. This process changed the accent of theory. Reproduction to experimental accuracy of a few kHz lines belonging to low lying vibrational states became a secondary issue. The major problem gradually changed to the task of calculating the

lines with infrared accuracy (about 10^{-3} of cm^{-1}) but for all the vibrational-rotational states up to dissociation.

Fortunately lasers as a tool of experimentalists appeared about the same time as computers, the tool for theoreticians began to develop explosively. The key technique for calculations of vibration-rotation energy levels for triatomic molecules was the numerical computer simulation of spectra based on variational calculations. The exact kinetic energy operator in internal coordinates developed by Sutcliffe and the numerical technique developed by Tennyson and Sutcliffe [3] allows us to switch from phenomenological perturbation calculations of the rotational levels in the low lying vibrational states to the calculation of all the rotation-vibration levels up to dissociation. This technique gives us the opportunity to calculate these energy levels to infinite accuracy, provided the Born-Oppenheimer approximation holds and we find the way to calculate infinitely accurate potential energe surfaces (PES).

This is a critical point. Comparison of the accuracy of calculations of energy levels using two PES - one obtained by pure fitting of the PES to experimental energy levels (PJT) [4] and the other - using a very accurate *ab initio* PES as a starting point for the subsequent fit to the experimental levels due to Partridge and Schwenke (PS) [5] shows, that the improvment is of about one order of magnitude. This extremely important fact alone necessitates the development of methods for very accurate *ab initio* potential calculations. Apart from the necessity of using *ab initio* PES as a starting point for better fitted surfaces, with the final goal of obtaining experimental accuracy for the fitted energy levels, there are other reasons for the accurate *ab initio* calculations of PES. Among them are problems with the extrapolation using fitted surfaces. It is well known, that whereas the optimisation of parameters gives excellent results for the interpolation - the extrapolation of the energy levels beyound the scope of energies used in the fit is often problematic. This problem is even more severe for the important problem of the calculation of intensities - fitted dipole moment surfaces turn out to be much less reliable, then the *ab initio* ones.

The conclusion is that accurate *ab initio* surfaces are indispensible for accurate variational calculations of rotation-vibration energy levels of molecules in highly excited states. The use of such calculated energy levels in spectral analysis of molecular spectra would result in better understanding of experimentally observed molecular spectra. Let me give you few examples.

1. Already mentioned Carrington's H_3^+ spectrum which has defied interpretation for 20 years since its first observation [2]

2. The sunspot spectrum [6], only a portion of which - up to 15 % of the lines - we managed to assign.

3. Difference bands spectra of water [7] which we assigned only due to

accurate variational calculations of water PES [4].

4. The weak lines of the infrared and optical spectrum of water up to ultraviolet spectral region. Analysis of these lines is necessary for the accurate modelling of water in the Earth's atmosphere.

5. High temperature water spectra in the laboratory and in the atmosphere of cool stars.

As most examples of spectra given in the previous paragraph belong to water, it is appropriate to say a few words on the second part of the motivation for this work. The reason we concentrated on the water molecule is twofold. The importance of water for the atmospheric absorption, astrophysics and flame analysis resulted in very extensive experimental observations of the spectra of this molecule. Hence thousands of energy levels of different water isotopomers up to very highly excited vibrational and rotational quantum numbers are known experimentally, which allows us to make the comparison of our calculations on water energy levels with this extensive set of experimental data. Almost 18 000 levels were used to calcualte the standard deviation of our calculations. In turn it allows us to produce reliable predictions for the levels not yet observed experimentally and waiting their assignment and understanding.

As the question of motivation of our developments is covered by the above paragraphs let us consider the details of our most recent calculations.

The best previous water potential has been published in 1997 by Partridge and Schwenke [5]. For that calculation the MOLPRO program was used [8] at the multireference configuration interaction (MRCI) level. A basis set with the partially augmented 5z level was used. A core-valence correction to this surface was also calculated. Already in that paper [5] it was clear, that the futher increase of the basis set to 6z level would give quite significant contribution to at least angular dependence of the *ab initio* energies. In [5] a table was presented where the deviation of 6z basis set calculations from partially augmented 5z was up to 60 cm^{-1} from equilibrium at about 104° to linear - 180° positions. This deviation might contribute up to a few tens of cm^{-1} to the bending vibrational levels. Our calculations of the relativistic correction in [9] gave a significant improvement in the stretching energy levels in comparison with PS, but worsened bending levels by up to 20 cm^{-1}. It became clear, that a further increase of the basis set up to 6z or even higher was necessary in order to obtain better agreement with experiment. Our phenomenological one-dimensional correction to the barrier to linearity to PS potential [10], which modelled a possible effect of a 6z basis set calculation, proved that at least few times better standard deviation was achievable, provided we could use 6z basis set for our calculations. These calculations proved to be computationally very demanding, but doable with the modern computer power. 64 processors

TABLE I: Predicted vibrational band origins (VBOs) for various theoretical models [1]. Results are presented as differences from the observed values in cm^{-1}. The standard deviation, σ, is for all experimentally known VBOs.

state	obs [19]	5Z	6Z	CBS	CBS+CV	+rel	+qed	+BODC
(010)	1594.74	−2.99	−2.29	−0.32	0.48	−0.81	−0.75	−0.32
(020)	3151.63	−4.22	−2.38	−0.78	1.16	−1.57	−1.44	−0.56
(030)	4666.78	−6.30	−3.24	−1.52	2.05	−2.37	−2.16	−0.78
(040)	6134.01	−9.81	−5.53	−2.74	3.20	−3.30	−3.00	−1.06
(050)	7542.43	−14.70	−9.18	−4.71	4.82	−4.45	−4.02	−1.41
(101)	7249.81	12.51	10.76	9.32	−5.35	1.70	1.43	0.60
(201)	10613.35	18.72	16.46	13.97	−7.47	2.98	2.57	1.23
(301)	13830.93	25.72	22.81	18.74	1.95	4.59	4.06	2.05
(401)	16898.84	32.56	28.92	23.06	−10.17	6.11	5.49	2.74
(501)	19781.10	40.72	35.96	28.68	−10.72	9.04	8.28	4.65
(601)	22529.44	51.14	43.41	34.17	−11.88	11.69	10.81	5.94
(701)	25120.27	63.29	51.75	38.66	−13.13	13.70	12.75	6.46
all	σ	22.84	19.74	16.56	7.85	4.23	3.83	1.90

5Z=aug-cc-pV5Z MRCI; 6Z=aug-cc-pV6Z MRCI; CBS=MRCI extrapolated to the complete basis set limit; CBS+CV=CBS + core correlation relation; rel=CBS+CV with relativistic effects; QED=rel with one electron Lamb shift; BODC=QED with Born-Oppenheimer Diag. Correc.

calculation on the 512 processor Origin3000 at Manchester University computer center turned out to be necessary to calculate one point at the MRCI level with a 6z basis set. Up to three hours per point was the computer time requirement. We calculated about 400 points in order to produce *ab initio* PES valid up to 30000 cm^{-1}. Modelling of the behaviour of infinite basis set by the complete basis set extrapolation [7] of the set of quadruple-zeta, 5z and 6z basis set proved to be also important to improve further the overall accuracy of the final results (see below). However, just brute force increase in the basis set is limited (a 7z basis set is hardly doable at present at the MRCI level) and does not completely solve the accuracy problem when the goal is to obtain better then 1 cm^{-1} results.

A matter of immense importance for that purpose is the effects of the breakdown of Born-Oppenheimer approximation. In [11] several years ago we showed, using phenomenologically constructed surfaces, that the problem of deuterium isotopomers of H_3^+ could be solved using the adiabatic mass dependent correction to the Born-Oppenheimer surface. High quality *ab initio* surfaces accurate to 1 cm^{-1} [9] were obtained for H_3^+ already 10 years ago, since

TABLE II: Standard deviation (σ) with which our final (CBS+CV+rel+QED+BODC) potential reproduces the vibrational-rotation term values. [7]

Isotopomer	σ	$J_{\max}$	N(levels)	Maximum Deviation	
	cm^{-1}			obs−calc	J
$H_2{}^{16}O$	1.17	20	9426	6.5	7
$H_2{}^{17}O$	0.56	12	1083	1.4	12
$H_2{}^{18}O$	0.65	12	2460	2.3	6
$D_2{}^{16}O$	0.71	12	2807	3.0	7
$HD^{16}O$	0.47	12	2019	−1.2	11
All	0.95	20	17795		

it helps to have only 2 electrons. The spectroscopically determined PES using *ab initio* methods [9] as a starting point gave an excellent wtandard deviation of 0.01 cm^{-1}. It was a shock for us at the time, when this very same surface gave only a 2 cm^{-1} accuracy for H_2D^+ and D_2H^+ isotopomers. Adiabatic effects proved to be the reason [11]. We used a primitive, SCF level of theory to calculate the adiabatic surface for H_3^+ and it showed some significant contribution to the rotation-vibration energy levels. We decided to model the nonadiabatic effects using the mass manipulation following diatomic results. That proved to be very successful for H_3^+ [12]. We achieved 0.03 cm^{-1} overall accuracy for all isotopomers using the *ab initio* potential of Kutzellnigg et al. [13]. The first *ab initio* adiabatic surface of water was published by Zobov et al. [14] using an SCF level calculation. More accurate up to date calculations of both adiabatic and nonadiabatic effects were provided by Schwenke [15, 16] and they are included in our final PES [1]. One more correction to the nonrelativistic BO PES is worth mentioning. I am talking about the quantum electrodinamic correction [17] which contributes up to 1 cm^{-1} to the rotation-vibration energy levels calculation. Our overall accuracy is so high, that the inclusion of this exotic correction results in the significant lowering of the overall standard deviation. Our final results are presented in the Tables 1 and 2. Table 1 illustrates the change in accuracy of water energy levels calculations. From this table one can see the contribution of different factors to the improved accuracy. These factors are - increase of the basis set, extrapolation to the basis set limit and inclusion of various corrections. Our final results are presented in Table 2. Table 2 illustrates that on average for all major isotopomers and most of the known experimentally values of the rotational quantum numbers of J, our accuracy is better then 1 cm^{-1} .

In conclusion I would like to mention that we also performed spectroscopic fitting of the PES using a starting point different from that of PS, though as yet not our present final surface [18]. We used PS's *ab initio* surface augmented with our relativistic and quantum electrodinamic corrections together with Schwenke's adiabatic correction. As the complete basis set extrapolated 6z basis surface

was unavailable to us at the time, we use our phenomenological one-dimensional correction to the barrier to linearity instead [10] . We produced the fitted surface which gives the standard deviation of 0.1 cm^{-1} for the rovibrational data up to 25 000 cm^{-1}. We hope, that our final goal in the water project - to achieve experimental accuracy of about 0.01 cm^{-1} for all known experimental energy levels of water and its isotopomers - will be feasible with the present *ab initio* PES as a starting point.

---

[1] O.L. Polyansky, A.G. Császár, S.V. Shirin, N.F. Zobov, P. Barletta, J. Tennyson, D.W. Schwenke and P.J. Knowles, *Science*, **299**, 539-542 (2003).

[2] A. Carrington and R.A. Kennedy, *J. Chem. Phys.* **81**, 91 (1984).

[3] J. Tennyson and B.T. Sutcliffe *J. Chem. Phys.*, **77**, 4061-4072 (1982)

[4] O.L. Polyansky, P. Jensen and J. Tennyson, *J. Chem. Phys.*, **101**, 7651-7657 (1994)

[5] H. Partridge and D. W. Schwenke, *J. Chem. Phys.* **106**, 4618 (1997).

[6] O. L. Polyansky, N. F. Zobov, S. Viti, J. Tennyson and P. F. Bernath, L. Wallace, *Science* **277**, 346 (1997).

[7] O.L. Polyansky, J. Tennyson and P.F. Bernath, *J. Molec. Spectrosc.*, **186**, 213-221 (1997)

[8] MOLPRO (version 2002.1) is a package of ab initio programs designed by H.-J. Werner and P.J. Knowles.

[9] A. G. Császár, J. S. Kain, O. L. Polyansky, N. F. Zobov and J. Tennyson, *Chem. Phys. Lett.*, **293**, 317 (1998).

[10] J.S. Kain, O.L. Polyansky and J. Tennyson, *Chem. Phys. Letts.*, **317**, 365-371 (2000).

[11] J. Tennyson and O.L. Polyansky, *Phys. Rev. A*, **50**, 314-316 (1994)

[12] O. L. Polyansky and J. Tennyson, *J. Chem. Phys.* **110**, 5056 (1999).

[13] W. Cencek, J. Rychlewski, R. Jaquet and W. Kutzelnigg, *J. Chem. Phys.* **108**, 2831 (1998).

[14] N.F. Zobov, O.L. Polyansky, C.R. Le Sueur and J. Tennyson, *Chem. Phys. Letts.*, **260**, 381-387 (1996).

[15] D. W. Schwenke, *J. Chem. Phys.* **118**, 6898 (2003).

[16] D. W. Schwenke, *J. Phys. Chem. A* **105**, 2352 (2001).

[17] P. Pyykkö, K. Dyall, A. G. Császár, G. Tarczay, O. L. Polyansky and J. Tennyson, *Phys. Rev. A* **63**, 024502 (2001).

[18] S.V. Shirin, O.L. Polyansky, N.F. Zobov, P. Barletta and J. Tennyson, *J. Chem. Phys.*, **118**, 2124-2129 (2003)

[19] J. Tennyson, N.F.Zobov, R. Williamson, O.L. Polyansky and P.F. Bernath, *J. Phys. Chem. Ref. Data* **30**, 735-831 (2001).

A. Miani, J. Tennyson and T. van Mourik (eds.)
High Accuracy Potentials for Quantum Dynamics

Analytical Energy Gradients for Internally Contracted Second-Order Multi-reference Perturbation Theory (CASPT2)

Hans-Joachim Werner and Paolo Celani

Institut für Theoretische Chemie, Universität Stuttgart, Pfaffenwaldring 55, D-70569 Stuttgart, Germany

I. ANALYTICAL ENERGY GRADIENTS FOR MRPT2

The theory for computing analytical energy gradients for second-order multi-reference perturbation theory (MRPT2) with arbitrary MCSCF reference functions has been derived and implemented[1]. In our method the configurations with two electrons in the external orbital space are internally contracted. This ansatz strongly reduces the length of the configuration expansion as compared to uncontracted wavefunctions, but avoids bottlenecks occurring when fully contracted first-order wavefunctions are used. The theory is based on Hylleraas functional for the second order energy and a Lagrange functional to account for the stationary conditions which determine the reference wavefunction. The method has been implemented into the `MOLPRO` *ab initio* program[2], using the gradient integral package `ALASKA` of Lindh[3]. The MCSCF Z-vector equations are solved using the available routines from our second-order MCSCF program[4, 5]. Conventional and integral-direct options are available. The back transformation of the effective second-order density matrix into the Atomi Orbital (AO) basis is the same as that used for MP2 gradients. This transformation is always direct, i.e. the transformed density elements are immediately contracted with the AO integral derivatives and not stored.

II. APPLICATION TO PYRROLE

As an example the new method has been applied to geometry optimizations for selected states of Pyrrole. This molecule has served in the past as a benchmark system for computing electronic excitation energies, and therefore comparison is possible with many previous calculations. In particular, extensive CASSCF and

CASPT2 calculations have been performed by Serrano-Andrés et al.[6]. More recently, coupled cluster methods (CCSD, CC2, CC3) have been applied by Christiansen et al.[7] to compute excitation energies. In the latter work, also the equilibrium structures of some states have been determined. For a review of other previous calculations and experimental work see Refs. 6, 7.

As examples for valence excited states we have chosen the $^1A_1^-$, $^1A_1^+$ and $^1B_1$ states. On the other hand, as typical Rydberg states we choose the 1^1B_1 ($1a_2 \rightarrow 3p_y$), 2^1B_1 ($2b_1 \rightarrow 3s$), 1^1A_2 ($1a_2 \rightarrow 3s$), and 2^1A_2 ($1a_2 \rightarrow 3p_z$) states. According to the findings of Christiansen et al.[7] the structures were confined to be planar in the current calculations. We note, however, that preliminary calculations in C_S-symmetry indicate that the excited-states have non-planar equilibrium structures. The full optimization of the equilibrium structures as well as of the vibrational frequencies is currently in progress.

The basis set used for all calculations (unless otherwise noted) was derived from the aug-cc-pVTZ basis[10]. It was found that the d-functions on the hydrogen atoms have a negligible effect on the excitation energies, and therefore these were omitted in the geometry optimizations. It has also been tested that additional diffuse functions are not needed for the states under consideration. The resulting basis set comprised 295 contracted GTOs.

In Table I the structures and excitation energies of the valence excited states of Pyrrole are compared. The vertical excitation energies T_v are in good agreement with the results of Serrano-Andrés et al.[6], but significantly lower than the CC3 results of Christiansen et al.[7]. The adiabatic excitation energies T_e are lower than the T_v values by 0.36 eV for the $^1A_1$ states and even by 0.48 eV for the $^1B_2$ state. These significant relaxation effects are due to changes of the bonding character caused by the excitations. In case of the $^1A_1$ states, the strongest effect is seen for the C_1-C_2 bond, which is elongated by about 0.08 Å. This is due to the excitation from the $1a_2$ orbital, which is bonding for C_1-C_2 and anti-bonding for C_2-C_3. A similar elongation of this bond is found for the $^1B_2$ state, but in this case this is accompanied by a significant shortening of the C_2-C_3 bond. This is due to the fact that the dominant excitation is from the anti-bonding $1a_2$ orbital into the bonding $9a_1$ orbital.

Serrano-Andrés et al.[6] have concluded that their excitation energies are in close agreement with the experimental data. The most intense band in the spectrum starts at 7 eV and extends well beyond 8 eV. These bands have been assigned to the $^1A^+$ valence state. The first maximum is at about 7.25 eV and the strongest peak at 7.54 eV[9]. The latter value agrees well with the computed vertical excitation energy. The significant bond elongations in this state indicate that the zero-point correction will be negative and probably quite larger. We estimate the zero-point correction to be -0.1 eV or even more. This means that the CASPT2 would predict the 0-0 transition at about 7.1 eV, just

TABLE I: Comparison of optimized structures and excitation energies for the valence states of Pyrrole[a]

	1^1A_1	$^1A_1^-$	$^1A_1^+$	$^1B_2$
N-C_1	1.368	1.389	1.380	1.409
C_1-C_2	1.375	1.455	1.460	1.457
C_2-C_3	1.419	1.462	1.452	1.361
N-H_1	1.000	1.000	1.007	0.999
C_1-H_2	1.072	1.070	1.071	1.074
C_2-H_3	1.073	1.071	1.072	1.072
H_1-N-C_1	125.1	123.7	123.0	126.4
N-C_1-H_2	121.2	121.9	121.3	121.3
C_1-C_2-H_3	125.7	126.1	125.3	123.8
T_e (eV)		5.62	7.18	5.66
T_v (eV)		5.98	7.54	6.14
CASPT2[6]		5.92	7.46	6.00
CC3[7]		6.37	8.07	6.63

a) Basis cc-pVTZ without d-functions on hydrogens. Bond lengths in Å, angles in deg, C_{2v} symmetry was enforced. Level shift 0.3 h.
States $1^1A_1 - 3^1A_1$, $^1B_2$ averaged in CASSCF

in the region where the band starts. Similar conclusions apply to the 2^1B_2 valence state, which has been assigned to the band system starting at 5.6 eV, with a maximum at 5.98 eV. The vacuum UV spectrum shows a 0-0 transition at 5.864 eV and another one at 5.818 eV[10]. The previous CASPT2 calculations predicted a vertical excitation energy of 6.0 eV, in good agreement with the band maximum. However, if geometry relaxation and zero-point corrections are added, the CASPT2 0-0 energy will likely be lower than the onset of the band. From these results it seems very likely that the CASPT2 method quite strongly underestimates the valence excitation energies. The apparently good agreement of previous CASPT2 calculations with experimental data is probably due to an error compensation effect. The results for the Rydberg states are presented in Table II. It is found that in this case the results of the CASPT2 and CC3 calculations are in close agreement. Inspection of the state-averaged CASSCF wavefunctions shows that in $^1B_1$ symmetry there is significant mixing of the $2b_1 \rightarrow 3s$ and $1a_2 \rightarrow 3p_y$ states.

TABLE II: Comparison of optimized structures and excitation energies (in eV) for selected Rydberg states of pyrrole[a]

	1^1A_1	1^1B_1	2^1B_1	1^1A_2	2^1A_2
		$(2b_1 \rightarrow 3s,\ 1a_2 \rightarrow 3p_y)$		$1a_2 \rightarrow 3s$	$1a_2 \rightarrow 3p_z$
N-C_1	1.370	1.365	1.362	1.343	1.357
C_1-C_2	1.377	1.369	1.393	1.433	1.426
C_2-C_3	1.421	1.498	1.436	1.369	1.370
N-H_1	1.002	1.054	1.035	1.054	1.017
C_1-H_2	1.074	1.075	1.076	1.078	1.077
C_2-H_3	1.075	1.076	1.075	1.076	1.073
H_1-N-C_1	125.0	123.6	124.3	125.3	125.5
N-C_1-H_2	121.1	120.5	121.1	120.6	121.8
C_1-C_2-H_3	125.7	127.3	125.1	125.0	124.7
T_e		5.83	5.94	4.98	5.85
T_v		5.92	6.00	5.22	6.01
T_v CASPT2[6]		5.85	5.97	5.08	5.83
T_v CC3[7]		5.85	6.00	5.10	5.86
T_{00} (best estimates)[7]		5.84	5.97	4.83	5.75

a) Basis aug-cc-pVTZ without d-functions on hydrogens
Bond lengths in Å, angles in deg, C_{2v} symmetry was enforced.
Level shift 0.2 h, analytical gradients for the shifted energy.
Only π-electrons active, orbitals $10a_1, 11a_1, 1b_1 - 3b_1, 7b_2, 1a_2, 2a_2$ active
$1^1A_1, 1^1B_1, 2^1B_1, 1^1A_2, 2^1A_2$ states averaged.

We find that at the ground-state structure the $1a_2 \rightarrow 3p_y$ state is the lowest (as found in previous work), but at the optimized 1^1B_1 structure the wavefunction is dominated by the $2b_1 \rightarrow 3s$ excitation. At the optimized 2^1B_1 structure, both excitations have about the same weight. This indicates that there is an avoided crossing of the two states near the geometry of the 2^1B_1 state. The strong mixing makes it very difficult to predict the structure of the two lowest $^1B_1$ states reliably. A multi-state CASPT2 treatment would be necessary to account for the mixing of the states more accurately.

[1] P. Celani and H.-J. Werner, J. Chem. Phys. (submitted for publication).
[2] H.-J. Werner, P. J. Knowles, R. Lindh, M. Schütz, and others (see `http://www.molpro.net`), `MOLPRO`, version 2002.7, 2003.
[3] R. Lindh, Theor. Chim. Acta 85 (1993) 423.
[4] H.-J. Werner and P. J. Knowles, J. Chem. Phys. 82 (1985) 5053.
[5] P. J. Knowles and H.-J. Werner, Chem. Phys. Lett. 115 (1985) 259.
[6] L. Serrano-Andrés, M. Merchán, I. Nebot-Gil, B. O. Roos, and M. Fülscher, J. Am. Chem. Soc. 115 (1993) 6184.
[7] O. Christiansen, J. Gauss, J. F. Stanton, and P. Jørgensen, J. Chem. Phys. 111 (1999) 525.
[10] R. A. Kendall, T. H. Dunning, and R. H. Harrison, J. Chem. Phys. 96 (1992) 6796.
[9] W. M. Flicker, O. A. Mosher, and A. Kuppermann, J. Chem. Phys. 64 (1976) 1315.
[10] M. Bavia, F. Bertinelli, C. Taliani, and C. Zauli, Mol. Phys. 31 (1985) 479.

A. Miani, J. Tennyson and T. van Mourik (eds.)
High Accuracy Potentials for Quantum Dynamics

Model Hamiltonians for Accelerating Orbital Basis Convergence

Peter J. Knowles

School of Chemical Sciences, University of Birmingham, Birmingham B15 2TT, United Kingdom

I. INTRODUCTION

First-principles computations of the spectroscopy and dynamics of small molecular systems can now be carried out with extraordinary accuracy. For example, recent computations on the vibration-rotation spectrum of water contain a standard deviation of less than 1 cm^{-1} on a set of more than 17,000 empirical energy levels. [1] The contributions to the remaining error in such calculations can be classified under the following headings: (a) solution of the nuclear motion problem, e.g. restriction to a finite basis of vibrational functions; (b) incomplete inclusion of beyond-Born-Oppenheimer effects; (c) incomplete inclusion of relativistic effects; (d) the use of an approximate electronic structure ansatz instead of full configuration interaction (the "N-electron" error); (e) incompleteness of the basis set in which orbitals are represented ("1-electron" error). In very small systems using the best available methodology, the contribution of each of these sources of error is similar, and the challenge in attaining even greater accuracy is therefore considerable. In larger molecules, where the realistic error target is inevitably larger, the emphasis on these five sources of error is different. For systems reasonably well described by Hartree-Fock theory, standard methodology for the N-electron problem based on coupled-cluster theory is very successful, and with appropriate exploitation of spatial locality can be applied to molecules with hundreds of atoms. [2–4] Although in such calculations the computational resource requirements can be made to scale roughly linear with system size, their dependence on the level of treatment of the 1-electron error is very strong. The computational effort for nearly all correlated wavefunction methods inevitably scales as the fourth power of the size of orbital basis set, with no possibility of help from localization; indeed, large basis sets that include diffuse orbitals actually impair the exploitation of locality. Given that convergence of errors with orbital

basis size is slow, these considerations show that small improvements in overall accuracy demand very large increases in computational resource, rendering a practical barrier to further improvements in accuracy.

Most electronic structure computations that represent electron correlation effects with a wavefunction have as their physical basis a configuration interaction expansion of two-electron wavefunctions represented as linear combinations of products of orbitals. The advantages and defects of this approach are well known: computational simplicity arises from the orthogonality of the orbitals; however such wavefunctions are not well adapted to the true, cusped shape of the wavefunction near the coalescence point. As a result of this, convergence of the energy and other properties to the basis-set limit is slow. Using the correlation-consistent basis sets developed by Dunning and co-workers[5], it is found empirically[6] that to a reasonable approximation, the correlation energy follows the asymptotic relationship

$$E^x_{\rm corr} = E^\infty_{\rm corr} + A\,x^{-3} \tag{1}$$

where x is the integer $2, 3, 4, 5, \ldots$ that characterizes the bases cc-pVDZ, cc-pVTZ, cc-pVQZ, cc-pV5Z,.... Unfortunately, this convergence pattern means that accurate correlation energies are difficult to attain; however, the asymptotic relationship can successfully be used as an extrapolation formula for $E^\infty_{\rm corr}$ based on two successive members of the $E^x_{\rm corr}$ sequence[6].

An alternative to orbital-product methods is the adoption of wavefunctions that contain explicit reference to the interelectronic coordinate r_{12}. The R12 methods[7, 8] offers a practical approximation to Hylleraas-type wavefunctions in the many electron case, and has been very successful in delivering very accurate results. However, because of the complication of implementing the R12 approach for each desired N-electron method, it remains desirable to seek improvements in the orbital-basis approach.

A systematic sequence of basis sets (e.g., cc-pVxZ, $x = 2, 3, \ldots$) that is capable of converging to completeness can be considered to define a sequence of model hamiltonians, written in second-quantized formulation as

$$\hat{H}^x = \sum_{pq}^{n^x} h_{pq} p^\dagger q - \tfrac{1}{2} \sum_{pqrs}^{n^x} (pq|rs) p^\dagger r^\dagger s q\,, \tag{2}$$

for which we solve Schrödinger's equation in principle exactly to get E^x. It is of interest to investigate the the corresponding extrapolated *hamiltonians*

$$\hat{H}^x_{\rm extrap} = \sum_y^x C_y\,\hat{H}^y \tag{3}$$

where C_y are fixed parameters chosen from, for example, the asymptotic relationship (1). We might then be able to get an approximation to the basis-set limit of the wavefunction as well as the energy. It might also be possible to find a modified hamiltonian that is not dependent on the existence and regularity of any sequence, thereby eliminating any ad-hoc dependence on x^{-3} convergence.

II. SCALING THE FLUCTUATION POTENTIAL

An interesting approach to effective elimination of basis-set errors is the Scaled External Correlation approach[9], in which correlation energies are adjusted according to a prescription designed to deliver exact results for certain known quantities such as individual bond energies. Such a philosophy can be applied to generate an effective hamiltonian operator. Consider a system described qualitatively correctly by the Hartree-Fock method. We can adopt the usual Rayleigh-Schrödinger partitioning of the hamiltonian

$$\hat{H}(z) = \hat{H}^{(0)} + z\hat{H}^{(1)} + (1-z)E^{(1)} \tag{4}$$

where the zero-order hamiltonian $\hat{H}^{(0)}$ is the Møller-Plesset choice of the Fock operator. $\hat{H}(1)$ is the true hamiltonian, and the additive term $(1-z)E^{(1)}$ is introduced merely so that the Hartree-Fock wavefunction always has the energy $E^{(0)}+E^{(1)}$ for any value of z. The normal development of Møller-Plesset theory is a series expansion in powers of z to give a series for the value of the correlation energy at $z=1$. In this context, in the first instance for molecules consisting of only a single chemical element, we choose a value of z different from unity such that a particular known quantity is reproduced exactly. This quantity would typically be the basis limit of the atomic correlation energy using the chosen N-electron methodology, but other choices, such as homonuclear diatomic bond energies, are also possible. Perturbation theory arguments show that the energy $E(z)$ is expected to decrease monotonically with z, and so the optimum z will be a single-valued function of the error in the calibration quantity, an important consideration for defining a unique model. z will also be greater than unity, reflecting the fact that the ansatz increases the strength of the fluctuation potential in order to compensate for deficiencies in the wavefunction arising from insufficient flexibility in the basis set.

As an example, we consider the interatomic Ne_2 potential. We use the aug-cc-pVxZ orbital basis set sequence[10], the CCSD(T) energy function, and choose the scaling factor z such that a best estimate of the valence CCSD(T) atomic correlation energy is reproduced. Table I shows that the performance of the method, in terms of the computed binding energy at a fixed

TABLE I: Orbital basis set convergence of the dissociation energy of Ne_2

x^a	$E_{\rm corr}$(Ne) ^{b}	z^c	D_e ^{d} (raw)	D_e $(x^{-3})^e$	D_e (scaled)
2	0.212945	1.2236	0.000004		0.000072
3	0.279375	1.0723	0.000072	0.000099	0.000103
4	0.303704	1.0296	0.000102	0.000124	0.000117
5	0.313051	1.0145	0.000116	0.000132	0.000124
6	0.316974	1.0083	0.000121	0.000130	0.000126
∞	0.322362				

[a] Cardinal index x in aug-cc-pVxZ orbital basis set sequence
[b] Valence CCSD(T) correlation energy of atom
[c] Scale factor to deliver $E_{\rm corr}(\mathrm{Ne}) = 0.322362$
[d] $E(R=\infty) - E(R=5.8a_0)$ using valence CCSD(T) ansatz.
[e] Extrapolation through (1) using x and $x-1$ raw energies

internuclear separation, is comparable to that obtained with the conventional x^{-3} extrapolation of the energy.

Figure 1 shows a part of a potential energy curve for F_2 using both the regular cc-pVTZ hamiltonian and that obtained by scaling through (4). The CCSD(T) ansatz with only valence electrons correlated has been used. It is seen that the effect of scaling is disastrous; the potential energy curve is strongly repulsive near to the equilibrium bond length, and at around 1.72 Å there is an unphysical dip in the curve. This feature is related to the convergence properties of the Møller-Plesset perturbation series; either increasing z or the bond length introduces divergencies because of the presence of intruder states. Thus the formulation as presented above is probably applicable in cases only where Møller-Plesset theory is convergent. Elsewhere it will be necessary to develop a formulation based, for example, on a multiconfigurational reference state.

III. EFFECTIVE KINETIC ENERGY OPERATORS

An alternative to the construction of parameterized effective operators is to seek approaches that work from first-principles understanding of the defects of finite-basis approaches. We start by considering for the ground-state helium atom a sequence of orbital basis sets that are radially complete, but contain angular functions only up to a certain angular momentum L. Instead of constructing two-electron wavefunctions using the variational principle, we imagine that we have knowledge of the exact wavefunction $\Psi_{\rm exact}$, and from it we project into the finite basis:

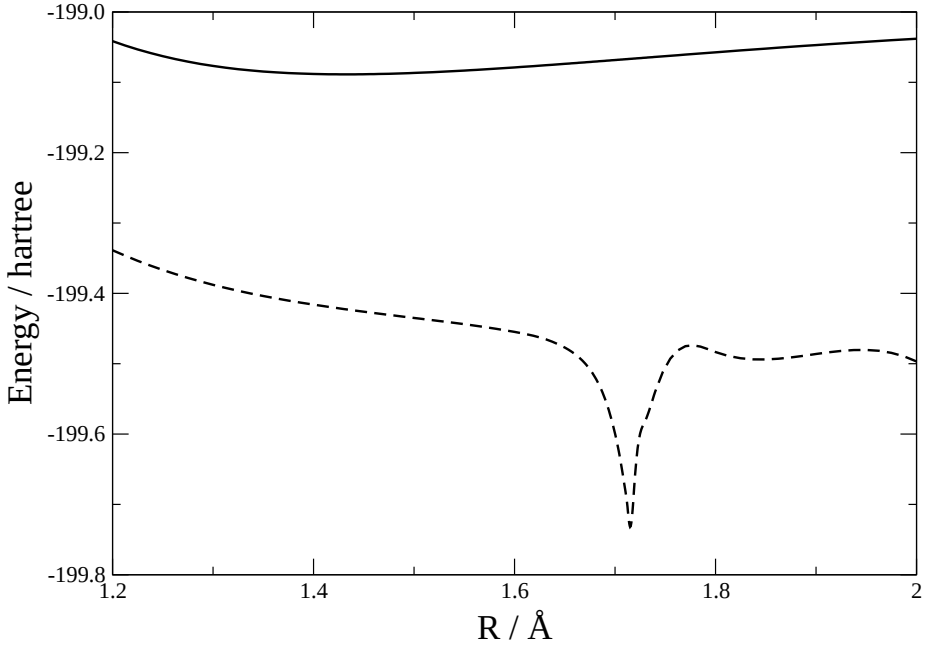

FIG. 1: Valence CCSD(T) potential energy curve for F_2 with scaled hamiltonian. Solid line: cc-pVTZ basis; dashed line: scaled hamiltonian.

$$\hat{P}\Psi_{\text{exact}} = \sum_{l}^{L} |l, m, l, -m\rangle\langle l, m, l, -m| \, \Psi_{\text{exact}} \tag{5}$$

Instead of following the conventional approach of analyzing the truncated wavefunction $\hat{P}\Psi_{\text{exact}}$, we cast all the basis dependence into an effective hamiltonian operator $\hat{P}\hat{H}\hat{P}$. This model hamiltonian contains a projected non-local interelectronic potential $\hat{P}r_{12}^{-1}\hat{P}$, which can be visualized through its action on the exact wavefunction, $\hat{P}r_{12}^{-1}\hat{P}\Psi_{\text{exact}}/\hat{P}\Psi_{\text{exact}}$, shown in figure 2 for the example of $L = 4$. The smoothing by the projection of the r_{12}^{-1} singularity provides a rationale for understanding why in the finite-basis wavefunction the Coulomb hole is underestimated. However, it is also important to consider the kinetic energy, and indeed it is the consideration of the kinetic rather than potential energy that appears important when considering the local energy,

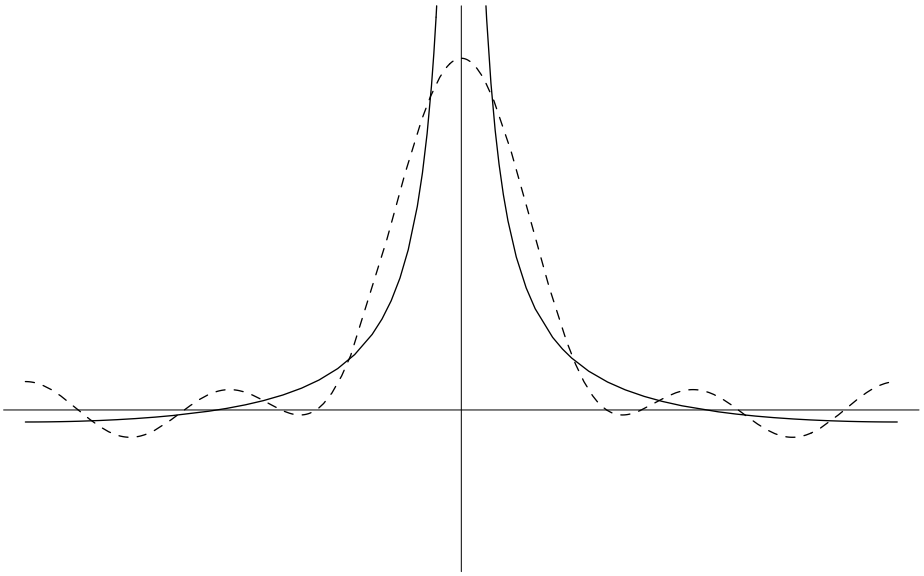

FIG. 2: Effective local potential $\hat{P}r_{12}^{-1}\hat{P}\Psi_{\rm exact}/\hat{P}\Psi_{\rm exact}$ with $L = 4$

defined as

$$E_{\rm local} = \frac{\hat{H}\Psi}{\Psi} \equiv \frac{\hat{H}\hat{P}\Psi_{\rm exact}}{\hat{P}\Psi_{\rm exact}}$$
$$= \frac{\hat{T}\hat{P}\Psi_{\rm exact}}{\hat{P}\Psi_{\rm exact}} + r_{12}^{-1} + V(\vec{r}_1) + V(\vec{r}_2)\,. \qquad (6)$$

Except in the case of the complete basis, where the local kinetic energy has an exact $-r_{12}^{-1}$ behaviour, $E_{\rm local}$ is positive and singular at $r_{12} \to 0$. In detail, the potential energy is singular, but the corresponding negative singularity in the kinetic energy is suppressed by $\hat{P}$ for any finite basis, and the integrated kinetic energy is overestimated. Figure 3 shows this effect of the projection on the local kinetic energy. Note that this analysis applies to the special case of $\Psi = \hat{P}\Psi_{\rm exact}$; in a real finite-basis calculation, variational procedures will subsequently adjust the wavefunction to the wrong shape, in the end *reducing* the kinetic energy in accordance with the virial theorem, but the argument we follow is a more natural one when looking for causes and remedies of errors.

In contrast, if it were possible to perform the projection after the hamiltonian,

$$E_{\rm exact} = \frac{\hat{P}\hat{H}\Psi_{\rm exact}}{\hat{P}\Psi_{\rm exact}} = \frac{\hat{P}\hat{T}\Psi_{\rm exact}}{\hat{P}\Psi_{\rm exact}} + r_{12}^{-1} + V(\vec{r}_1) + V(\vec{r}_2) \qquad (7)$$

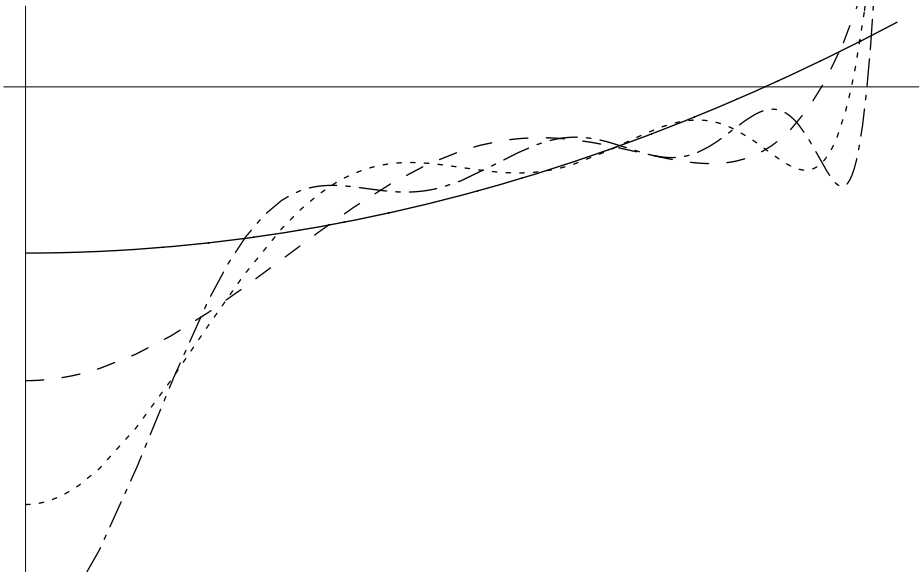

FIG. 3: Projected local kinetic energy for helium as a function of r_{12} with both electrons constrained to be a distance $1a_0$ from the nucleus. Solid line: $L = 2$; dashed: $L = 4$; dotted: $L = 6$; dot-dash: $L = 8$.

the singularities would cancel, and E_{local} would be constant. Of course, such a formulation offers no practical route forward, since for any real problem Ψ_{exact} is unknown. However, we seek to use the relationship between (6) and (7) to quantify and remedy the basis incompleteness error.

In order to develop a general theory, it is necessary to avoid using quantities such as L or anything else that relies on a central potential or a particular kind of basis set. The projector $\hat{P}$, however, does readily translate to the general molecular case, and can be used as an indicator basis incompleteness. For 2-electron systems,

$$\hat{P} = \sum_{pqrs} |pq\rangle S^{-1}_{pr} S^{-1}_{qs} \langle rs| \tag{8}$$

where $S_{pq} = \langle p|q\rangle$, and more generally an equivalent second-quantized formulation can be adopted.

We seek to address the kinetic energy deficiency by changing the 2-electron

operator in the second quantized hamiltonian, adding

$$\hat{M} = \frac{1}{2} \sum_{pqrs} M_{pq,rs}\, p^\dagger r^\dagger sq \tag{9}$$

such that

$$\hat{P}(\hat{T} + \hat{M})\hat{P}\Phi = \hat{P}\hat{T}\Phi \tag{10}$$

for some 2-electron trial functions Φ. The modified operator would then be applied to many-electron systems. The potential advantage of this approach is that it completely avoids any discussion of representing the shape of the Coulomb hole in the many-electron case, where explicitly correlated wavefunctions implicate the calculation of many-electron integrals. In contrast, here we retain a two-electron hamiltonian operator that works only on a tensor-product space, and therefore will require at most two-electron integration.

A suitable choice of trial functions might be $(1+\frac{1}{2}r_{12})\psi_t(1)\psi_u(2)$ for all ψ_t, ψ_u in the orbital basis. We define the following two-electron operators.

$$\hat{T} = -\tfrac{1}{2}\nabla_1^2 - \tfrac{1}{2}\nabla_2^2 \tag{11}$$

$$\hat{G} = r_{12}^{-1} \tag{12}$$

$$\hat{R} = r_{12} \tag{13}$$

$$\hat{Q} = r_{12}\hat{T} \tag{14}$$

$$\hat{U} = r_{12}^{-1}(\vec{r}_1 - \vec{r}_2) \cdot (\vec{\nabla}_1 - \vec{\nabla}_2) \tag{15}$$

$$\hat{V} = [\hat{R}, \hat{T}] = 2\hat{G} + \hat{U} \tag{16}$$

We then get

$$\hat{P}(\hat{T} + \hat{M})\hat{P}(1 + \tfrac{1}{2}\hat{R})\hat{P} = \hat{P}\hat{T}(1 + \tfrac{1}{2}\hat{R})\hat{P} \tag{17}$$

$$2\hat{P}\hat{M}\hat{P} + \hat{P}\hat{M}\hat{P}\hat{R}\hat{P} = \hat{P}\hat{Q}\hat{P} - \hat{P}\hat{V}\hat{P} - \hat{P}\hat{T}\hat{P}\hat{R}\hat{P} \tag{18}$$

which is a linear system for $\hat{M}$ driven by $\hat{T}R - \hat{T}\hat{P}\hat{R}$, which vanishes in the complete basis limit. In explicit matrix element form the linear equations may be written as

$$\langle pq|(\hat{T} + \hat{M})\hat{P}(1 + \tfrac{1}{2}\hat{R})|rs\rangle = \langle pq|\hat{T}(1 + \tfrac{1}{2}\hat{R})|rs\rangle \tag{19}$$

and their solution requires the computation of the two-electron integrals over the basis of the operators $\hat{R}, \hat{Q}, \hat{V}$. This ansatz, or others that might be based on it, offers a simple route to establishing an effective hamiltonian operator that can be used with existing second-quantized codes, but which addresses

the kinetic energy defect associated with the finite orbital-product space. The effort required is the calculation of additional two electron integrals, and the solution of linear equations (the effort for the latter can probably be reduced by exploiting locality). Future work will evaluate the effectiveness of the method.

Acknowledgments

PJK is grateful to Dr. Fred Manby (University of Bristol) for technical assistance.

---

[1] O. L. Polyansky, A. G. Császár, S. V. Shirin, N. F. Zobov, P. Barletta, J. Tennyson, D. W. Schwenke, and P. J. Knowles, Science **299**, 539 (2003).
[2] S. Saebø and P. Pulay, Ann. Rev. Phys. Chem. **44**, 213 (1993).
[3] M. Schütz and H.-J. Werner, J. Chem. Phys **111**, 5691 (1999).
[4] M. Schütz, J. Chem. Phys **116**, 8772 (2002).
[5] T. H. Dunning, J. Chem. Phys **90**, 1007 (1989).
[6] A. Halkier, T. Helgaker, P. Jørgensen, W. Klopper, H. Koch, J. Olsen, and A. K. Wilson, Chem. Phys. Letters **286**, 243 (1998).
[7] W. Kutzelnigg, Theor. Chim. Acta **68**, 445 (1985).
[8] W. Kutzelnigg and W. Klopper, J. Chem. Phys **94**, 1985 (1991).
[9] F. B. Brown and D. G. Truhlar, Chem. Phys. Letters **117**, 307 (1985).
[10] R. A. Kendall, T. H. Dunning, Jr., and R. J. Harrison, J. Chem. Phys **96**, 6796 (1992).